A.D. MDLXII

DEPARTMENT OF BIOMEDICAL SCIENCES

PhD COURSE IN LIFE SCIENCES AND BIOTECHNOLOGIES

UNIVERSITY OF SASSARI

Director: Prof. Leonardo Antonio Sechi

Cycle XXXV

Identification of the mechanism of innate immune response against SARS-CoV-2

By

Tang Chao

Supervisors: Prof. Salvatore Rubino
Ph.D. School in Life Sciences and Biotechnologies
Department of Biomedical Sciences University of Sassari

Prof. David J. Kelvin
Division of Immunology, International Institute of Infection and Immunity
Shantou University Medical College

Academic Year: 2019-2022

ABSTRACT

The globe is currently experiencing a situation that is similar to the Spanish flu pandemic of 1918: Coronavirus Disease 2019 (COVID-19), which is brought on by the severe acute respiratory syndrome coronavirus 2 (SARS-CoV-2), has been producing a pandemic since March 2020. The exact pathogenesis of SARS-CoV-2 and the innate immune system induced by the virus remain poorly understood. However, using rapid genome sequencing will help researchers elucidate the structure and function of the virus, which could lead to a better understanding of SARS-CoV-2.

The harm posed by COVID-19 to human health and life is grave. Since the COVID-19 epidemic till the present, there have been improvements in treatment medications and vaccinations as well as modifications in the pathogenicity of the virus itself. Although the rates of severe sickness and mortality have greatly decreased, the elderly population (>65) still has high hospitalization and mortality rates. The death rate is higher in the senior population, regardless of whether it is a breakthrough infection, a typical illness, or another variation strain. This is likely brought on by the elderly's brittle innate immune system and diminished capacity to heal injured cells [1-2]. It is uncertain how innate immunity to viruses works in the elderly. For treatment efforts, it is essential to comprehend the host's innate immune response during early SARS-CoV-2 infection.

In response to viral infection, cells of the innate immune system produce antiviral cytokines, which are crucial in preventing viral reinfection and reducing viral replication and pathogenesis. Angiotensin-converting enzyme 2 (ACE2) membrane protein overexpression in airway epithelial cells has been found to be mediated by the antiviral cytokines INF-γ and TNF-α.

The SARS-CoV-2 connects to and infects host cells through the ACE2 receptor. We now understand additional details about how SARS-CoV-2 causes excessive proinflammatory cytokine release and transcriptional control of ACE2. Our findings imply that VSV-Spike in the LPS group can bind macrophages and dendritic cells more selectively. A portion of the

innate immune system's ACE2-expressing cells may also produce cytokines as a result of this. In the LPS group, VSV-Spike induces innate immunity while inhibiting adaptive immunity. This demonstrates that antiviral drugs that activate the innate immune system may have a considerable impact on the early stages of viral infection.

The spike protein is essential for endogenous immunity and a major element in setting off a cytokine storm since it is the main binding protein of SARS-CoV-2. It is feasible to identify the main immune regulatory pathways in the severe disease caused by the virus in the elderly by researching the immunological mechanism of viral invasion triggered by the spike protein. By blocking these pathways, clinical symptoms may be eased and mortality may be decreased. In this study, the differential gene expression of the cell experimental group was examined using RNA sequencing technology, and the results were compared to those from clinical sample analysis. Thirty-eight genes with the greatest association were discovered using Venn analysis. Most of these genes, such as CCL2, CXCL10, CCL8, DDX60L, and others, are involved in immunity and antiviral defense. Twenty-nine of the 38 frequent genes show downregulation, whereas 9 show upregulation. The most frequently down-regulated genes are those related to the adaptive immune system. IFI35 and SAMD9L linked to macrophages and innate immunity, were both activated. This demonstrates how crucial innate immunity is in protecting against viruses. These genes' primary roles in PPI analysis include immunological responses, type I interferon responses, and viral defense responses. Immune cell enrichment analysis revealed that cell subsets linked to innate immunity were considerably increased in COVID-19 compared to healthy controls, but cell subsets related to adaptive immunity were downregulated.

Immune cell genotyping research showed that innate immune cell subtypes (DC, monocytes, and neutrophils) were higher in the COVID-19 group as compared to healthy controls. The clinical link between 38 essential genes and SARS-CoV-2 was shown by ROC analysis of the association between 38 key genes and subsets of innate immune cells.

Toll-like receptors (TLRs) play a crucial role in the innate immune system, which uses them to identify various viral proteins and release type I interferons and pro-inflammatory

cytokines to combat infection. In our study, when comparing to the elderly patient group with the healthy control group, we found that TLR2, TLR5, TLR7/8 are activated, which activate the NF-κB pathway via the downstream MyD88 complex, leading to the release of inflammatory factors, but IRF3/7 cannot be activated, resulting in failed activation of type I interferons. Our study also showed that cytokine detection in the in vitro cell studies confirmed the increased expression of IL-2, IL-6, INF-γ, and TNF-α. Clinical COVID-19 patients had higher levels of IL-2, IL-6, INF-γ, and TNF-α expression while having fewer lymphocytes, which may play a significant role in cytokine storm. The inflammatory response can be balanced and the recovery of severe patients is aided by cytokine storm-blocking medications. It is important to find new prediction molecules or proteins for severe COVID-19 disease.

Index

Background

A significant group of coronaviruses known as human coronaviruses (HCoV) is linked to a number of respiratory illnesses of varied severity, such as the common cold, pneumonia, and bronchitis [3]. Due to their high genomic nucleotide replacement rate and recombination, HCoVs is considered to be one of the fastest-evolving viruses.

Currently, seven types of coronaviruses have been found to infect humans. including human coronavirus 229E (HCoV-229E), human coronavirus NL63 (HCoV-NL63) which encompasses α-coronavirus, and β-coronavirus: human coronavirus OC43 (HCoV-OC43), human coronavirus HKU1 (HCoV-HKU1) , severe acute respiratory syndrome virus (SARS-CoV), Middle East respiratory syndrome virus (MERS-CoV); and severe acute respiratory syndrome coronavirus-2 (SARS-CoV-2) [4-5]. A brand-new coronavirus called SARS-CoV-2 is to responsible for the ongoing 2019–2022 pandemic, which has already claimed millions of lives. due to its recurring infections across species and sporadic spillover incidents [6]. Two of these β-coronaviruses were responsible for significant outbreaks in the previous twenty years: SARS-CoV in 2002-2003 and MERS-CoV in 2012 [7-8]. All three of these coronaviruses are thought to have zoonotic origins and are capable of inflicting serious and even lethal sickness on people. SARS-CoV-2 has spread to more than 200 countries worldwide, with a total of 559 million confirmed cases and 6.4 million fatalities, in comparison to these three coronaviruses (data as of July 2022) [9]. With a total of 8096 confirmed cases and 774 fatalities, SARS-CoV spread to 26 countries [10]. There were 2562 confirmed cases of MERS-CoV in 27 countries, and 858 people died as a result. (Table 1) [11]. Due to the coronavirus's high genetic diversity, rapid genome reorganization, and frequent contact with human activities, SASR-CoV-2 is expected to continue to develop and spread seasonally [12]. The dilemma of new coronaviruses, which represent a severe danger to the world economy and healthcare system, persists despite our advances in medicine and fundamental science.

Table 1: Comparison of SARS-CoV-2, SARS-CoV and MERS-CoV

Name	Pandemic/epidemic year	Coronavirus subfamily	Country spread	Total cases	Total deaths	Fatality rate
SARS-CoV-2	2019-Present	β-Coronavirus	Globally	>559 Million	>6.4 Million	1.14%
SARS-CoV	2002-2003	β-Coronavirus	26	8096	774	9.6%
MERS-CoV	2012	β-Coronavirus	27	2468	851	34.5%

*The number of the COVID-19 confirmed cases and related deaths are change with the ongoing COVID-19 pandemic [9-11].

1. Introduction and review

1.1 Coronavirus and SARS-CoV-2

1.1.1 Coronavirus

Coronavirus belongs to the orders Nidovirales, Coronaviridae, and Orthocoronavirinae, and the subfamily Coronavirus is divided into four different genera: α, β, γ and δ Coronavirus. α- and β-coronaviruses originate from mammals, mainly bats, and are thought to cause more severe and fatal diseases in humans, while γ- and δ-viruses mainly originate from birds and pigs and are thought to cause asymptomatic or mild disease in humans [13].

The virions of coronaviruses are spherical, have a nuclear envelope, and have proteins on their surface that provide the appearance of a solar corona. They are positive sense, single-stranded RNA viruses that are enclosed [14].

Coronaviruses have a large RNA genome (26–32 kb) of coronaviruses.). Characteristics that they all share include a highly conserved genomic organization with a large replicase gene preceding structural and accessory genes; ribosomal frameshifting for the expression of nonstructural genes; specific enzymatic activities encoded within the replicating polyprotein; and expression of downstream genes through the synthesis of 3'-nested mRNAs are all characteristics that they share [15].

Humans and other vertebrates are hosts for the coronavirus, which mostly causes respiratory and intestinal infections and exhibits a range of clinical signs [16]. Since they cause both moderate and severe respiratory illness in humans, coronaviruses have long been regarded as one of the most significant infections in domestic and companion animals.

1.1.2 SARS-CoV-2 Viral morphology

SARS-CoV-2 belongs to the β-coronavirus family. Under an electron microscope, the virus surface has spikes that resemble a crown (Figure 1A) [17].

The inner nucleocapsid, translucent middle zone, and envelope comprise SARS-CoV-2. The Spike (S), Membrane (M), and Envelope (E) proteins are three crucial glycoproteins that constitute the double-layer lipid envelope. During the infection, the S proteins will break into S1 and S2. The S2 subunit facilitates membrane fusion, which leads to viral entrance into the host cell, whereas the S1 subunit mediates viral attachment to the cell membrane receptor. The coronavirus membrane structure is a result of the interaction between M protein, the most prevalent membrane protein, and E protein. The N protein, which composes the protein portion of the helical nucleocapsid that contains the genome RNA, is another part of the beta-coronavirus (Figure 1B) [18].

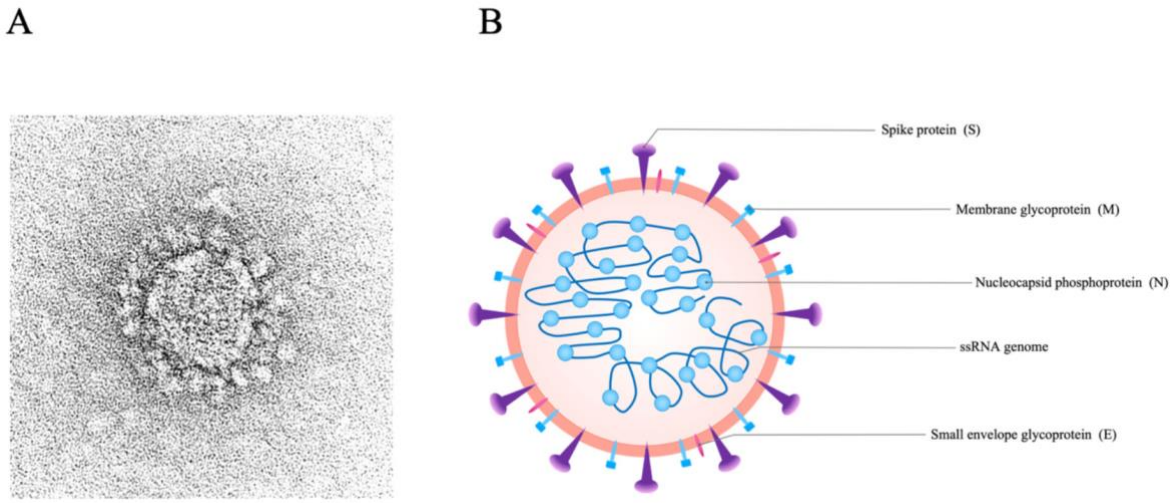

Figure 1: Electron microscopy image of SARS-CoV-2 virions and SARS-CoV-2 Structure

Fig 1 | A: Electron micrograph of a negatively stained particle of SARS-CoV-2, the causative agent of COVID -19. Note the prominent spines from which coronavirus gets its name: "corona" or "crown-like." Photo provided by Cynthia S. Goldsmith and A.Tamin to the CDC, 2020, ID#:23640. Available online at:https://phil.cdc.gov/Details.aspx?pid=23640. **B:** Viral structure with its protein components and viral RNA.

1.1.3 Biology of SARS-CoV-2

1.1.3.1 Biology of Coronaviruses

A spiral symmetrical nucleocapsid that surrounds the single-stranded sense RNA genome inside the coronavirus particle makes up the broad family of single-stranded enclosed RNA viruses known as coronaviruses [19]. The RNA chain has a polyA tail structure at the 3'end and a methylation cap structure at the 5'end. Translation is based on the genomic RNA as a template. The genome encodes and translates the proteins replicase and transcriptase. All of the viral byproducts in the open reading frame downstream come from subgenomic mRNA.

The coronavirus replicase gene spans about 2/3 of the whole genome's 5' end and is made up of two overlapping open reading frames (ORFs), ORF1a and ORF1b, which together code for 16 non-structural proteins. Four typical coronavirus structural proteins are encoded by the coronavirus genome's leftover RNA. Additionally, the number and distribution of additional ORFs in the structural protein genes vary depending on the kind of CoV [20-21].

1.1.3.2 SARS-CoV-2 genome characteristics

Since the emergence of SARS-CoV-2, genomic sequence research has helped to shed additional light on this unique coronavirus' features [22-24].

Seven pathogenic Human CoVs have been identified so far [25-26]. The SARS-CoV-2 genome is around 29.9 kb long, whereas the SARS-CoV and MERS-CoV genomes are 27.9 kb and 30.1 kb, respectively [27]. Additionally, out of the six other known human pathogenic CoVs, SARS-CoV-2 and SARS-CoV have the greatest nucleotide sequence similarity (79.7%) with SARS-CoV. Given this genomic sequence homology, it is assumed that SARS-CoV-2 and SARS-CoV share a number of biological characteristics. A conserved leader sequence with 9 transcribed sequences and 2 untranslated sections is present in the SARS-CoV-2 mRNA. Twelve anticipated functional ORFs are co-expressed by 9 nested subgenomic mRNAs. The pp1a and pp1ab polyproteins, which are cleaved into 16 non-structural proteins like RNA-dependent RNA polymerase, are encoded by the 5'-terminal two-thirds of the genome. The 3'-terminal portion of the genome encodes the structural proteins S, E, M, and N. (Figure 2A) [28-29].

The poly(A) tail of viral RNA is typically composed of 47 adenosines, and the poly(A) tail of full-length viral RNA is longer than subgenomic RNA, according to nanopore

sequencing of a single molecule. There is a link between the modified RNA and the 3′ poly(A) tail, as shown by the fact that the modified RNA's poly(A) tail is shorter than that of unmodified RNA. Furthermore, the study discovered that SARS-CoV-2 also creates transcripts that encode unknown ORFs to the conventional genome and nine subgenomic RNAs [30].

The amino acid sequences of NSP2 and NSP3 in the genes that code for the spike proteins have reportedly undergone some alterations. As RNA viruses are more prone to acquire genetic alterations that help them to avoid the host immune system and develop medication resistance, multiple SARS-CoV-2 gene mutations have been discovered. These mutations most likely boost the infectivity of SARS-CoV-2 [31-32]. Researchers have discovered that NSPs and spike proteins make use of several unique mutation sites in various gene sequencing studies throughout the world, indicating that the viruses may be adjusting to different host conditions [33].

Currently, many pharmaceuticals' research and development targets overlap with the locations of these mutations, including inhibiting the spike site and other locations, and the mutation of these sites may prevent the successful development and use of drugs. Therefore, developing the pharmacological target in the invariant area of the virus would be a superior approach for developing novel drugs.

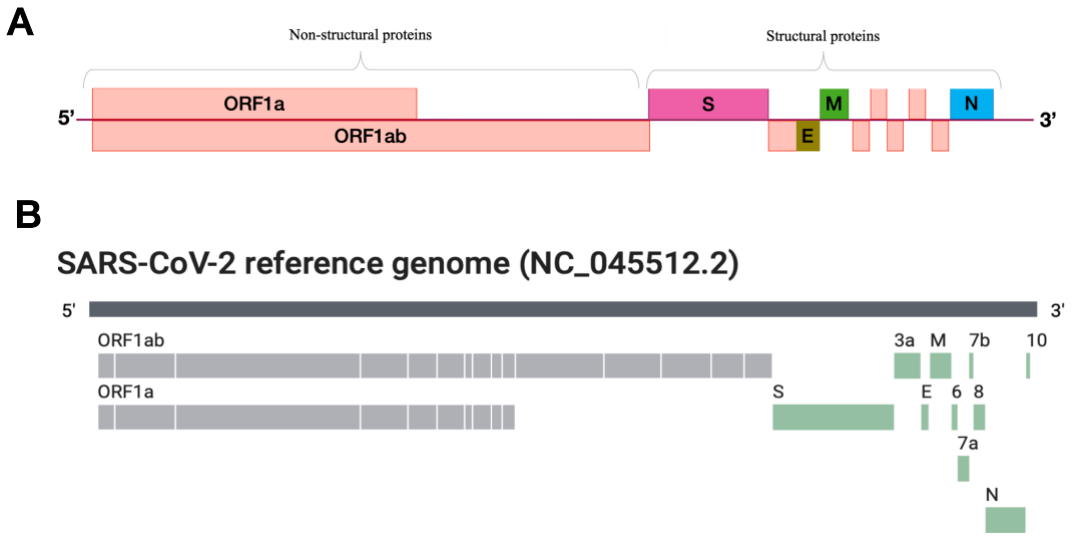

Figure 2: The genome structure of SARS-CoV-2

Fig.2 | **A:** genome of SARS-CoV-2. The S, E, M and N structural proteins are encoded in the 3′-terminal one-third of the genome [34]. **B:** SARS-CoV-2 reference genome which annotation from NCBI RefSeq. Retrieved https://www.ncbi.nlm.nih.gov/labs/data-hub/taxonomy/2697049/

1.1.3.3 SARS-CoV-2 protein characteristics

The foundation for understanding the pathogenesis of a virus is the study of the properties of viral proteins. The 3′-terminal part of the genome encodes structural proteins, which are made up of the four S, E, M, and N proteins [35]. The single positive stranded RNA (ribonucleic acid) that constitutes the viral genome and is encircled by the N protein serves as both the genome and the messenger RNA (mRNA).

On the coronavirus's surface, the S protein serves as a significant marker protein. Additionally, because glycosides are covalently bonded to one another to produce glycoproteins, it possesses a number of N-glycosylation sites [36]. The S protein is a transmembrane protein that has two subunits: the S1 at the N-terminus and the S2 at the C-terminus. While the S2 component resembles a handle and promotes fusion between the membranes of the virus and the host cell, the S1 subunit has a spherical shape and is in charge of binding to cell receptors [37].

The N-terminal domain (NTD), receptor binding domain (RBD), fusion peptide (FP), two heptad repeats (HR1/2), Central Helix (CH), intracellular domain (ID), transmembrane domain (TD), and S1/2 and S2′ sections make up the majority of the S protein's sequence [38].

The S protein trimer's three HR1 domains coil into a parallel trimer at its core, while the three HR2 domains that surround it are twisted into an antiparallel configuration. These two domains mostly interact through hydrophobic force. The deep hydrophobic grooves formed by each pair of neighboring HR1 helices serve as binding sites for the hydrophobic residues of the HR2 domain [39]. The amino acid sequence of Spike protein (GenBank: AAP41037.1) was found from the NCBI gene bank, and the PSIPRED function was used to estimate its secondary structure (Figure 3A).

In the HR1 domain's fusion core region, SARS-CoV-2 differs from SARS-CoV by 8 amino acid residues. According to crystallographic studies, this could enhance the interaction between HR1 and HR2. Additionally, it can aid in maintaining the 6-HB conformation of SARS-CoV-2, which could make SARS-CoV-2 more contagious [40]. The RBD directly interacts with ACE2 in the SARS-CoV-2 spike trimer, according to data from cryo-electron microscopy [41-42]. A carboxypeptidase with zinc called ACE2 serves as the major receptor for SARS-CoV-2 to enter host cells [43]. It is a type I transmembrane protein with 805 amino acid residues that is found on the surface of cell membranes. [44]. The SARS-CoV-2 RBD utilises ACE2 as the cell receptor, identically to the SARS-CoV RBD. Structural research revealed residues in the SARS-CoV-2 RBD that are crucial for ACE2 binding [45]. The majority of these residues either exhibit side-chain characteristics that are comparable to those seen in the SARS-CoV RBD or are substantially conserved.

Researchers may create protein models with various degrees of complexity using SWISS-MODEL. Models of the ACE-2 isoform 1 precursor protein and the SARS-CoV-2 spike protein were created using it (Figure 3B). In vitro binding studies have further shown that the SARS-CoV-2 RBD binds ACE2 with a high affinity, demonstrating that RBD is a crucial functional component of the S1 subunit involved in binding SARS-CoV-2 via ACE2 [46-47]. The conformational study of the S protein performed by electron microscopy revealed that the binding efficiency of ACE2 and the S protein of SARS-CoV-2 was significantly higher than that of the original SARS-CoV [48-49]. By carefully examining the virus's host receptor's binding site and efficiency, researchers can develop specific antiviral neutralizing antibodies and drugs.

A

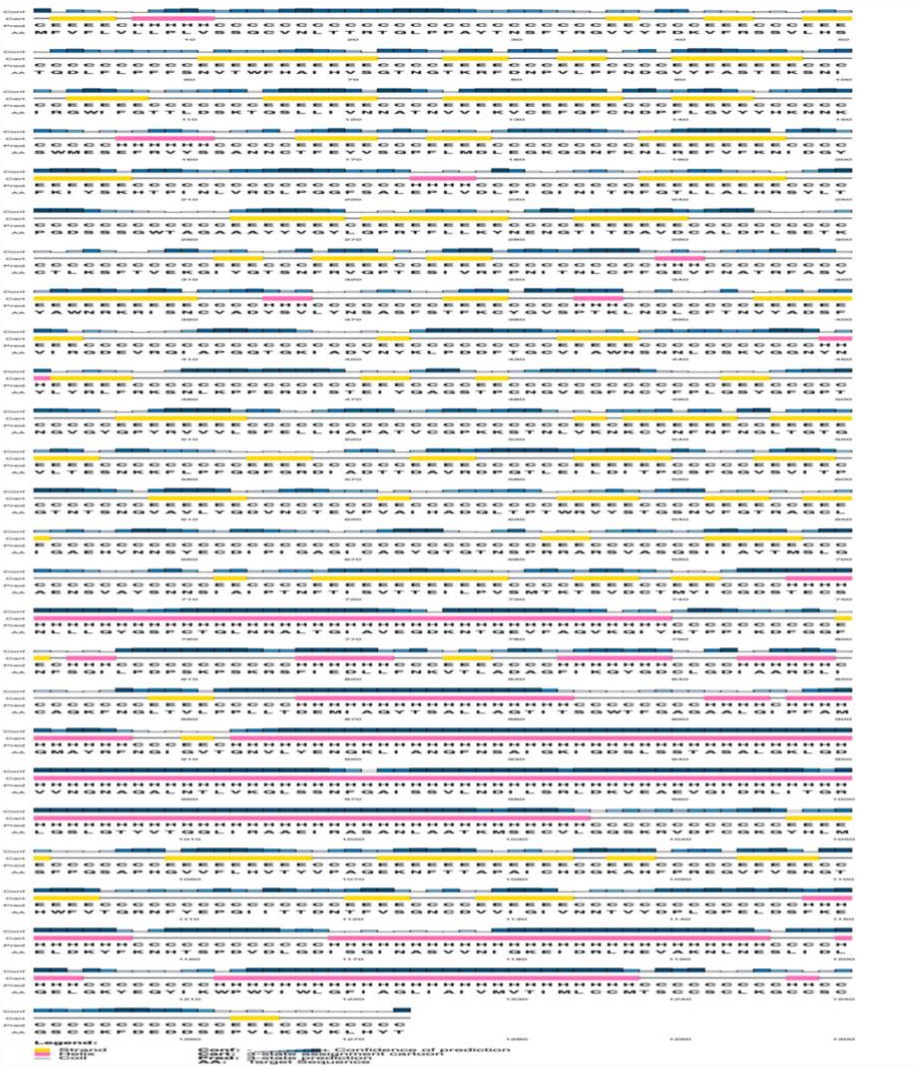

B

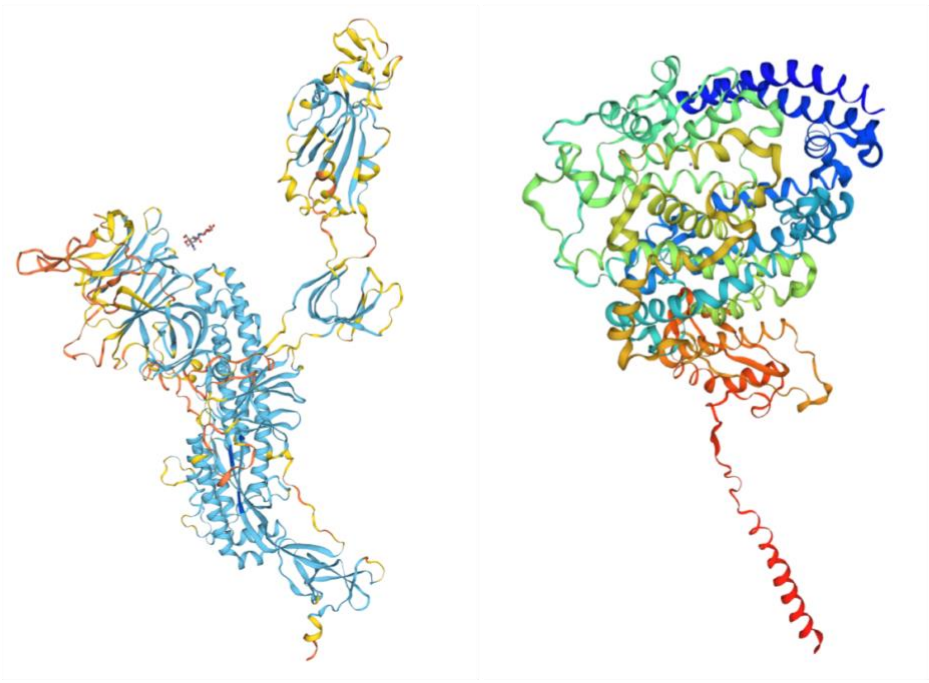

SARS-CoV-2 Spike protein

ACE-2 isoform 1 precursor

Figure 3: Overall structure of SARS-CoV-2 RBD bound to ACE2 [50]

Fig.3 | **A:** Protein secondary structure prediction of spike protein. Retrieved from http://bioinf.cs.ucl.ac.uk. **B:** The three-dimensional structures of the spike protein and the ACE-2 isoform1 precursor protein were predicted. and used QMEANDisCo to estimate the quality of the predicted protein tertiary structure. Scale 0-1, Spike protein score: 0.70 ± 0.05, ACE-2 isoform 1 precursor score: 0.83 ± 0.05, between 0.7 and 0.9, the results are confident. Retrieved from https://swissmodel.expasy.org.

1.1.4 Life cycle of SARS-CoV-2

The processes involved in a virus infecting a host cell include binding to the cell and entry; release of the viral genome, translation of the viral polymerase protein; replication of the viral genome and transcription of mRNAs; translation of the viral structural proteins; formation of the mature virion; and budding of freshly packaged virions. This procedure, which depends on host cell proteins, is essential for the virus' survival and pathogenicity [51].

SARS-CoV-2 infection begins by binding to a particular host cell receptor and entering by membrane fusion, endocytosis, or a combination of both as an obligate intracellular parasite envelope virus [52]. Endosomal cysteine protease cathepsins and the low pH in the cellular milieu may encourage membrane fusion and endosomal coronavirus cell invasion [53].

The primary determinant of viral pathogenicity, tissue tropism, and host range is the host receptor [54]. Similar to SARS-CoV, SARS-CoV-2 has been demonstrated to enter cells through the ACE2 receptor [55]. The ACE2 receptor on the host is particularly recognized by the S protein of SARS-CoV-2. S protein can be activated by membrane fusion, and rely on the host cell protease to cleave the S protein at the S1/S2 and S2 sites, which is an essential step for the virus to enter the cell. The S1 subunit binds to the receptor and viral membrane fusing with the host-cell membrane via S2 subunit. The S protein of SARS-CoV-2 possesses a Furin protease cleavage site, which is a mutation that other coronavirus β-genus do not have, in contrast to SARS-CoV and MERS-CoV [56]. According to previous studies, S1/S2 can be broken down by the cell protease Furin, and this cleavage is necessary for S proteins

to facilitate cell fusion and entrance into human lung cells. This discovery implies that SARS-CoV-2 transmission may be facilitated by genetic recombination in the S protein [57].

The transmembrane serine protease 2 (TMPRSS2) is a crucial mediator of S protein activation, assisting the virus to enter the host cell following contact. Membrane fusion is a multi-step process [58]. Respiratory epithelial cells contain ACE2 and TMPRSS2, which appears to be the major route for SARS-CoV-2 to enter the respiratory tissue [59]. SARS-CoV-2 can enter cells via the endocytic route as well. With the aid of cathepsin B/L, the virus that was bound to ACE-2 in the endosome is liberated from the endosome and into the cytoplasm [60].

After viral genomic RNA has entered the cell, it uses host ribosomes like RNA-dependent RNA polymerase (RdRP) to make its own mRNA, translate it into four structural proteins (S, E, M, and N), and then modify those proteins in the host cell's endoplasmic reticulum and Golgi complex. Finally, the structural proteins and genomic RNA are reassembled into fresh virus particles and discharged by exocytosis [61-62]. These freshly created viral particles have the capacity to infect nearby healthy cells, and after accumulation, they are also capable of being discharged into the environment through highly contagious respiratory droplets, possibly causing sickness to healthy individuals (Figure 4).

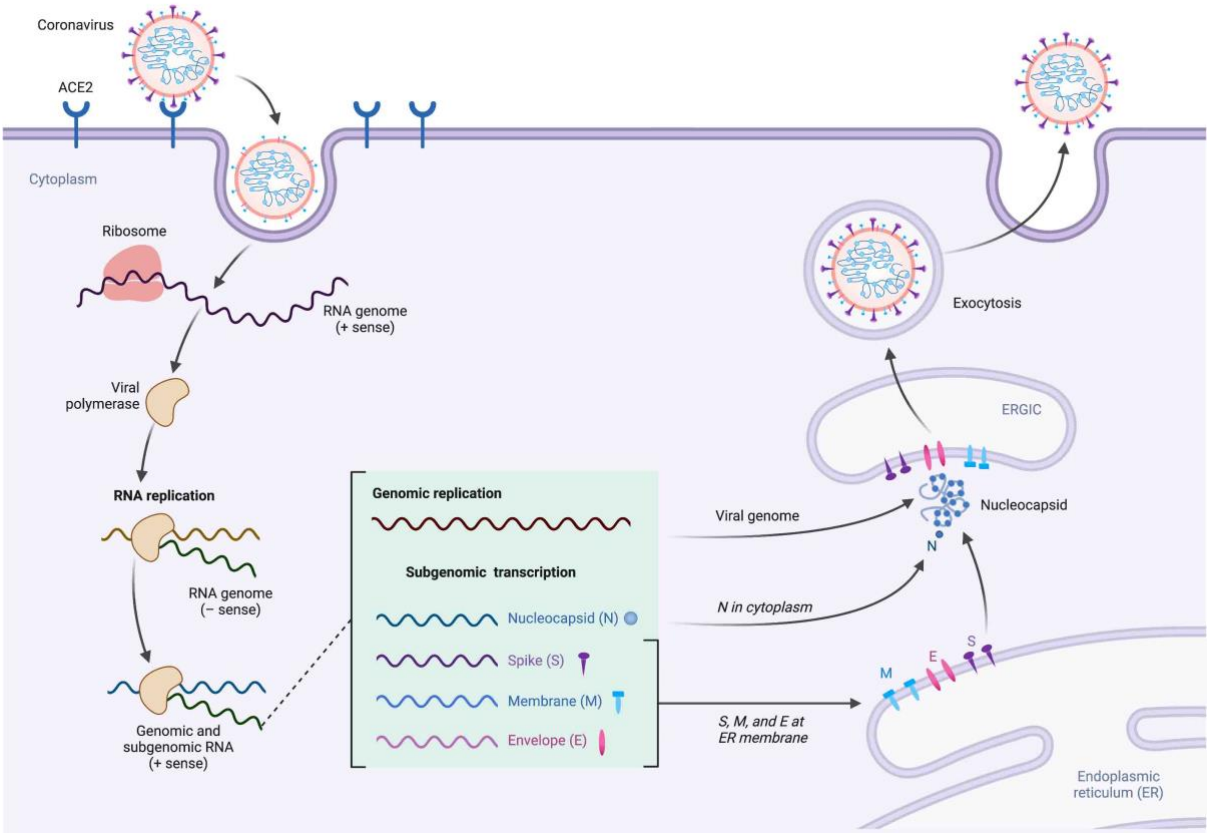

Figure 4: The life cycle of SARS-CoV-2 [63]

Fig.4 | There are nine major steps in coronavirus replication: step 1 is binding to the receptor on the host cell; step 2 is releasing the viral genome; steps 3–4 are the viral genomic RNA being replicated and translated into non-structural proteins; steps 5–7 are the translation of the viral structural proteins (S, E, and M); steps 8–9 are the assembly of the virus particles; and steps 9–10 are the mature virus being transported and released from the cell through the exocytosis pathway. This figure was adapted from "Life Cycle of Coronavirus", by BioRender.com (2022). Retrieved from https://app.biorender.com/biorender-templates.

1.1.5 Different variants of SARS-CoV-2

All creatures in the evolutionary process of life and viruses will continuously mutate in response to environmental changes. Viruses are no exception to the rule that living things that can adapt to their environment survive, while those that cannot are wiped out.

SARS-CoV-2 will evolve over time to adapt to environmental changes brought on by vaccines or human immune regulation. In particular, SARS-CoV-2, a single stranded RNA virus, is more likely to mutate than DNA virus, and the majority of the mutations are mild,

not significantly altering the characteristics of the virus. The human immune system will also carry out a continuous immune fight against the virus. However, a small number of mutant virus strains will gain special advantages that are helpful for adjusting to the environment, such as increasing the virus's ability to infect quickly and effectively, or escaping the host's immune system, rendering the antibodies produced by the current vaccine useless. It is even possible that increased virus virulence to the host results in an increase in the rate of hospitalization, serious illness, and mortality.

The Global Initiative on Sharing All Influenza Data (GISAID), Nextstrain, and Pang are the three key organizations that will continue to monitor and label the genetic mutation spectrum system of SARS-CoV-2 [64-65].

Each naming scheme has a distinct scientific foundation and significance that may be used by researchers to categorize various mutation types. For non-scientists, however, the same epidemic virus variation may occasionally go by several names, and there are too many SARS-CoV-2 variants, making them easily confused. As a result, people often do not know which variants are responsible for the current epidemic.

The SARS-CoV-2 epidemic in 2019 has caused the virus to grow quickly and extend globally. The World Health Organization (WHO) has created special variants that threaten global public health: variants of interest (VOIs), variants of concern (VOCs), and variants under monitoring (VUM). These variants are classified according to their level of hazard, and the variants that are already on the list are updated in real time with progress and changes.

The variations that are currently listed as VOCs are displayed in (Table 2). The creation of this system makes it will be possible to more effectively prevent the spread of the variants and introduce the necessary controls to control them globally, allowing for a better understanding of which variants are prevalent globally and how contagious and lethal they are in the countries where the epidemic is occurring.

Table 2 | The WHO designated variants of concern(VOCs) [66]

WHO label	Pango lineage	GISAID clade	Nextstrain clade	Earliest documented samples	Country of first detection	Date of designation

Alpha	B.1.1.7	GR/501Y.V1	20I/501Y.V1	Sept-2020	United Kingdom	18-Dec-2020
Beta	B.1.351	GH/501Y.V2	20H/501Y.V2	May-2020	South Africa	18-Dec-2020
Gamma	P.1	GR/501Y.V3	20J/501Y.V3	Nov-2020	Brazil	11-Jan-2021
Delta	B.1.617.2	G/452R.V3	21A, 21I, 21J	Oct-2020	India	11-May-2021
Omicron	B.1.1.529	GRA/484A	21K, 21L, 21M, 22A,22B,22C,22D	Nov-2021	Multiple countries	26-Nov-2021

There are five SARS-CoV-2 lineages identified as the VOC, including the Omicron variation, alpha, beta, gamma, and delta variants, as of November 26, 2021. They are more contagious than the original virus, have the ability to make the disease worse, and pose a greater threat to public health [67-68]. Alpha, beta, gamma, and delta versions were recorded in the UK, South Africa, Brazil, and India between May 2020 and November 2020 [69-72]. They mostly result in spike protein gene mutation, increasing the stability of spike protein and ACE2 binding or enhancing the binding affinity to human ACE2, raising the risk of infection [73-75].

Globally, the epidemic may be loosely split into three stages (waves) based on time, with the number of cases continuing to rise and COVID-19 continuing to pose a major threat to public health and safety (Figure 5).

The first wave of the epidemic occurred from December 2019 to September 2020, and the global Case Fatality Rate (CFR) was 3.12% (Table 3), with the original virus being the primary cause. Vaccines were not available, and the public was not be sufficiently aware of the virus due to their ignorance of its high fatality rate and rapid spread, and the corresponding precautions, such as isolation and mask use, were insufficient, leading to a large number of infected patients entering hospitals for treatment, while the available medical resources are relatively scarce and insufficient. This leads to a relatively high mortality rate in patients with underlying chronic diseases and the elderly (those over 65 years old) [76].

The second wave of the pandemic, which lasted from October 2020 to November 2021, is mostly brought on by many variations, including B.1.1.7 (Alpha), B.1.351 (Beta), P.1 (Gamma), and B.1.617.2 (Delta), with a CFR of 1.81% (Table 3), which is significantly lower than the CFR of the original virus. All nations have implemented travel bans and health promotion measures, and the overall vaccination rate has greatly increased [77].

The third wave of the epidemic is currently ongoing (December 2021 to July 2022) mainly due to the Omicron variant, which has many mutation sites in the spike protein gene, some of which are considered to enhance immune escape and have higher transfection, but the severe rate and mortality caused by it have decreased significantly, and the CFR is 0.38% (Table 3). The potential causes include: 1. A crucial part was played by the vaccination. According to studies, the hospitalization rate for those who received the full course of immunization (2 doses of the mRNA vaccine) and the booster population is dramatically lowered as compared to the unvaccinated population. 2. The toxicity of Omicron itself is weakened. According to clinical research, the majority of symptoms usually start in the throat and seldom spread to the lungs. This scenario also demonstrates how viral mutations may not result in pneumonia and significant mortality rates as before [78]. Furthermore, there is a concentration of virus replication in the throat, which makes it easier for the virus to transmit by breathing, saliva, and other methods. This clinical phenomena has a higher transmissibility.

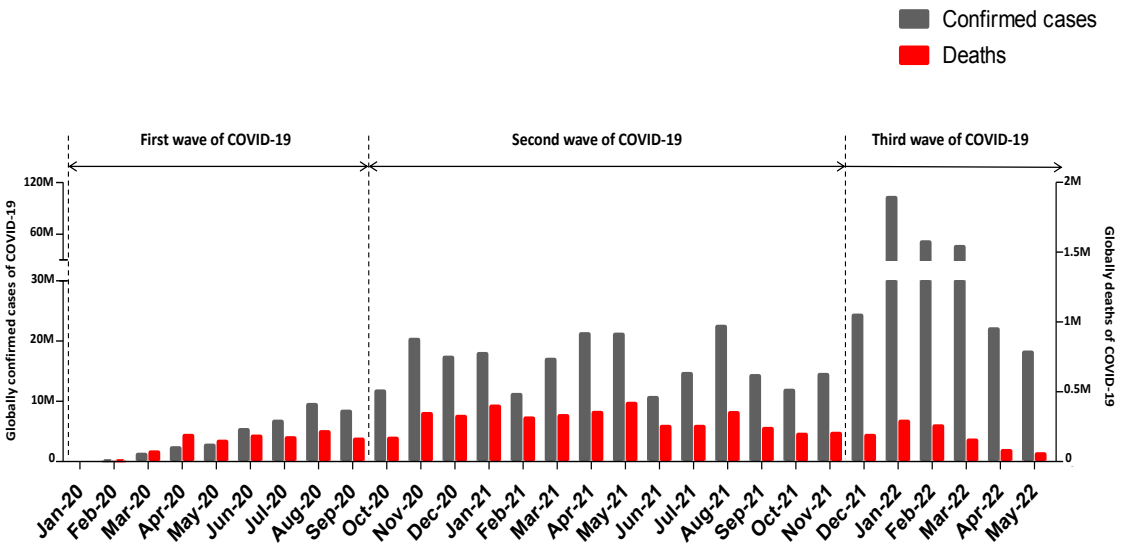

Figure 5: Pandemic diagnoses and deaths in 3 different stage.

Original data and continuously updated data can be found at https://covid19.who.int

Fig.5 | The vertical axis on the left represents the number of confirmed cases of COVID-19 in the world, and the vertical axis on the right represents the number of deaths from COVID-19 in the world, divided into 3 different time periods depending on the variant.

When we examine the Case Fatality Rate(CFR) brought on by SARS-CoV-2 at various stages worldwide and in important nations, we discover that the CFR is quite high at the early stage, especially in aging nations such as Italy, where the CFR has exceeded 11.14%. Italy has a population of 59.64 million people, with roughly 23.2% of whom are over 65. According to the Italian National Bureau of Statistics, the average age of Italians will rise from 45.7 to 50.7 years old between 2020 and 2050, and the percentage of individuals over 65 in the general population will rise from 23.2% to 35% [79].

The CFR caused by SARS-CoV-2 has considerably decreased over time in the latter stage, mainly as a result of Omicron, decreasing to 0.59% in the United States, 0.26% in Italy, and below 0.37% in China (Table 3). It may also be because the Omicron variant's own toxicity has decreased, medical resources have been completely employed, flight isolation and other epidemic prevention measures have been effective, and the main countries of the globe have undertaken widespread immunization and booster vaccination.

In China, where the vaccination rate for inactivated vaccines is above 85%, the number of individuals who have received vaccinations is high, but the infection rate is quite low, more information has to be acquired through scientific study and assessment, and more research focusing on case data is required.

Table 3. Case Fatality Rate(%) of SARS-CoV-2 variants in different countries and globally in different periods.

Stage	Period	Global	United States	Italy	China
First wave	**Dec-2019 to Sept-2020**	3.12	2.88	11.14	5.21
Second wave	**Oct-2020 to Nov-2021**	1.81	1.38	2.06	2.56
Third wave	**Dec-2021 to May-2022***	0.38	0.59	0.26	0.37

* Date collecting until May-2022, the pandemic still going. Data Source: https://covid19.who.int

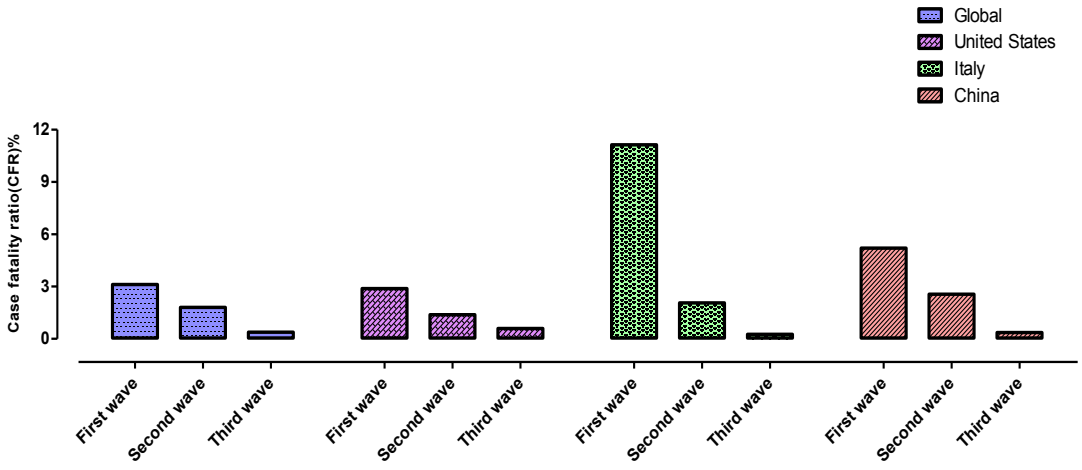

Figure 6: The CFR of COVID-19 by different stage group in major countries and global

Fig.6 | In China, the United States, Italy, and worldwide, the COVID-19 mortality rate has consistently declined over time.

1.2 Aging and Immunity of COVID-19

According to clinical research, COVID-19 and cancer are related. patients with underlying diseases with COVID-19 appear to have a worse prognosis and a higher probability of dying, and the virus itself can also cause a variety of cardiovascular disorders owing to irregularities in coagulation [80-81].

Epidemiological data show serious illness and mortality are highly common among the elderly and people with pre-existing diseases [82]. The tendency toward an increase in inflammatory macrophages with age may be the cause of the age-related rise in death rates of COVID-19. For instance, pro-inflammatory cytokines and chemokines such as TNF-α and IL-6 are overproduced by the immune system, causing numerous organ damage [83], especially in the geriatric population which has a weakened innate immune system [84].

Age-related declines in innate antiviral immunity may be caused by impaired activation of interferon regulatory factor 3/7 (IRF3/7) in Toll-like receptor (TLR) signaling due to decreased Sirtuin1 protein expression, which causes very low and delayed production of type I IFNs in elderly patients [85]. This may account for the higher frequency of chronic inflammatory conditions and the high prevalence of severe COVID-19 cases in the elderly.

Similar to this, it is understandable why SARS-CoV-2 infections had higher clinical morbidity of severe illness and increased death in those with underlying conditions.

1.2.1 Risk factors for severe illness

The risk of developing COVID-19 severe disease is influenced by a number of variables, such as age, ethnicity, genetics, immunization status, and other circumstances that increase the risk of developing severe disease [86]. The most significant risk factor for serious disease, complications, and mortality among them is age [87-92]. Clinical diagnosis and intensive care therapy of COVID-19 depend on an understanding of the underlying illness processes and hazards for various age groups.

Our study evaluates the association between COVID-19 mortality and different age groups in 4 typical nations of the globe, including China, the United States, Italy, and France, and finds that age has a significant impact on the risk of death from the disease. In China, Early data from China indicate that aging is associated with a rise in the case fatality rate (CFR) of COVID-19. Among those younger than 40 years, mortality was 0.2%; among those aged 40-49 years, 0.4%; among those aged 50-59 years, 1.3%; among those aged 60-69 years, 3.6%; among those aged 70-79 years, 8.0%; and among those aged 80 years and older, 14.8% [93]. In the United States, early epidemiologic data (as of March 16, 2020) was as follows: among those younger than 40 years, mortality was 0.15%; among those aged 40-49 years, 0.65%; among those aged 50-59 years, 2.0%; among those aged 60-69 years, 3.8%; among those aged 70-79 years, 7.4%; and among those aged 80 years and older, 18.85% [94]. In Italy, COVID-19 CFR data from Italy show a more profound impact of aging, likely due to the higher proportion of the elderly population in that country. Among those younger than 40 years, mortality was 0.2%; among those aged 40-49 years, 0.4%; among those aged 50-59 years, 1.0%; among those aged 60-69 years, 3.5%; among those aged 70-79 years, 12.8%; and among those aged 80 years and older, 20.2% [95]. In France, national epidemiological data (as of May 7, 2020) show a linear relationship between mortality rates and increasing age. Among those younger than 40 years, mortality was 0.01%; among those aged 40-49 years, 0.05%; among those aged 50-59 years, 0.2%; among those aged 60-69 years, 0.7%;

among those aged 70-79 years, 1.9%; and among those aged 80 years and older, 8.3% [96] (Table 4).

Regardless of the underlying illness prevalence, population base, genetic background, medical circumstances, etc. in China, the United States, Italy, or France, the mortality rate rises with age, especially beyond age 65, when the CFR increases dramatically (Figure 7). Aging is unquestionably a significant risk factor for severe COVID-19 illnesses and the case fatality rate.

Table 4. Case Fatality Rate(%) by Age Group in China, Italy, France and United States.

Age	China	Italy	France	United States
<40	0.20	0.20	0.01	0.15
40-49	0.40	0.40	0.05	0.65
50-59	1.30	1.00	0.20	2.00
60-69	3.60	3.50	0.70	3.80
70-79	8.00	12.80	1.90	7.40
80+	14.80	20.20	8.30	18.85

* Age group of China was not available for 1 patient. The Data of United States were taken by the median. All data comes from references [93-96].

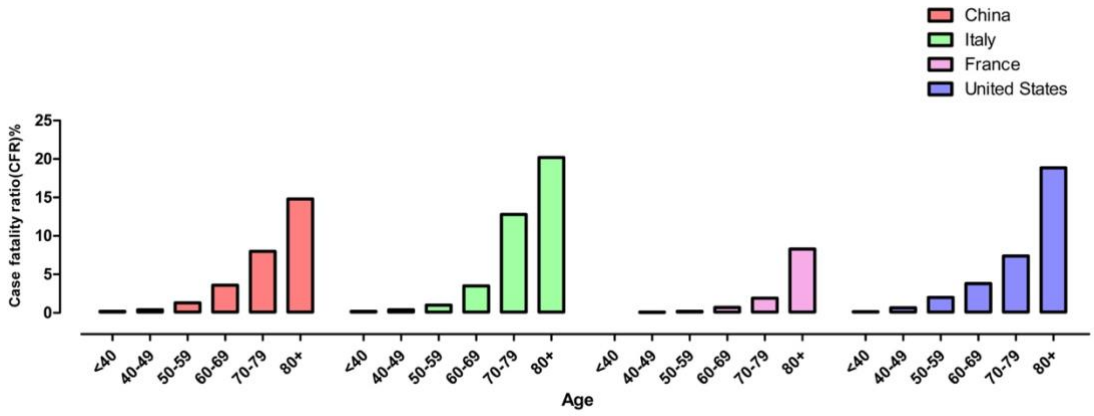

Figure 7: The case fatality ratio of COVID-19 by age group in major countries in the world

Fig.7 | China, the United States, Italy, and France all have mortality rates that increase with age, especially after age 65.

1.2.2 Immune system against pathogens

The host's antiviral immunity is crucial in the fight against viruses. Innate immunity, cellular immunity, humoral immunity, and other immunological mechanisms are all included. can successfully combat, control, and eradicate viral infection and bodily harm. The body's ability to adapt to its surroundings is a crucial assurance [97].

The innate immune system is the initial immune battleground of host defense against pathogens. Limiting viral invasion, translation, replication, and assembly; assisting in the detection and eradication of infected somatic cells; and promoting and coordinating the antiviral activity of adaptive immunity are all functions of the innate immune response [98].

Adaptive immunity triggers the inflammatory response; releases inflammatory factors that bind and encourage cell death following infection; and releases targeted antibodies to block the viral invasion site, stop virus invasion and reproduction, and encourage virus clearance. The virus will get more severe as a result of inaction and overactivation of the immune system, and it will use an appropriate mutation strategy to thwart the immune system's onslaught. Future pandemics can be avoided and their severity and mortality can be decreased by having a better knowledge of the molecular mechanisms underlying immunity and viral suppression.

1.2.2.1 Immune response to SARS-CoV-2

Before the SARS-CoV-2 vaccine was developed, the entire population was susceptible to the virus. No one's immune system was unable to identify the virus since SARS-CoV-2 was a novel coronavirus type. The virus is also very infectious, making it simple for the entire population to contract it. In the battle against viruses, both innate and adaptive immunity are crucial. A greater knowledge of the immune system may lead to better resistance to SARS-CoV-2.

The Th1 (T helper cell type 1) immune response is crucial for developing adaptive protection against viral infections. Antigen-presenting cells create a milieu of cytokines that controls how T cells react. Helper T cells regulate the adaptive response and are directly linked to the release of antibodies, whereas effector T cells are essential for eliminating virus-infected cells [99]. By restricting viral infection and avoiding future reinfection, humoral

adaptive immunity, in particular the development of neutralizing antibodies, may provide protection in the late stages of viral infection. Although the T-cell response in SARS-CoV-2 has been widely investigated, the mechanism of the immune response to SARS-CoV-2 after infection remains unclear. Coronavirus-infected macrophages then provide coronavirus-related antigens to T lymphocytes. T cell activation and differentiation result from this process, which is followed by a significant release of cytokines to intensify the immunological response. Directly destroying virus-infected cells can be ensured by CD8+T cells [100].

After activation of viral antigen presentation, the humoral response to SARS-CoV-2 is identical to the response to viral infection, with B cells generating antibodies to the N and S proteins [101]. The majority of individuals experience an antibody response 10 days following the start of their illness. Patient sera may be used to detect viral IgG antibody subtypes, and the multi-antibody sera of SARS-CoV-2 are directed against the full-length viral S protein as well as the RBD and N protein [102]. IgM and IgG antibodies generated by SARS-CoV-2 patients have been shown to have no cross-reactivity with other human coronaviruses. IgG was not found until 14 days after the onset of symptoms, whereas IgM and IgA antibodies were found 5 days after the onset of symptoms [103].

After infection, the majority of patients nearly always acquire antiviral humoral immunity. The original infection can cause a very effective adaptive immune response, which can produce immunological memory and provide a protective immune response to eradicate the virus [104]. By boosting immunity, certain conventional herbal treatments for COVID-19 patients may lower viral loads and mortality [105].

According to these findings, isolated high-efficiency monoclonal antibody sequences can be used to isolate particular viral targets for vaccine development and to analyze their epitopes.

1.2.2.2 Changes in immune cells after infection with SARS-CoV-2

Immune cells in the body go through a sequence of antiviral reactions after contracting SARS-CoV-2. While certain immune cells are stimulated to create antiviral substances,

others engage in a variety of immunological responses that either increase in number or are inhibited and diminished. The evolution of the patients' clinical symptoms is strongly correlated with the alterations in these immune cells.

Changes of macrophages and dendritic cells: While a decline in resident reparative alveolar macrophages was seen in the lung tissue of severe COVID-19 patients, a large number of inflammatory monocytes were found in the PBMCs of symptomatic COVID-19 patients. The development of acute respiratory distress syndrome (ARDS) may be facilitated by an increase in inflammatory-monocyte-derived macrophages and activation of IFN signaling [106]. Type I INF is blocked upon viral activation, and inflammatory macrophages produce large amounts of pro-inflammatory cytokines such IL-1, IL-12, and IFN-γ, which trigger pathogenic T-cell responses and encourage the release of downstream cytokine cascades, aggravating the condition [107]. Early research suggests that dendritic cells are involved in the pulmonary response to SARS-CoV-2 infection because their density is comparatively elevated in patient bronchial veolar lavage fluid [108].

However, myeloid and plasma cytoid dendritic cell subsets are frequently diminished in patients' blood and lungs. This shows that in the early phases of SARS-CoV-2 infection, poor dendritic cell activity resulted in lower interferon production and a drop in innate immune function [109]. Dendritic cells infected with SARS-CoV-2 in COVID-19 patients are immature and unable to directly deliver antigens to activate T lymphocytes. Further research is required to determine the precise function of dendritic cells in the pathophysiology of COVID-19.

Changes in NK cells: Innate immunity is strongly influenced by NK cells, and in the PBMCs of COVID-19 patients, a decline in NK cell numbers was revealed to be one of the key contributors to the severity and course of the illness. IgG antibodies produced after SARS-CoV-2 infection can either attach to antigens on the surface of infected cells to activate NK cells or kill the virus at the site of infection. ARDS may result from the process in which the activated NK cells produce perforin and granzymes and engage in antibody-dependent cell-mediated cytotoxicity, which lyses virus-infected cells [110].

In the peripheral blood of COVID-19 patients, higher levels of IL-6 and TNF have been found. In vitro NK cell production of perforin and granzyme B may be reduced as a result of IL-6 binding to its receptors, reducing the cytotoxic impact. The ability of TNF-α from monocytes to bind to receptors on NK cells and impair NK cell function raises the possibility that SARS-CoV-2 may negatively affect the development of effective acquired immunity by preventing NK cells from recognizing and eliminating infected cells through a variety of pathways in the early stages of infection [111].

Changes in T cells: After contracting SARS-CoV-2, macrophages get active and present virus-related antigens to T cells, which causes T cells to become activated and differentiate, producing a significant number of cytokines to boost the immune response, and CD8+ T cells may immediately clear virus-infected cells [112].

Most effector T cells undergo apoptosis following the removal of the virus and any accompanying antigens, and CD4+ memory T cells and CD8+ memory T cells are generated. After viral restimulation, CD4+ memory T cells produce cytokines that activate B cells and other immune cells, whereas CD8+ memory T cells contribute to fast growth after repeated infection and destroy infected cells [113-114].

The examination of many cohorts of COVID-19 clinical cases revealed that patients' helper T cells began to rise steadily on day 7; activated CD4+ T and CD8+ cells reached a peak on day 9 and then began to drop [115]. Another clinical trial on SARS-CoV revealed that from three months to six years, both CD4+ and CD8+ memory T cells successfully stimulated an immunological response [116]. This work reveals that certain populations may be targeted for quick viral clearance using efficient antigen vaccines that probe T-cell epitopes [117].

Changes in B cells:

Most patients experience an antibody response on or after day 10 of a viral infection. In the serum of patients, viral antibody subtypes of IgG and IgM can be found. Most patients can likely acquire close to antiviral humoral immunity following infection because the SARS-CoV-2 multi-antibody serum specifically targets the whole S protein, RBD, and N

proteins of the virus [118]. Additionally, studies on animals have demonstrated that the antibodies and memory B cells created following SARS-CoV-2 infection can provide immunological defense [119]. Although it should be used under strict supervision, the clinical use of convalescent plasma as a source of polyclonal antibodies for therapy can lower patient mortality and respiratory virus load [120].

This strategy will make it possible to treat SARS-CoV-2 with neutralizing antibodies. Antigen epitope analysis using isolated high-efficiency monoclonal antibody sequences may aid researchers in identifying particular viral targets that might make good vaccine candidates.

1.3 The pathogenic mechanism of SARS-CoV-2

While the majority of SARS-CoV-2 patients generally have minor symptoms, a tiny percentage of individuals experience serious lung damage or even multiple organ failure. SARS-CoV-2-related deaths can be caused by a variety of variables, including age and underlying chronic diseases. Cytokine storm, evading innate immunity, and other mechanisms are the key variables.

1.3.1 Pro-inflammatory cytokine storm

Studies on pathogenic human coronaviruses that cause the Middle East respiratory syndrome and severe acute respiratory syndrome have demonstrated that viral replication achieves a high titer in the early stages of infection [121-122]. The virus can cause the necrosis of infected cells and produce a significant number of cytokines, such as interferons, interleukins, chemokines, colony stimulating factors, tumor necrosis factors, etc. as a result of its fast and widespread replication in the body [123-125].

The production of these cytokines disrupts the body's normal cytokine balance, especially when pro-inflammatory substances are released. This finally results in a cytokine storm, which is one of the major reasons people die. Early clinical sample showed that individuals with COVID-19 had considerably higher expression levels of inflammatory markers such as TNF-α, IL-6, G-SCF, IL-10, and MCP1. Through the activation of the

pattern recognition receptor (PRR), macrophages and dendritic cells all produce cytokines to some extent [126].

Type I interferon production is blocked by viral proteins in the early stages of SARS-CoV-2 infection, and its postponed release causes an influx of pro-inflammatory neutrophils and monocyte-derived macrophages. These cytokines' expression can encourage the in vivo expression of ACE2, continually increase the synthesis of significant amounts of inflammatory substances, and also encourage viral infection. Type I interferon autoantibodies are more prevalent in severe COVID-19 patients than in moderate patients or healthy people. Early inhibition of type I interferon function may increase viral replication, attract more inflammatory factors, and activate the immune system excessively, aggravating the illness brought on by SARS-CoV-2 infection and resulting in pulmonary immunopathologic symptoms such as pneumonia or acute respiratory distress syndrome [127-128].

Early in the course of viral infection, it may be possible to control immune imbalance and stop the death of critically ill patients by suppressing excessive immune responses through the administration of antiviral medications to stop viral replication, and the use of IFN injections to activate the type I IFN pathway. Moreover, at various phases of symptom onset, patients show a drop in the overall number of T cells, this decline reaches a critical level and is inversely connected with patient survival. Additionally, there was a negative correlation between the patients' blood levels of IL-6, IL-10, and TNF-a and the total number of T cells. Serum cytokine levels declined along with the patient's recovery, and the T-cell count progressively reverted to normal [129]. ICU patients also had a higher expression of cytokines in their plasma, as well as a higher total number of neutrophils and a lower total number of lymphocytes in their blood [130].

As it invades the human lung, SARS-CoV-2 releases cytokines, stimulates adaptive T- and B-cell immune responses; and mobilizes macrophages and monocytes to fight the infection. The patient produces a pro-inflammatory cytokine storm that immunologically damages the body and then leads to lesions in other organs such as the liver and lung, which worsens the development of the disease. Sustained high pro-inflammatory response and T-

cell exhaustion, which results in a decrease in lymphocytes, an increase in neutrophil granulocytes, and high expression of pro-inflammatory cytokines [131].

1.3.2 SARS-CoV-2 evades innate immunity

The antiviral innate immune response is extremely important during the first infection of the host with SARS-CoV-2, particularly in triggering the production of type I interferon (mostly IFN-α/β) and type III interferon (IFN-λ). The adaptive immunity phase occurs when type II interferon (IFN-γ) begins to perform its primary role. Type I interferon is released externally once it is created. It has antiviral effects by binding to the type I interferon receptor on the cell surface, which causes the phosphorylation and activation of downstream signal transduction and transcriptional activator proteins, resulting in the synthesis of several pro-inflammatory molecules [132]. A positive cycle is created by innate immunity, which also stimulates and activates innate immune cells including macrophages and dendritic cells during the release of cytokines [133], but according to clinical investigations, people who have a severe SARS-CoV-2 infection only have a small level of type I interferon in their serum [134]. indicating that SARS-CoV-2 may have a unique method to prevent the generation of IFNs by hosts and avoid their innate defenses.

By thwarting the recognition of PRRs recognition by downregulating MHC-II molecules in infected macrophages or dendritic cells, SARS-CoV-2 avoids detection by the innate immune system which can result in reduced antigen presentation and diminished T-cell activation. The virus-encoded protein may attach to the transcriptional signal downstream of PRRs, limit the release of antiviral cytokine cascades, or they may impede the binding and signaling of type I interferon [135]. The single-stranded RNA of SARS-CoV-2 virus forms a double-stranded intermediate during replication that can be recognized by TLR3 within the package [136].

Inside, the RNA is detected by TLR7/TLR8, which in turn activates PRR and starts the TLR signaling cascade response, encouraging the production of pro-inflammatory cytokines and IFNs as well as activation of NF-B signaling. To help SARS-CoV-2 escape from the

innate immune system, however, may be due to antagonistic interactions between the viral or nonstructural proteins of SARS-CoV-2 and the PRRs signaling cascade.

Studies have demonstrated that SARS-CoV-2 ORF9b and non-structural proteins NSP13, NPS15, etc. can interact with signal transducers or signaling intermediates to activate the host innate immune response and block the activation of downstream signaling pathways. The host's nonspecific antiviral defensive activities are restricted due to the inhibition of cytokine synthesis [137].

IFNs serve a protective function in the early stages of the illness and may aggravate pathogenicity in the later stages due to dysregulation of the IFNs response, which is a major factor in the pathogenicity of COVID-19. SARS-CoV-2 can promote pathological inflammatory responses while inhibiting IFN signaling and activating other inflammatory pathways. Additionally, research has shown that SARS-CoV-2 may prevent the production of interferon both in vitro and in vivo achieve the goal of immune evasion. Patients with severe pneumonia produce much less IFN-γ than those with mild or moderate COVID-19 [138].

Furthermore, innate immunity against SARS-CoV-2 infection depends heavily on NK cells. NK cells have the ability to destroy and degrade virus-infected cells by releasing CD107a, granzyme B, and granulysin. Patients with COVID-19 had considerably lower levels of CD16 and KIR expression on their NK cells in their peripheral blood [139]. The growth of NK cells requires CD16 and KIR, which reduces their capacity to kill and their capacity to produce chemokines, thus allowing SARS-CoV-2 to evade the innate immune system.

1.4 The signaling pathway activated by SARS-CoV-2

Numerous signaling pathways are involved in controlling the production of inflammatory factors during SARS-CoV-2 host infection. These signaling pathways are crucial for the activating the immune system, preventing viral multiplication, and eliminating infected cells.

1.4.1. Major signaling pathway

Innate immunity can recognize PRRs of PAMPs (Pathogen-associated Molecular Patterns) of various pathogens by immune cells such as macrophages, monocytes, dendritic cells, neutrophils, and natural killer (NK) cells, etc. to trigger inflammatory signaling pathways and immune responses. This recognition is dependent on the genomic nucleic acid characteristics and replication strategies of pathogens. The TLRs: the retinoic acid-inducible gene I (RIG-I)-like receptors (RLRs): the nucleotide-binding oligomerization domains (NLRs); the C-type lectin receptors; and the receptors absent in melanoma 2 (AIM2)-like receptors are the major families of immune signaling pathways [140]. In the invasion of SARS-CoV-2, the activated TLR signaling pathway is crucial for the generation of inflammatory mediators and chemokines that cause infected cells to die and be eliminated. When immune cells recognize viral invasion, PPRs on their surface activate TLRs 3, 7, and 8, which leads to the production of interferons (IFNs) [141-142], and SARS-CoV-2 invasion can lead to IFN production and cytokines overexpressed, causes severe inflammatory response.

1.4.2 The function of Toll-like receptors signaling pathway

TLRs are members of the PRR family, which are produced in the endoplasmic reticulum and then transduced to the endosome or extramembrane to recognize molecules associated with various pathogens such as bacteria, viruses, and parasites, Pathogen-associated molecular patterns (PAMPs) trigger adaptive immune responses that suppress and eradicate invading pathogens by regulating cytokine production and activating innate immune responses [143].

1.4.2.1 Toll-like receptor family

TLRs play a crucial role in inducing the innate immune response to many infections. They cause the innate immune system's antiviral response by inducing the production of type I and type II interferons, pro-inflammatory cytokines, and other molecules. TLRs activate signaling pathways primarily by downstream linkage of the myeloid differentiation primary response 88 (MyD88) and the TIR domain containing adaptor-inducing interferon-β (TRIF),

promote activation of nuclear factor-κB (NF-κB), and induce type I expression of interferons and immunological inflammatory factors [144].

1.4.2.2 The function of TLRs

TLRs share a common structure that is separated into intracellular, transmembrane, and extracellular domains. They are all type I transmembrane proteins. In addition to TLR3, which is triggered by TRIF binding, TLR4 may also start a downstream signaling pathway via MyD88 or TRIF, and additional TLRs activate downstream signaling pathways via MyD88 after the TLR pathway has been started [145].

While other TLRs recruit IRAK4 via MyD88, IRAK1 binds TRAF6 and creates TAK1 complexes. TLR3 and TLR4 attract TRAF3, TRAF6, and RIP1 to form a complex, activate the downstream IKK complex, start NF-κB signaling downstream of IRF3, and promote type 1 interferon production. It stimulates the production of pro-inflammatory cytokines such IL-6, IL-12, TNF-α, IFN-α and activates the mitogen-activated protein kinase (MAPK) signaling and NF-κB signaling pathways (Figure 8). They eventually trigger the host's natural immunological defense against infections.

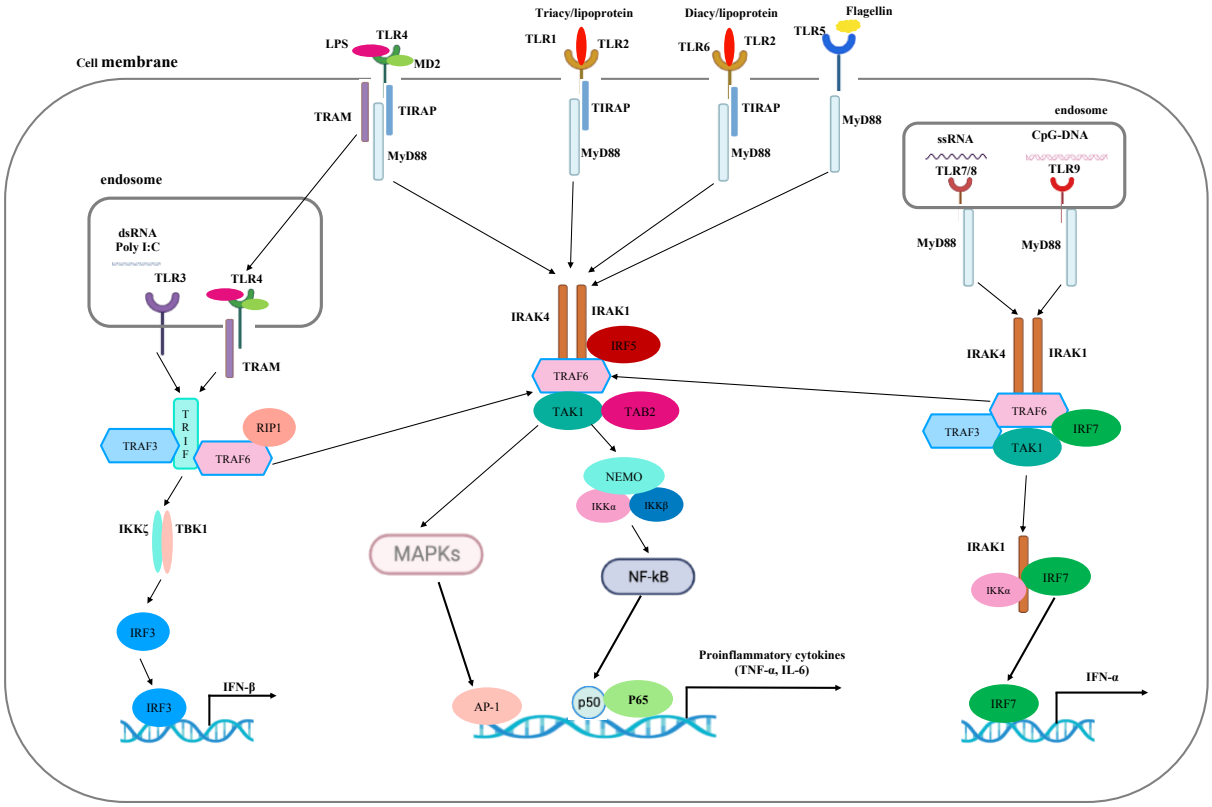

Figure 8: The overview of TLR signal pathway

Fig.8 | Different TLRs trigger the production of type I interferons or inflammatory factors by activating a variety of downstream signaling pathways, including the NF-κB and MAPK signaling pathways via MyD88 or TRIF [146]. This figure was adapted from "Yang L, Seki E. Toll-like receptors in liver fibrosis: cellular crosstalk and mechanisms. *Front Physiol*. 2012;3:138.

TLRs found in the human genome are TLR1 to TLR10 making up the TLR family [147]. TLR signaling is mostly activated on immune system cells such macrophages, monocytes, dendritic cells, and B cells, as well as on cell surfaces. TLRs primarily recognize PAMPs such lipids and lipoproteins [148].

TLR2 and TLR1 or TLR6 may combine to generate a complex. After recognizing PAMPs such as lipoproteins, lipopeptides, peptidoglycans, etc., the complex activates their cascade response with downstream MyD88, which causes activation of the NF-κB pathway. TLR4 mainly recognizes bacterial lipopolysaccharide, which ultimately activates the expression of inflammatory factors such as type I interferons and IL-6 [149]. TLR5 Can sense and recognize some special bacterial flagellins [150]. In B cells, TLR10 is mostly expressed; it is the only member of the TLR family that is known to have both pro- and anti-inflammatory properties [151].

Intracellular TLRs can detect nucleic acids from some autoimmune illnesses as well as nucleic acids from infections such as viruses and bacteria [152]. To activate IRF3 and cause the generation of type I and type III IFNs, TLR3 primarily identifies double-stranded RNA (dsRNA) and single-stranded RNA (ssRNA) viruses [153]. Monocytes or DCs are the major cell types that express TLR7 and TLR8. TLR7/8 can activate CD8+ T cells and initiate an immunological response in addition to recognizing ssRNA and promoting the development of type I IFNs through the MyD88 pathway [154-155]. By detecting PAMPs, TLR-9 can activate plasmacytoid dendritic cells (pDCs) to create strong antiviral activity. and is crucial in the transformation of innate immunity into adaptive immunity [156].

1.4.2.3 The function of TLRs with SARS-CoV-2

The TLR system is a crucial immunological signaling route for host defense against a variety of infections and is also crucial for SARS-CoV-2 resistance. The TLR family is capable of identifying different PAMPs, including viral proteins and RNAs, and activating

innate immune responses. By attaching to ACE-2 through the S protein, SARS-CoV-2 mostly merges with the surface of the host cell. The virus attaches to the cell surface concurrently. TLR2 is mostly found on the cell membrane surface of macrophages, monocytes, and lung epithelial cells. It identifies the S protein as the virus' PAMP and then heterodimers with TLR1 or TLR6 to trigger NF-κB and MAPK signaling through MyD88 signaling and leading to production of proinflammatory cytokines [157].

Further research has revealed that TLR2 is also capable of recognizing E and N proteins, initiating downstream signaling pathways, and releasing inflammatory factors that are crucial for the activation of the innate immune system, indicating that the severity of COVID-19 illness substantially correlates with the degree of TLR2 expression [158]. TLR4, a different TLR present on the cell membrane, was discovered to have a highly potent affinity for the S protein of SARS-CoV-2 [159]. TLR4 could therefore be able to detect SARS-CoV-2 directly. Studies conducted in vitro have demonstrated that TLR4/TLR2 may identify S1 of the S protein as a PAMP, activating the MyD88-dependent signaling pathway and increasing the production of pro-inflammatory cytokines [160]. In a MyD88-dependent way, S protein may also activate TLR4 to cause the generation of IL1B in a murine macrophage cell line (Raw 264.7) [161]. These studies show that TLR2 and TLR4 may identify the SARS-CoV-2 PAMP via the TLR signaling route, activating the downstream signaling pathway, resulting in the production of inflammatory factors, and activating the innate immune system's antiviral activity.

When SARS-CoV-2 infects a host, it produces single-stranded RNA (ssRNA), which is then replicated into double-stranded RNA (dsRNA) and translated into proteins in the cytoplasm. While ssRNAs are recognized by TLR7/8, these dsRNAs are likely identified by TLR3, a member of the TLR family. TLR3 signaling is dependent on the TRIF adaptor protein but not the MyD88 adaptor protein, and TLR3 and TLR7 detect SARS-CoV-2 RNA. Whereas TLR7 primarily stimulates the NF-κB transduction pathway and promotes the release of type I interferons, which are important in the control of innate immunity, it causes the activation of IRF3 and the release of cytokines [162]. In addition, another study reported

that young adults with severe COVID-19 disease were more likely to have mutations in the TLR7 gene [163].

In sum, TLR signaling is crucial for antiviral immunity during SARS-CoV-2 infection, and several TLRs each conduct immunological identification and innate immune response activation, which often contributes to viral eradication and illness remission.

1.5 Targeted drugs for COVID-19 treatment

Clinical treatments for COVID-19 primarily target broad-spectrum viruses, polymerase inhibitors, S-protein neutralizers, targeted drugs to control signaling pathways, immunomodulators, etc., blocking the virus's ability to bind to the host receptor and preventing the virus from replicating, or inducing an antiviral immune response to control or eradicate the virus. The U.S. Food and Drug Administration has authorized the emergency use of additional pharmaceuticals as well as two medications for the treatment of COVID-19. Veklury (remdesivir), an antiviral medication, is available for use in adults and certain pediatric COVID-19 patients, while Olumiant (baricitinib), an immune modulator, is available for use in some COVID-19 hospitalized adults [164].

SARS-CoV-2 replicates and copies its RNA through RdRp after entering host cells, and medications that target RdRp can prevent viral RNA replication. Remdesivir is an adenosine analog that can be incorporated into newly produced viral RNA and has inhibitory effect on RdRp. This inhibits viral RNA-dependent RNA polymerase activity and stops continuing transcription. It demonstrates antiviral action against a number of viruses, including coronavirus infections that have caused epidemics in the past, such as SARS-CoV-1, MERS-CoV, Nipah virus, and Ebola virus [165-168].

The median recovery time for adult COVID-19 patients treated with remdesivir was dramatically shortened (from 15 days to 10 days) compared to the placebo group, according to preliminary findings of a double-blind clinical trial. Additionally, it was shown that patients who received treatment with remdesivir had a higher likelihood of having reduced mortality than those who received placebo at days 15 and 29 after therapy (6.7% vs. 11.9% and 11.4% vs. 15.2%, respectively) [169]. Other RdRp inhibitors that prevent SARS-CoV-2

replication include molnupiravir and favipiravir. A study revealed that participants who treated with molnupiravir needed fewer respiratory interventions than those who took a placebo, resulting in a relative risk reduction of 34.3%. It also revealed that hospitalized participants who received treatment with molnupiravir were released from the hospital on average three days sooner than those who took a placebo [170].

Another trial examined the effectiveness of the lopinavir and ritonavir combination with the favipiravir group in treating COVID-19. In contrast to the control group's average viral clearance time of 11 days, the favipiravir treatment group's average viral clearance time was only 4 days, according to the data ($P < 0.001$). Additionally, the improvement rate of the chest CT was substantially ($P = 0.004$) higher in the favipiravir treatment group (91.43%) than in the control group (62.22%) [171].

Baricitinib (in combination with remdesivir) acts as an inhibitor of janus kinase (JAK), blocking the subtypes JAK1 and JAK2 [172]. Based on the clinical research, after 28 days, the death rate in the combination group was 9.091% compared to 14.29% in the remdesivir group for patients who got either remdesivir alone or remdesivir plus baricitinib concurrently, suggesting that using baricitinib and remdesivir together has a benefit in lowering mortality in people with moderate-to-severe cancer. COVID-19 [173]. Paxlovid is a protease inhibitor and functions by preventing the enzymes required for coronavirus replication. Ritonavir frequently has to be used with paxlovid since it makes protease inhibitors more effective. According to clinical research, paxlovid, an oral antiviral medication, considerably lowers hospitalization and death in COVID-19 patients who are critically sick compared with placebo (89% decrease in risk rate), when taken within three days after the beginning of symptoms [174].

SARS-CoV-2 attachment to the host is dependent on the ACE-2 cell surface receptor. By creating various monoclonal antibodies or monoclonal antibody combinations, one can limit viral invasion by interfering with the S protein's ability to connect to ACE-2 and preventing the virus from attaching to the host receptor. The S, S1-RBD, S1-NTD, or the S2 region can be specifically targeted by virus-neutralizing antibodies that have received EUA or that have

undergone clinical trials. Examples include Sotrovimab, Regdanvimab, and the monoclonal antibody cocktails Bamlanivimab+Etesevirmab, Tixagevimab+Cilgavimab, and Casirivimab+Imdevim.

In high-risk individuals with mild-to-moderate COVID-19 disease, sotrovimab decreased the risk of hospitalization and mortality by 85% when compared to placebo [175]. Regdanvimab significantly reduced the risk of progression to severe illness as compared to supportive therapy (9.6% vs. 2.1%, P <0.001) in moderate COVID-19 patients [176]. Bamlanivimab+Etesevirmab expedited the fall in SARS-CoV-2 viral load while reducing the related risk of hospitalization and mortality in high-risk ambulatory individuals by 70% when compared to placebo [177].

Studies using Tixagevimab+Cilgavimab have shown that it has the ability to reduce the rate of infection and severe illness in immunocompromised patients [178]. Clinical use of Casirivimab+Imdevimab was found to reduce hospitalization rates in high-risk patients [179]. With the great majority of these clinical studies including more than 1,000 individuals, it has been clinically demonstrated that each of these neutralizing antibodies plays a significant role in the treatment of COVID-19 patients. The majority of neutralizing antibodies significantly lower viral load, infection rates, hospitalizations, and death.

Tocilizumab (anti-IL-6 receptor mAb) and anti-GM-CSF mAbs offer immunomodulatory techniques in addition to functional medications based on small molecules and antibodies that prevent viral replication and binding of the viral S protein to the host. The host's innate immune system produces more type I interferons and other cytokines when it comes into contact with pathogens such as viruses. Overactivation of the immune system during acute and ongoing infections can also result in the emergence of a pro-inflammatory milieu, which can have detrimental effects, including fatal ones [180]. Increases in inflammatory cytokines such IL-6, IFNs, and granulocyte-monocyte stimulating factor(GM-CSF) are common in critically sick individuals. Clinical improvement might result from immunomodulation's suppression of this hyperinflammation [181].

Studies on the use of mesenchymal stromal cells (MSCs) in injectable treatment to treat COVID-19 are also available. Remestemcel-L, an allogeneic MSC product, was employed in the trial on patients with moderate-to-severe COVID-19 because MSCs exhibit anti-inflammatory capabilities. Results at day 28 indicated that all patients had a good tolerance for Remestemcel-L infusion and had better clinical results [182].

Despite these drugs being FDA-approved and EUA-authorized for the treatment of COVID-19, including small molecules, antibodies, cellular immunotherapies, and other therapies, many of these drugs have restricted therapeutic indications, and the majority of severe disease cases globally continue to be nonspecific. This, combined with their pricing models and location-specific medical conditions, results in a limited number of specific treatment options. The future development of particular COVID-19 medicines that might be helpful for treating outbreaks of novel COVID-19 mutations may be aided by increasing our knowledge of the genetic, immunological, and molecular pathways causing enhanced pathogenicity.

2. Objectives

Although the intensity of the illness and the fatality rate have greatly dropped since the COVID-19 pandemic, the infectivity and rate of transmission have grown, posing a major threat to human life and health, particularly for the frail senior population (> 65 years).

SARS-CoV-2 is effectively fought off by the immune system in both immunized and unimmunized people. The first line of defense against infections is made up of innate immune system cells including neutrophils, dendritic cells, and macrophages. When it comes to preventing viral invasion, translation, and replication, the innate immune system is crucial. While presenting antigens to activate the adaptive immune system, produce cytokines and inflammatory substances, and infiltrate the immune system, macrophages may identify and destroy contaminated host cells. The cycle of positivity fights viral infection and gets rid of contaminated cells. According to earlier research, severe COVID-19 patients in clinics had high levels of cytokines and chemokines including IL-6, TNF-α, CXCL1, CXCL10, etc. The

high expression of these cytokines often causes cytokine storms, leading to severe pneumonia and even endangering patients' lives, but excessive or insufficient immune responses are also fatal to patients. Among these immune responses, the innate immune system is very important for fighting COVID-19, but we still do not know the specific mechanism of how the innate immune response is activated after SARS-CoV-2 invasion, especially the mechanism of the innate antiviral immune system in the elderly, and which key cytokines or innate immune cells are more sensitive and preferential for fighting SARS-CoV-2.

Hypothesis: dysregulated innate immune pathways leads to poor outcome in patients infected with SARS-CoV-2. The innate immune system of the elderly is relatively fragile, and SARS-CoV-2 can regulate the expression of type I interferon through the TLR signaling pathway and directly mediate the release of cytokines. In the elderly population with SARS-CoV-2 infection, the expression of type I interferon may be inhibited in the early stage, while other cytokines, such as IL-6, IFN-γ, etc. are overexpressed, triggering cytokines in the late stage of virus infection.

Objectives: 1. Perform cell experiments to identify whether Spike protein stimulates innate immune pathways in PBMCs, and to identify the key immune genes and signaling pathways affected by Spike protein. In vitro investigations using cells that carried the packed VSV-Spike protein in certain peripheral blood mononuclear cells (PBMCs) under LPS stimulation were able to produce green fluorescent protein, demonstrating that the VSV spike protein may enter and interact with some PBMCs.

Studies have shown that ACE-2 can be expressed in proinflammatory macrophages. In addition, we analyzed the cell subsets expressing the Spike protein by flow cytometry and found that LPS can mainly stimulate macrophages and dendritic cells to bind to spike. This is closely related to innate immunity to viruses. previous studies also suggest that innate immunity may inhibit SARS-CoV-2 invasion and replication by controlling the expression of inflammatory factors via the TLR signaling pathway. Although it is unclear, we hypothesize that the TLR signaling pathway plays a crucial role in innate immunity, helping to control the production of inflammatory substances in the body and thwart viral invasion. In the elderly

population, innate immunity is weak and macrophage function is compromised. It is very likely that SARS-CoV-2 spreads quickly in the initial phase of viral replication because of the impaired macrophage function in the elderly population. As a result, the disease of pneumonia progresses more quickly in this age group, with a higher rate of severe illness and mortality.

Objectives: 2. Compare the COVID-19 patient group with healthy controls to identify the innate immune signaling pathways and genes regulated by SARS-CoV-2 infection. To clarify whether SARS-CoV-2 can affect the antiviral process by binding and activating innate immune cells such as macrophages DC, thereby mediating TLR signaling, we used high-throughput sequencing technology to performed cell experiments and samples from elderly patients were sequenced compared with volunteer groups. The TLR signaling pathway's downstream cytokines were all elevated and somewhat implicated in the antiviral process, according to the multi-cytokine detection approach.

Objectives: 3. Analyze the TLR signaling pathway to identify whether SARS-CoV-2 affects the TLR signaling pathway in elderly patients, and through which genes they regulate delayed type I interferon response, resulting in uncontrolled cytokine release. The innate immune molecular mechanism resistance to SARS-CoV-2 was first identified in this study by establishing the VSV-Spike virus expression vector, analyzing the signaling pathway and response mechanism of key genes on innate immunity and antivirus by RNA sequencing, and detecting the expression changes of downstream proteins of TLR by multicytokines. The possibility is suggested that SARS-CoV-2 has a high severity and mortality rate in the elderly population. This offers concepts for future immunologically-based vaccine development, which has significant theoretical and practical implications. Our research also demonstrates that the TLR signaling pathway is essential for patients who are old or critically ill, and future therapy development may focus on blocking these signaling pathways.

3. Materials and methods

3.1 Materials

3.1.1 Marjor reagent

No.	Name	Catalog number	Company
1	CD45	304012	Biolegend
2	CD3	317324	Biolegend
3	CD56	318332	Biolegend
4	CD16	302016	Biolegend
5	CD19	302234	Biolegend
6	CD11b	301306	Biolegend
7	CD14	367110	Biolegend
8	CD4	344634	Biolegend
9	CD8	344714	Biolegend
10	CD27	356412	Biolegend
11	CD45RO	304206	Biolegend
12	CD45RA	304130	Biolegend
13	CD25	302610	Biolegend
14	CD279	329920	Biolegend
15	CD163	333622	Biolegend
16	HLA-DR	307650	Biolegend
17	CD80	305222	Biolegend
18	CD86	374210	Biolegend
19	CD206	321140	Biolegend
20	Paraformaldehyde, 4% in PBS	J61899	Thermo
21	AbC Anti-Mouse Bead	A10344	Invitrogen
22	Falcon® 40 μm Cell Strainer	352340	Corning
23	RPMI 1640	72400047	Gibco
24	DMEM	11054001	Gibco
25	Fetal bovine serum(FBS)	A4766	Gibco
26	Sodium pyruvate	11360070	Invitrogen
27	Penicillin-Streptomycin-Glutamine	10378016	Gibco
28	Lipopolysaccharide (LPS)	00-4976	eBioscience
29	Concanavalin A (Con A)	00-4978	eBioscience
30	Phorbol 12-myristate 13-acetate (PMA)	P8139	Sigma
31	Ionomycin	I24222	Invitrogen
32	Ficoll Paque Plus	GE17-1440-02	Cytiva
33	PBS, pH 7.4	A1286301	Gibco
34	RiboPure™ RNA Purification Kit, blood	AM1928	Invitrogen
35	RNA*later*™ Stabilization Solution	AM7021	Invitrogen
36	RNA Quantification, high sensitivity	Q32852	Invitrogen
37	1X dsDNA, high sensitivity	Q33230	Invitrogen

38	Qubit RNA IQ Assay Kit	Q33221	Invitrogen
39	NEBNext® rRNA Depletion Kit (Human/Mouse/Rat)	E6310X	NEB
40	NEBNext® Ultra™ II Directional RNA Library Beads	E7765L	NEB
41	BD CBA Human Th1/Th2 Cytokine Kit II	551809	BD

3.1.2 Human peripheral blood mononuclear cells (PBMCs)

Blood collection and detection described in this paper were approved by the local Ethics committee. All the study subjects participated voluntarily and gave written, informed consent for use of their blood samples for academic purposes.

3.1.3 Plasmid and Cell line

VSV-eGFP-Spike plasmid is reserved by our laboratory. Vero-E6 cell line is from American type culture collection(ATCC). and Vero cells were cultured in with 90% DMEM, containing 10% FBS, 1 mM sodium pyruvate, Penicillin-Streptomycin-Glutamine (100X). A 37°C incubator with 5% CO_2 was used to incubate the cells.

3.1.4 Main experimental instruments and consumables

No.	Name	Company
1	Qubit 4.0	Invitrogen
2	Nanodrop 2000	Thermo Fisher
3	FACS Celesta	BD
4	Automated Cell Counters	Thermo Fisher
5	The 96-well T100 PCR thermal cycler	Bio-rad
6	CO_2 incubators	Thermo Fisher
7	Microscope	OLYMPUS
8	Pipettes	Eppendorf
9	Pipette Tips	Axygen
10	Stripette	Corning
11	Low temperature high speed centrifuge	Eppendorf
12	DynaMag™-PCR	Invitrogen
13	Biosafety cabinet	Thermo Fisher

3.1.5 Bioinformatics software

1.http://www.genome.jp/kegg/pathway.html

2.http://www.geneontology.org/

3.http://www.geneontology.org/GO.doc.shtml#cellular_component

4.http://www.geneontology.org/GO.doc.shtml#biological_process

5.http://www.geneontology.org/GO.doc.shtml#molecular_function

6.https://string-db.org/

7. https://cibersortx.stanford.edu/index.php

8. https://xcell.ucsf.edu

3.2 Methods

3.2.1 Collection and isolation of PBMC

Human PBMC samples were obtained from donors identifying as healthy and HIV-1 negative. Donors were recruited from the local research community and through the Dalhousie University of the IWK Health Centre. COVID-19 samples were from the elderly patients (>65 years old). PBMC were isolated using standard Ficoll-PAQUE Plus density gradient centrifugation: Aspirate the upper layer leaving the mononuclear cell layer after centrifuged. Transfer the mononuclear cell layer to a new tube. Washed the cells with PBS and centrifuge at 300×g for 10 minutes by two times. Collecting the cell pellet in an appropriate amount of PBS.

3.2.2 Pseduovirus packaging

Put the VSV-eGFP-Spike expression plasmid and Virus packaging plasmids into Vero cells, each plasmid is 1μg in $1x10^6$ cells, Cultured in standard medium, incubated at 37°for 48hr. The titer of infected virus was determined according to the expression of green protein fluorescence rate under microscope. Then using anti-VSV-G antibody to neutralization of residual VSV-G. We used the concentrated cell supernatant as the virus solution for infecting cells.

3.2.3 Analysis of PBMC after drug stimulated

Use different molecular drugs to stimulate PBMC, and test the transfection efficiency of VSV-Spike protein. Collect PBMC from more than 3 health volunteer's blood samples, after

isolation PBMCs in BSL-2 lab, make the cell concentration: $1X10^6$/mL, Divided into 5 groups, Group A is a blank control group (Control(-)); Group B was a positive control group with VSV-eGFP-Spike pseduovirus（Control(+)）, Group C to Group E were added with VSV-eGFP-Spike pseduovirus and different chemicals to stimulate and activate immune cells; Group C with LPS on concentration of 2.5 mg/mL (LPS group); Group D with Con A on concentration of 1.25 mg/mL (Con A group); Group E with PMA on concentration of 5ng/mL and Ionomycin on concentration of 500ng/mL (PMA+Ionomycin). The cells were cultured in medium containing with 90% RPMI 1640, containing 10% FBS, 1 mM sodium pyruvate, 100 U/mL Penicillin and 100ng/mL Streptomycin. Incubate in 5% CO_2 incubator at 37 ℃ for 48-72 hours, then detect the molecular protein, and repeat the independent experiment for 3 times.

3.2.4 Multi-color flow cytometry subtype detection

PBMC cells in different groups were stained with a variety of flow panels, the flow cytometry staining panels are show as (Table 5). Multiple staining plate combinations were used to complete the staining of all specified cell subtypes. To some extent, the three laser flow cytometry limits the selection of panels. PBMC was stained with various antibody combinations against cell surface proteins (CD45, CD3, CD4, CD8, CD56, CD16, CD19, CD11b, CD14, CD27, CD45RO, CD45RA, CD25, PD-1, CD11c, HLA-DR, CD80, CD86) in 4 panels for 30min, incubate in the dark. and then washed twice with PBS. After incubation is complete, Add an equal volume of the 4% stock to samples for a final concentration 1% PFA. Fix cells on ice for 20-30 minutes, and then wash twice with PBS with 300×g for 5 minutes, discard the supernatant. Resuspend cells by add 300uL PBS. Filter with 40μm, Prepare for flow cytometry. BD celesta instrument is used for flow detection, built-in flow software is used for data collection, and FlowJo Version 7.6 software is used for all flow data analysis in Windows system.

Table 5: for Panel-1 to Panel-4

Panel-1

No.	Name	Amount (μl)
1	CD45	2
2	CD3	1
3	CD56	1
4	CD16	2
5	CD19	2
6	CD11b	1
7	CD14	1

Panel-2

No.	Name	Amount (μl)
1	CD3	1
2	CD4	2
3	CD8	1
4	CD27	1
5	CD45RO	2
6	CD45RA	2

Panel-3

No.	Name	Amount (μl)
1	CD3	1
2	CD4	2
3	CD8	1
4	CD25	2
5	CD27	1
6	CD279 (PD-1)	2

Panel-4

No.	Name	Amount (μl)
1	CD11c	1

2	CD14	2
3	HLA-DR	1
4	CD80	2
5	CD86	1
6	CD11b	2

3.2.5 RNA extraction, Library preparation and RNA Sequencing

Biological samples are stored in RNAlater™ stabilization solution or directly derived from fresh samples. Use RNA Purification Kit to extract total RNA. The total RNA is combined with the magnetic beads with Poly(T) probe, the magnetic beads are harvested and the rRNA is removed, the mRNA bound to the magnetic beads is eluted, so the RNA is purified. Use Nanodrop 2000 to detect the concentration of RNA and the value of 260/280. To check whether RNA sample has degraded by using Qubit 4.0 Fluorometer. It can quickly assess the integrity of an RNA sample. The strategy we adopted was to reverse transcription of mRNA combined with oligo(dT), and then fragmentation of cDNA. The cDNA library is completed after a series of terminal repair, and sequencing adapter ligation. Library were made quality control by Qubit 4.0, Agilent 2100 and Q-PCR before sequenced on the Illumina NovaSeq 6000 Sequencing System.

3.2.6 Data processing and Differentially Expressed Gene(DEG) analysis

Following RNA sequencing, short reads are produced on the sequencing platform using tagged fluorescent sequences that have undergone a number of quality checks. The FASTQ format is used to store these quick readings. Each sample has a depth of 30 million reads throughout the sequencing process. The reads were first aligned with the reference genome Homo sapiens (human) genome assembly GRCh38 (hg38) using STAR, and the transcripts were then put together using the reads alignment data. In this work, RSEM software was used to avoid filtering reads that had multiple matching sites or numerous expression characteristics because doing further analysis on these reads might result in biased homologous and overlapping transcriptional data. Transcripts Per Kilo Base of Exon Model

per Million Mapped Reads (TPM) function was used to normalize read expression amount after Cufflinks program was used to filter and normalize read count to eliminate the impacts of sequencing depth, expression pattern, and technical bias.

An essential objective of RNA-seq research is to identify genes that are differently expressed across various samples and environments. The False Discovery Rate (FDR), also known as the p-value, and the log2 fold change between genes were used to screen the differential genes using DESeq2, which was utilized to examine the differential gene expression across various groups. The screening criteria in this study were: absolute correlation |log2| fold change >2 and p-value <0.05. The correlation strength is proportional to the abscissa's width.

3.2.7 GO enrichment and KEGG pathway analysis to characterize of differentially expressed genes

Each gene's fundamental function is based on the protein domains, and the scientific literature generally identifies the types of functions that genes have. Numerous gene function annotation databases have been created by scientists in an effort to address the issue of identifying genes by function. Gene Ontology (GO) and the Kyoto Encyclopedia of Genes and Genomes(KEGG) are two examples of the global ones.

The databases of gene-related functions known as GO and KEGG use several categorization schemes. One of these is the Gene Ontology Consortium's GO database, which intends to provide a semantic language standard that can be applied to different species, defines and characterizes the activities of genes and proteins, and can be updated as research into these topics progresses. The three subcategories of GO annotations are biological process(BP), molecular function(MF), and cellular component (CC). We may examine the roles and primary relationships of our target DEGs at the three levels of CC, MF, and BP using the GO database.

While KEGG not only includes gene sets but also specifies intricate interrelationships between genes and metabolites, GO term is a pure gene set and does not specify the interrelationships of the genes in it. A comprehensive database called KEGG combines data

on systemic, chemical, and genetic functions. KEGG Pathway, a database that specializes in recording details on many species' gene pathways, The KEGG Pathway The gene will take part in a number of pathways in the human body in addition to being annotated for its own function. The route-related database was created using the human body's pathway as a model. We can determine whether key signaling pathways DEGs are considerably enriched in compared to the control group by using KEGG, and the combined macroscopic outcome is the end result.

3.2.8 STRING Database PPI analysis

Protein-Protein Interaction (PPI) networks may be functionally analyzed using the database STRING (Search Tool for the Retrieval of Interacting Genes/Proteins). A group of differentially expressed genes or proteins are discovered between several groups of samples following RNA-Seq sequencing, etc. In order to characterize how these genes or proteins are connected to one another and eventually to find significant molecular regulatory networks in the organism, the potential connections between the various proteins may then be examined using STRING.

3.2.9 Multi-cytokine detection and analysis

In this work, BD Cytometric Bead Array (CBA) was used to detect the expression of cytokines in several experimental groups in order to determine the levels of expression of various cytokines in cell studies. CBA can be used to concurrently measure many proteins. for instance, cytokines. The CBA system employs antibody-coated beads, each of which has a distinct fluorescence intensity that can be resolved in a flow cytometer. This enables the simultaneous mixing and detection of multiple beads in a single experimental sample in order to obtain information on the expression of multiple proteins. In the cell experiment, spin the Control(-), Control(+), and LPS groups at 300xg for 10 minutes. Then, collect the cell culture supernatant and do the test in accordance with the kit's instructions..

4. Results

4.1 A pseudovirus expressing spike protein with high titer was prepared

SARS-CoV-2 spike(S) protein was used to pseudotype a recombinant replication-deficient vesicular stomatitis virus (VSV) vector that encodes green fluorescent protein (GFP) and luciferase and the spike protein (S) rather than the VSV-glycoprotein (VSV-G). High titer pseduovirus supernatants were collected after 48 and 72 hours, and used in the following experiments.

4.2 PBMC activation system capable of transfecting pseudovirus was constructed

Previous research has demonstrated that the SARS-CoV-2 virus may bind to the ACE-2 protein produced on the surface of epithelial cells and pass through [183-184]. Some COVID-19 patients exhibit neurological symptoms such as headache, nausea, and vomiting in a clinical setting. Respiratory distress is the most common symptom. Cytokine storm syndrome (CRS) is the primary cause of these symptoms and one of the key factors that contributes to the patient's mortality [185]. Unfortunately, the evidence for the regulation of how and which immune cell subgroups function is not apparent.

Here we identified the immune cell subgroups capable of adhering to spike protein by activating several cell subgroups using chemical agents. Lipopolysaccharides (LPS), which bind and activate B cells, monocytes, and dendritic cells, stimulate the release of cytokines that are pro-inflammatory [186]. Additionally, LPS can stimulate cellular stress responses in a variety of cell types that express TLR [187]. Concanavalin A (ConA) is extracted from jack-bean [188]. ConA is known to simulate T-cell activation and NK-T cells [189-190]. The signaling enzyme protein kinase C can be activated by phorbol 12-myristate 13-acetate (PMA) [191]. Further, ConA is frequently used with ionomycin to promote the activation, proliferation, and cytokine generation in T cells [192].

We utilized these chemical agents to activate the collected PBMCs from healty controls. The grouping and stimulation methods mentioned above are applied. After co-culturing PBMC cells for 72 hours, we conducted flow cytometry to confirm if VSV-Spike can infect PBMCs by assaying for the production of GFP. Green fluorescence was observed in a certain

subset of cells indicating that these cells were infected with pseudovirus containing spike and GFP (Figure 9).

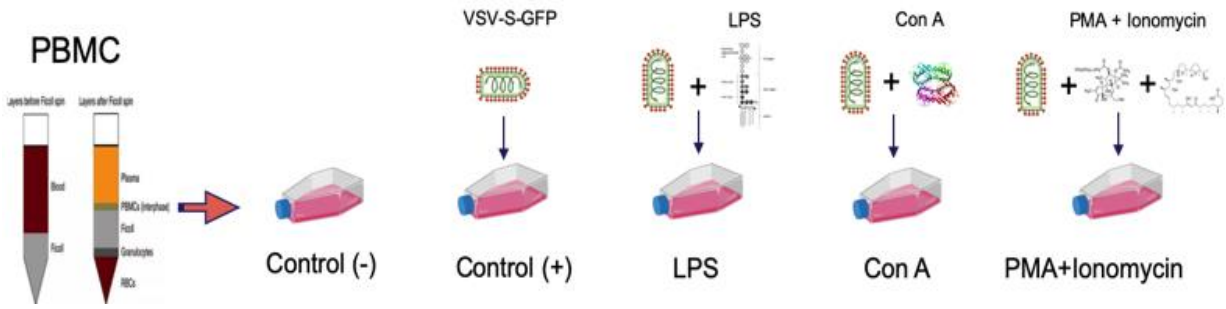

Figure 9: Stimulate PBMC with different molecular drugs

Fig 9 | Collect PBMC from volunteer blood samples to make the cell concentration: $1X10^6$/mL, add LPS (2.5 mg/mL), Con A (1.25 mg/mL), PMA (5ng/ml), Ionomycin (500ng/mL) in groups, Culture for 48-72hr.

4.3 VSV-Spike-GFP+ is highly expressed in the LPS+ group

The flow cytometry findings are displayed in (Figure 10A). According to the results, cells expressing GFP were Control (-): 0.89%; Control PBMCs (+): 4.75%; LPS stimulated PBMCs: 17.7%; Con A stimulated PBMCs: 5.01%; and PMA+Ionomycin stimulated PBMCs: 2.44%. This data indicates that LPS stimulates increased expression of ACE2 receptor on PBMCs and facilitates VSV-Spike binding and infection. An alternative explanation is that LPS stimulates increased phagocutosis and VSV-Spike is phagocytosed by macrophages. We see the same outcomes in (Figure 10B). Only the LPS group has a significant fluorescence expression when viewed with an inverted fluorescence microscope; the other groups did not have increased observable flourescence. SARS-CoV-2 primarily targets airway epithelial cells at the tissue level. This investigation demonstrates that the spike protein VSV can easily infect LPS-stimulated PBMCs. ACE2 is persistently and consistently expressed in enterocytes, renal tubules, the gallbladder, cardiomyocytes, male germ cells, placental trophoblasts, ductal cells, eyes, and arteries with modest expression in

cell subsets as a host receptor for SARS-CoV-2 [193-194].

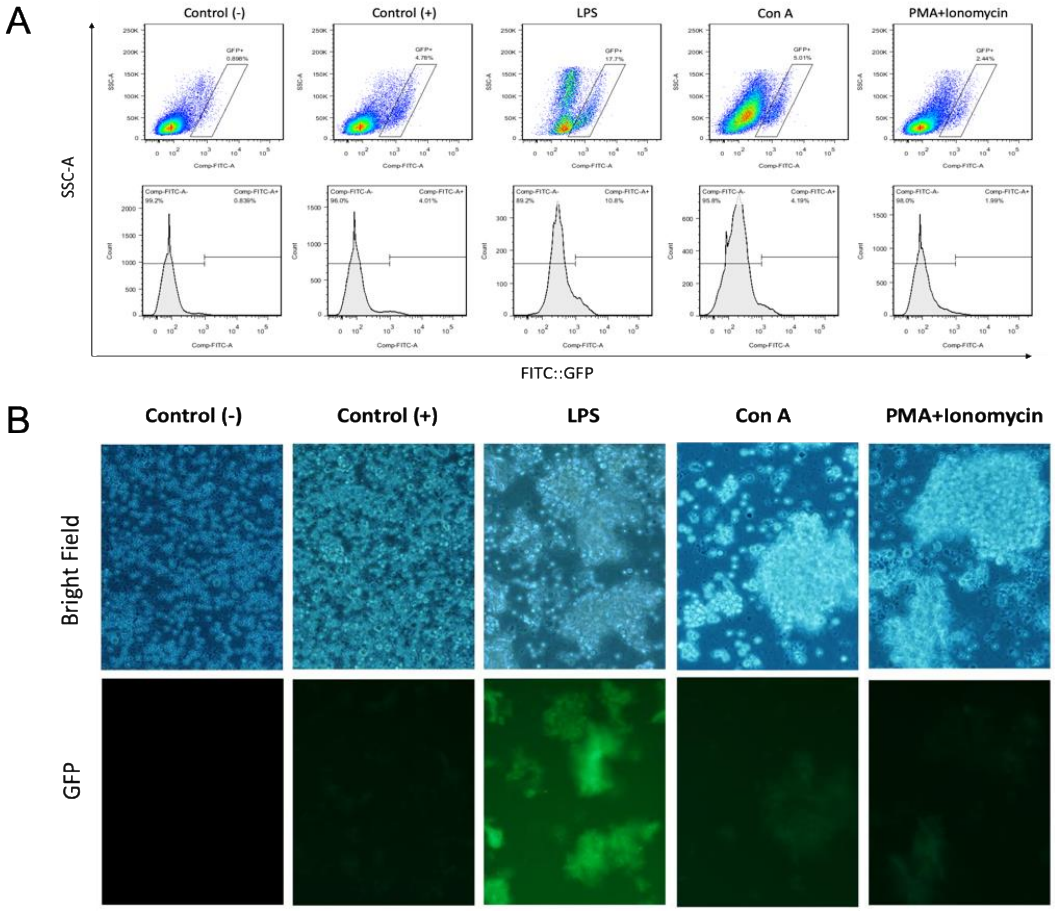

Figure 10: Infectivity to VSV-Spike-GFP+ differs between groups

Fig 10 | **A:** Incubated PBMCs with different drugs, The expression of infected VSV with Spike protein: Control (-): 0.89%; Control (+): 4.75%; LPS: 17.7%; Con A: 5.01%; PMA+Ionomycin: 2.44%. **B:** The GFP fluorescence intensity among different groups.

4.4 sets of repeated independent experimental data results

Four separate experiments were done, and the findings and the statistical significance was assessed using t-tests (Figure 11). There was a significant difference at **P< 0.05 and ***P< 0.01. The highest significant difference was observed between the LPS group and the control (-) group (P = 0.0082) and between the control (-) group and the control (+) group (P = 0.0184).

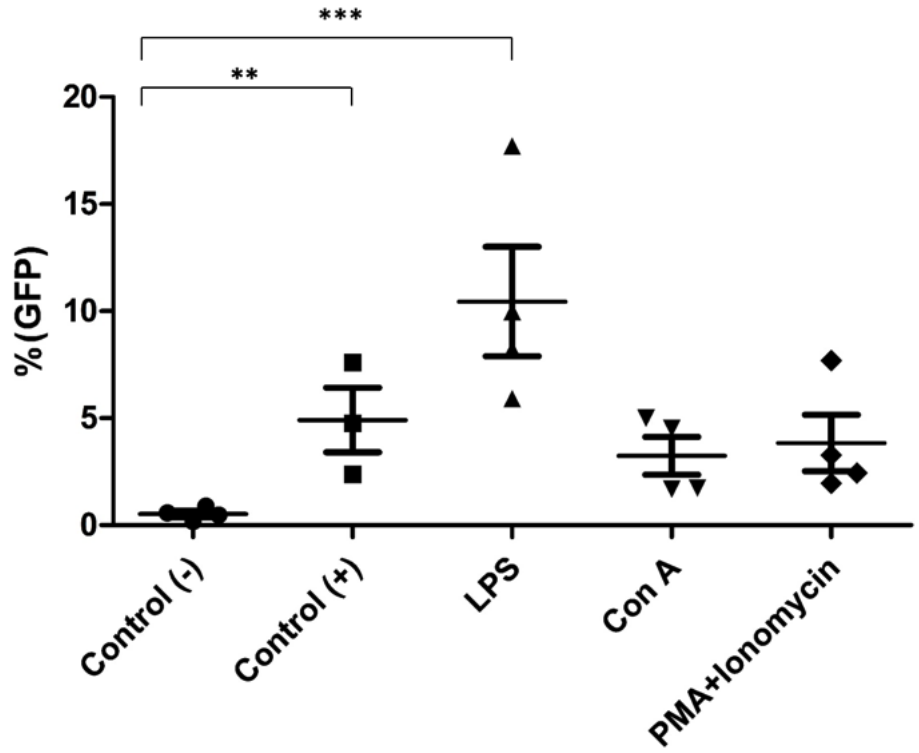

Figure 11: The infectivity to VSV-Spike-GFP+ differs between different groups of multiple repetitions

Fig 11 | Incubated PBMCs with different drugs, the difference in infected VSV with Spike and GFP+ , Control(-) vs LPS, P=0.0082, Control(+) vs Control(+), P=0.0184, **means P < 0.05, ***means P < 0.01.

4.5 Flow cytometric phenotyping of cell subtypes bound to VSV-Spike protein

4.5.1 Flow cytometric results analysis

To determine which cell subsets can bind to VSV spike, we identified cell subsets using flow cytometry. The antibody usage strategy is shown in the table above (Table 5). Different panels have been tested for different cell subtypes. Flow cytometry gating strategy for T cell, B cell, NK-T cell, NK cell and macrophage are detailed in Panel 1: T cell (CD3+CD19-), B cell (CD3+CD19+), NK-T cell (CD3+CD56+CD16+), NK cell （CD3-CD56+CD16+), and macrophage (CD14+CD11b+) were identified within CD45+. And in Panel 2: For identification of CD4+ T cells and subsets as naïve/resting T cell (CD4+CD45RA+) and memory/activated T cell (CD4+CD45RO+), subdivide the naïve/resting T cell as the subsets of Naïve T (CD27+CD45RO-), and Effector T (CD27-CD45RO-); Subdivide the memory/activated T cell as the subsets of Central memory T (CD27+CD45RO+) and Effector memory T (CD27-CD45RO+); For identification of CD8+ T cell and subsets such as

naïve/resting T cell (CD8+CD45RA+) and memory/activated T cell(CD8+CD45RO+), the naïve/resting T cell e subsets were Naïve T (CD27+CD45RO-), and Effector T (CD27-CD45RO-); and memory/activated T cell as the subsets of Central memory T (CD27+CD45RO+) and Effector memory T (CD27-CD45RO+). To identify PD-1+ T cells in Panel 3, we detected PD1+ cells in the CD8+ T cell subset as Effector CD8+ PD-1+ T cell (CD3+CD8+CD27+PD-1+), and also identified Treg cells (CD3+CD4+CD25+). In panel 4, we identified different subpopulations of macrophage and dendritic cells Subsets of the macrophage group we identified were primitive macrophage (CD45+CD14+CD11b+), M1 macrophage (CD45+CD14+HLA-DR+), and M2 macrophage (CD45+CD14+CD80-CD163+CD206+). Cell subsets were further subdivided into dendritic cells: immature dendritic cells (CD45+CD14-HLA-DR+CD86+) and mature dendritic cells (CD45+CD14-HLA-DR+CD80+). The common control antibody experiment and fluorescence minus one (FMO) group were set up to reduce the interference of fluorescence channel.

Flow analysis was performed on the Control (-), Control (+) and LPS groups, because Control (-) has no VSV-Spike infection, and we wanted to compare the infection of the pseudovirus Control(+) group, and the LPS group which had LPS stimulation. Secondly, we wanted to further study, among the subpopulations of infected cells (GFP+), which cell subpopulations are most likely to be infected. From (Figure 12A), we can see that in the LPS group, the positive rate of PBMC (CD45+) cells is higher, reaching 63.7%, while the positive control group is only 41.8%, suggesting that PBMC subsets can more easily bind to Spike protein; Furthermore, we found that among the CD45+ positive cell population, the expression rate of macrophages (CD14+CD11b+) in the Control (+) group was 1.22%, while the expression rate in the LPS group was 12.1%. The results showed that increases in macrophage cell subsets correlate with infection of VSV-Spike. However, we see that there is no significant difference between the two groups in T cells (CD3+) and NK cells (CD56+CD16+). The reason for these results may be that ACE2 expression on the surface of T cell immune cell subsets is less, or because macrophages stimulated by LPS can participate in the recognition of spike protein in the early stage, thereby exerting a certain antiviral

effect. Alternatively, or it may be because LPS-activated macrophages can swallow spike protein-carrying pseduovirus, and thus spit out spike protein with fluorescent label protein on the surface and be detected. The probability of this hypothesis is low because it is not clear how the spike protein is transferred to macrophages after phagocytosis.

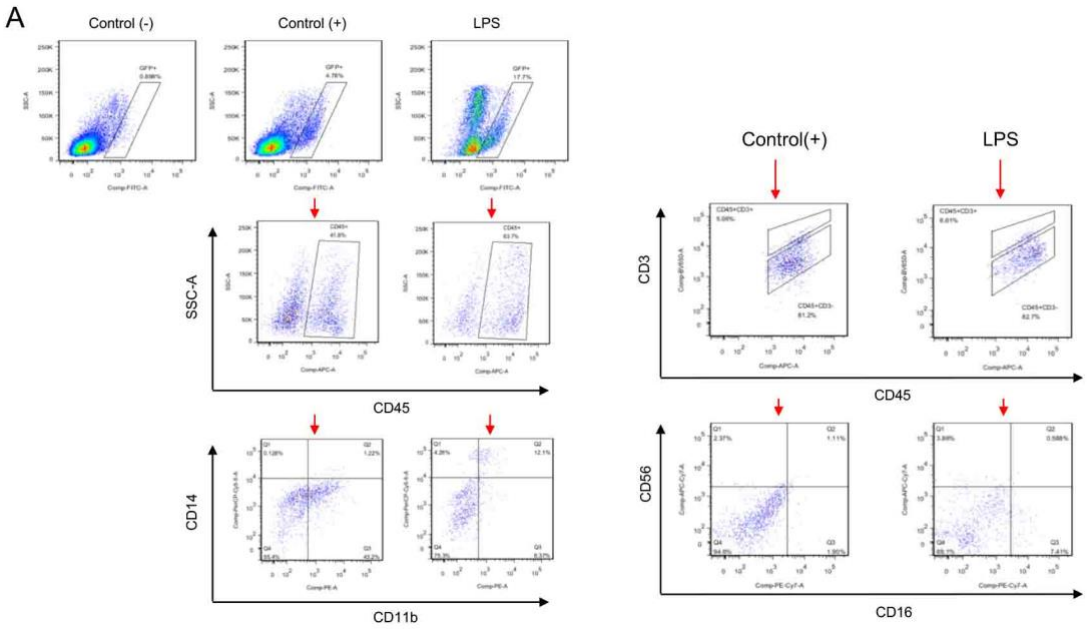

Figure 12: Analysis of VSV-Spike-GFP+ cell subtype ratios

Fig 12 | **A**：In GFP+ population analyzed cell subsets, including PBMC (CD45+)，Macrophages (CD14+CD11b+)，T cells (CD3+) and NK cells (CD56+CD16+).

In addition, we analyzed other cell subsets, including DC (CD45+CD14-), immature DC (CD45+CD14-HLA-DR+CD86+), mature DC (CD45+CD14-HLA-DR+CD80+), monocytes (CD45+CD14+) and MΦ-2 cells (CD45+CD14+CD163+CD206+), Flow phenotype analysis showed (Figure 12B) VSV-Spike GFP was highly expressed in DC cell subsets in the LPS-stimulated group.

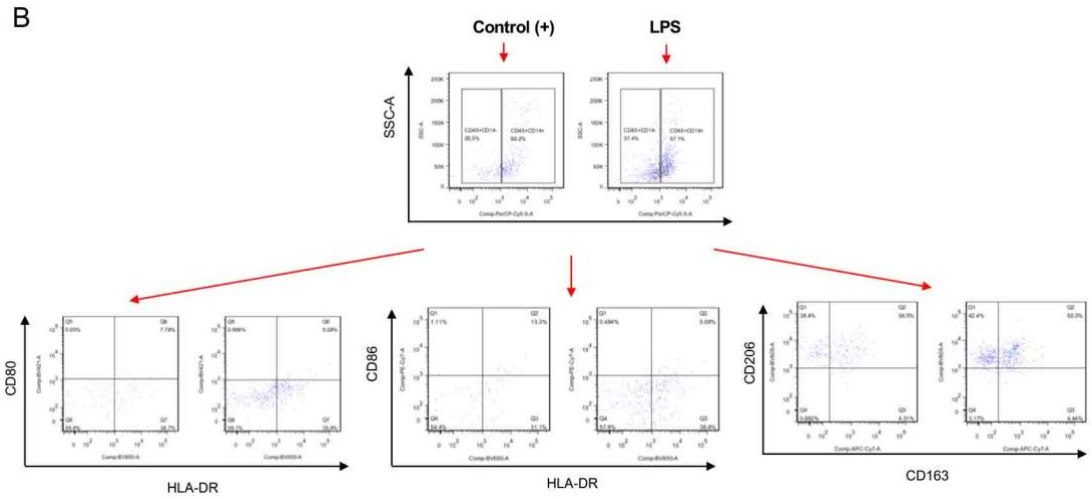

Figure 12: Analysis of VSV-Spike-GFP+ cell subtype ratios

Fig 12 | B： In GFP+ population analyzed cell subsets, including DC (CD45+CD14-), Immature DC (CD45+CD14-HLA-DR+CD86+), Mature DC (CD45+CD14-HLA-DR+CD80+), Monocytes (CD45+CD14+) and MΦ-2 cells (CD45+CD14+CD163+CD206+).

4.5.2 Summary of VSV-Spike findings

Studies have revealed that while it is challenging for SARS-CoV-2 to infect immune cells in the blood, certain monocytes can be infected and that the main immune cell type that can produce ACE2 is proinflammatory macrophages [195-196].

In this study, summarized in (Table 6), the results show LPS increases VSV-Spike infection in the macrophages and dendritic cells. Infection of immature DCs significantly downregulated when LPS-stimulated.

Table 6：Overall differences in VSV-Spike-GFP+ immune cell subtype ratios in LPS and Control(+) groups

Group	Control(+)	LPS
PBMC(CD45+)	41.8%	63.7%
MΦ cell(CD14+CD11b+)	1.22%	12.1%
T Cell (CD45+CD3+)	5.06%	6.61%
NK Cell (CD45+CD3-CD56+CD16+)	1.11%	0.588%
DC (CD45+CD14-)	26.5%	37.4%

Immature DC(CD45+CD14-HLA-DR+CD86+)	13.3%	**5.08%**
Mature DC(CD45+CD14-HLA-DR+CD80+)	7.78%	5.08%
Monocytes (CD45+CD14+)	68.2%	57.1%
MΦ-2 cell (CD45+CD14+CD163+CD206+)	56.5%	50.0%

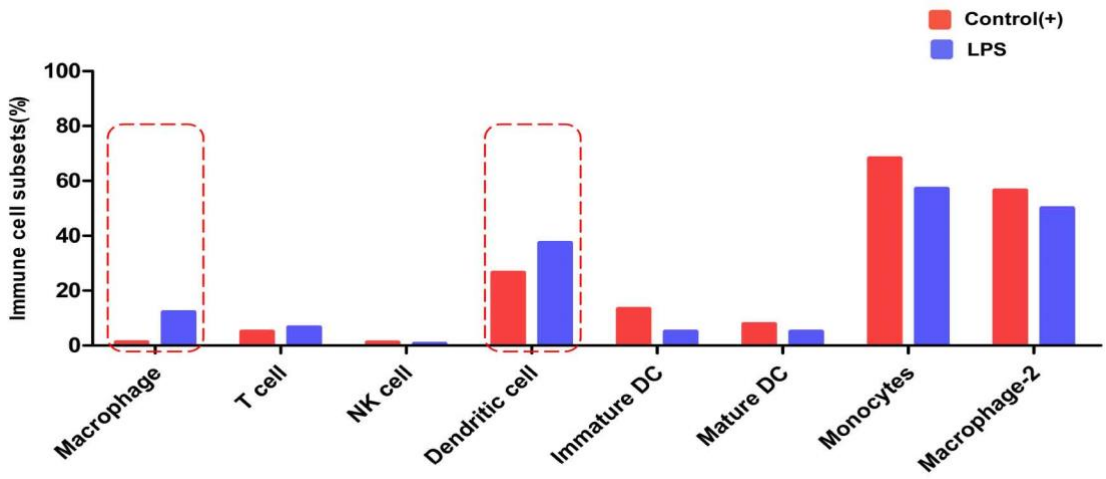

Figure 13: Histogram of the overall differences in the ratios of immune cell subtypes

Fig 13 | Compared with the control(+) group, the VSV-S-LPS+ group Spike protein mainly bind to these immune cell subsets in DC and Macrophages.

4.6 Flow cytometric typing of different cell subtypes after stimulation with various leukocyte activators

4.6.1 Flow cytometric results analysis

We examined PBMC cell subsets to better understand if cell subsets of PBMCs are altered after infection with VSV-Spike protein and after LPS stimulation.

Studies have shown that after SARS-CoV-2 virus infection, lymphocyte subsets, including B lymphocyte subsets and T lymphocyte subsets, will decrease significantly, which may affect the body's normal cellular immune function and antibody responses, and even cause IL-6, IL-10, and TNF-α and other cytokines to be significantly up- or down-regulated, causing cytokine dysregulation that typically results in severe disease [197-199].

We proceeded to perform an overall immune cell subset analysis in the Control (-), Control (+) and LPS-stimulated groups. Our results (Figure 14A), show that Control (-),

Control (+) and LPS groups had no significance in different cell types in PBMCs (CD45+) which were as follows: 99.5%, 94.5% and 97.9%. T cell (CD45+CD3+) subgroup, the LPS group was lower than those in the other groups, 59.5%, 64.1% and 57.1%; but in B cells (CD45+CD3-CD19+) there was no significant change, 2.04%, 4.23% and 3.41%;

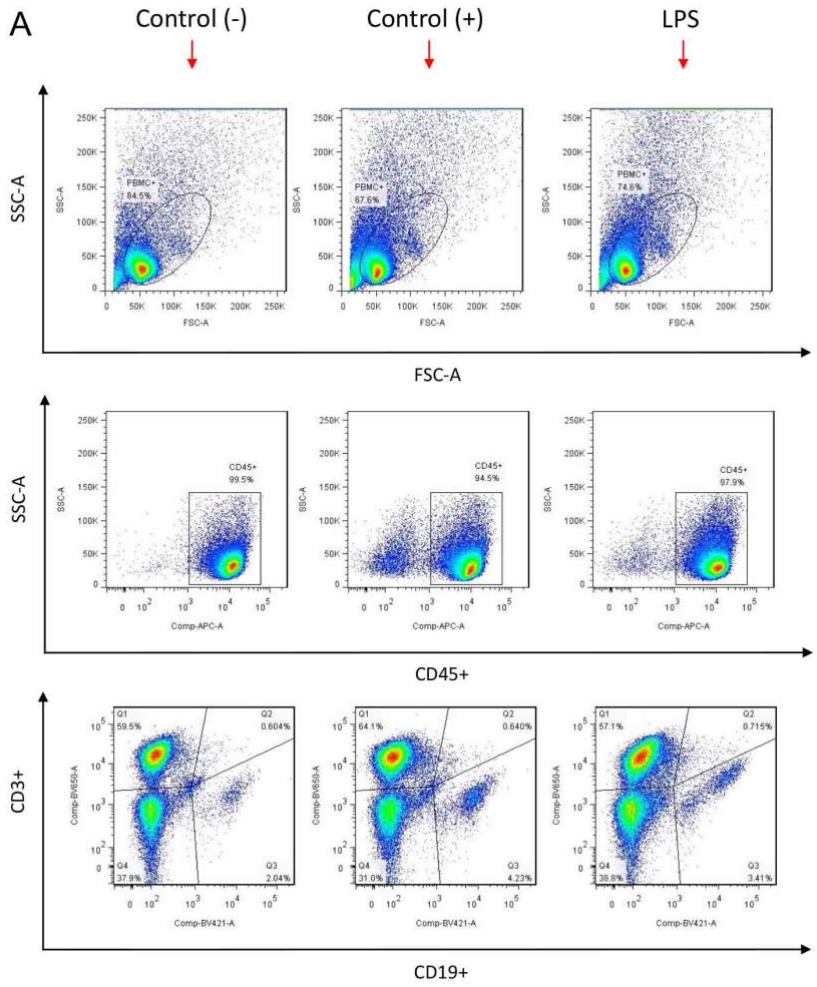

Figure 14: Analysis of the proportion of whole cell subtypes in different groups

Fig 14 | **A:** Analyzed cell subsets, including PBMC ($CD45^+$), T cells (CD3+) and B cells (CD45+CD3-CD19+).

As shown in (Figure 14B), NK-T cells (CD3+CD56+ CD16+) were 0.064%, 0.112%, and 0.143% with no significant change, and NK cells (CD3-CD56+CD16+) were 5.25%, 3.06% and 4.88% with no significant change.

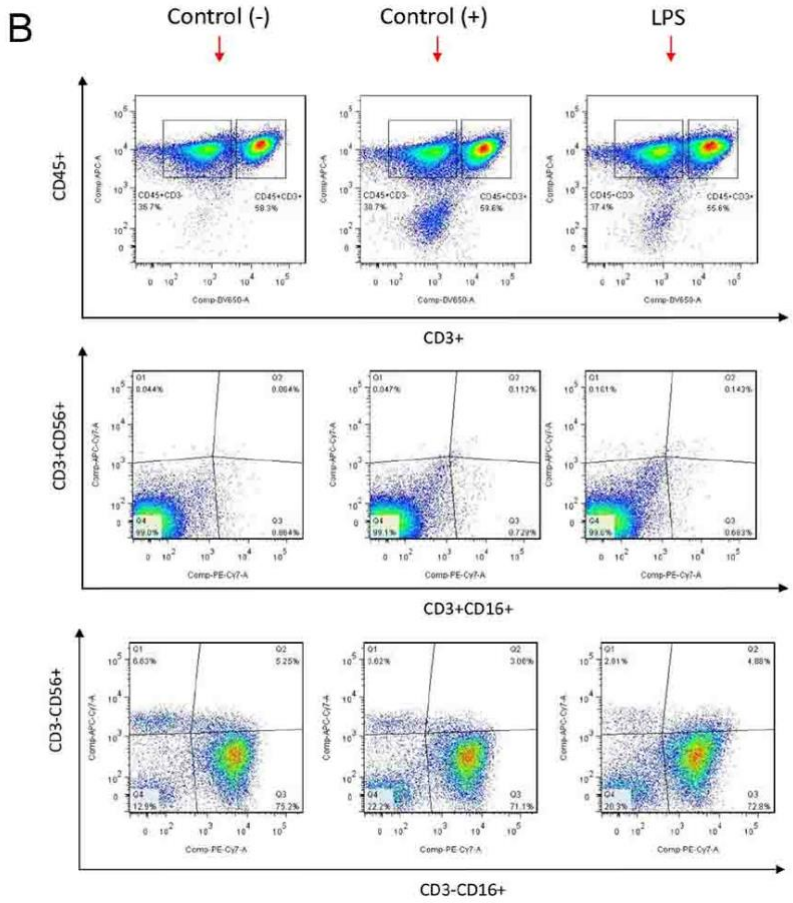

Figure 14: Analysis of the proportion of whole cell subtypes in different groups

Fig 14 | **B:** Analyzed cell subsets, including NK-T cells (CD3+CD56+ CD16+) and NK cells (CD3-CD56+CD16+).

Figure 14C shows, CD8+ T Cell (CD3+CD8+) were 34.4%, 34.2% and 31.9% with no significant change; CD4+ T Cell (CD3+CD4+) were 43.7%, 42.7% and 46.7%, highest in the LPS group; CD8+ naive T cells (CD8+CD45RA+) were 31.0%, 26.4% and 35.5%, and the LPS group was relatively higher by immune activation; CD8+ memory T cells (CD8+CD45RO+) were 53.5%, 54.6% and 46.1%, which was significantly down-regulated in the LPS group, and CD4+ naive T cells (CD4+CD45RA+) were 30.5%, 29.2% and 25.9% less in the LPS group; CD4+ memory T cells (CD4+CD45RO+) were 61.4%, 61.7% and 64.2% with no significant changes; central memory T (CD27+CD45RO+) were 38.9%, 40.7%, and 32.9% with a decrease in comparison; (CD27+CD45RO-) were 25.8%, 22.9%, and 23.5% with no significant change; effector memory T (CD27-CD45RO+) were 25.2%,

26.6% and 32.4% with a significant increase; effector T (CD27-CD45RO-) were 10.1%, 9.74% and 11.2% with no significant change.

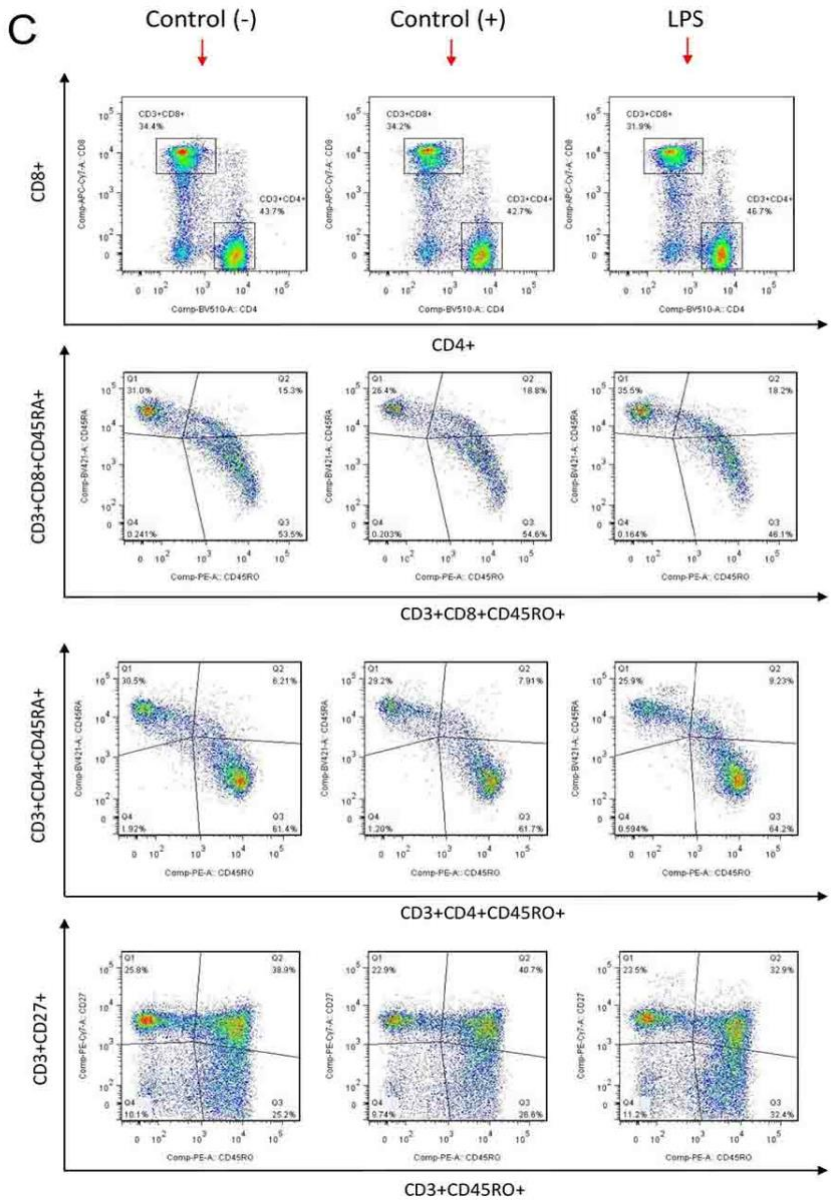

Figure 14: Analysis of the proportion of whole cell subtypes in different groups

Fig 14 | **C:** Analyzed cell subsets, including CD8+ T Cell (CD3+CD8+), CD4+ T Cell (CD3+CD4+), CD8+ naive T cells (CD8+CD45RA+), CD8+ memory T cells (CD8+CD45RO+), CD4+ naive T cells (CD4+CD45RA+), CD4+ memory T cells (CD4+CD45RO+), central memory T (CD27+CD45RO+), (CD27+CD45RO-), effector memory T (CD27-CD45RO+) and effector T (CD27-CD45RO-).

Figure 14D shows, PD1+ T cells (CD3+PD-1+) were 5.43%, 6.19% and 3.98% significantly reduced in LPS group; effector CD8+ PD-1+ T cells (CD3+CD8+CD27+PD-

1+) were 13.0%, 12.8% and 9.43% with decreased ratios; effector CD8+ T cells (CD3+CD8+CD27+) were 39.2%, 37.2% and 39.4% no significant changes; Treg cells (CD3+CD4+ CD25+) were 6.63%, 7.21% and 6.7% with no significant change.

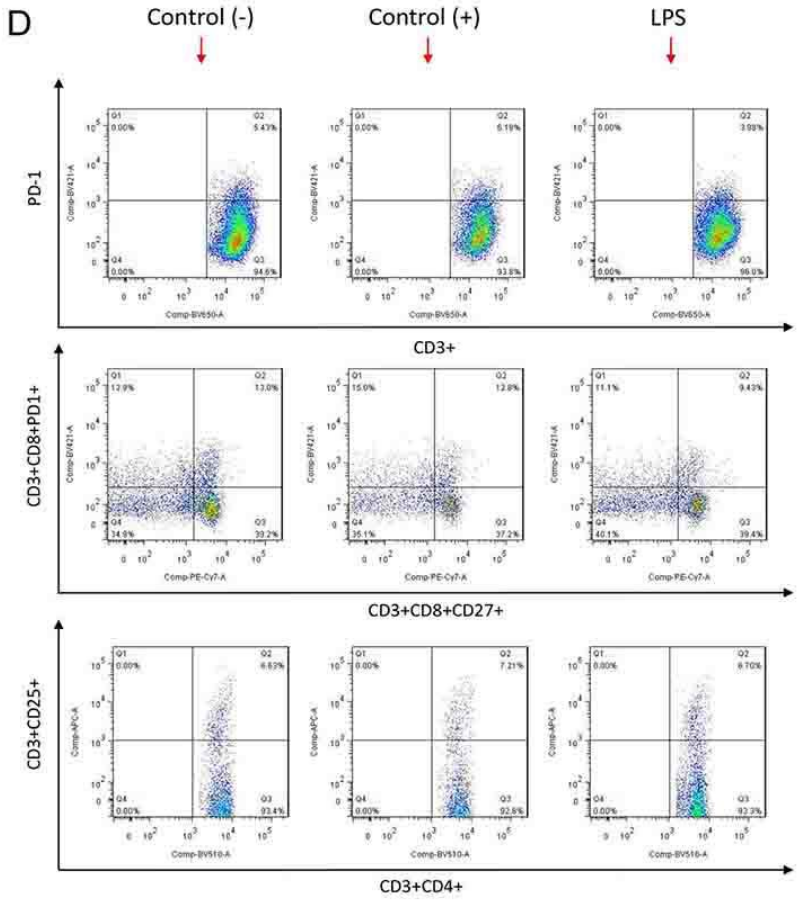

Figure 14: Analysis of the proportion of whole cell subtypes in different groups

Fig 14 | D: Analyzed cell subsets, including PD1+ T cells (CD3+PD-1+), effector CD8+ PD-1+ T cells (CD3+CD8+CD27+PD-1+), effector CD8+ T cells (CD3+CD8+CD27+) and Treg cells (CD3+CD4+ CD25+).

Figure 14E shows, MΦ cells (CD14+CD11b+) were 2.34%, 1.54% and 3.57% up-regulated; MΦ-1 cells (CD14+HLA-DR+) were 2.55%, 2.12% and 2.95% no significant changes.

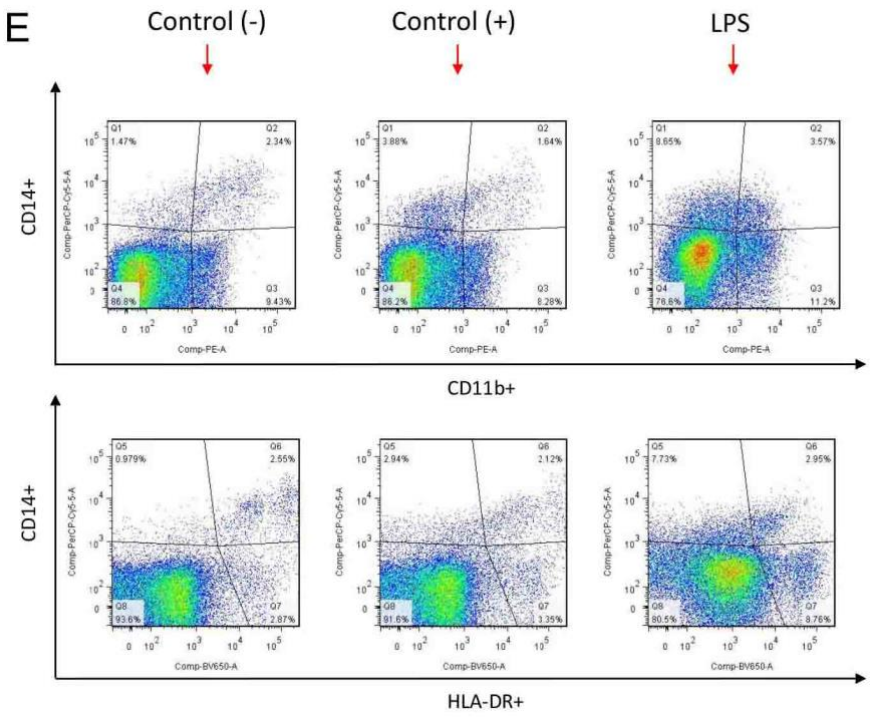

Figure 14: Analysis of the proportion of whole cell subtypes in different groups

Fig 14 | **E:** Analyzed cell subsets, including MΦ cells (CD14+CD11b+) and MΦ-1 cells (CD14+HLA-DR+).

As shows in Figure 14F: monocytes (CD45+CD14+) were 4.34%, 6.68% and 14.5%, significantly up-regulated in LPS group; MΦ-2 cells (CD45+CD14+CD163+CD206+) were 50.7%, 58.4% and 55.5 %, no significant change; DC (CD45+CD14-) were 89.9%, 86.5% and 81.7%, slightly decreased; immature DC (CD45+CD14-HLA-DR+CD86+) were 0.666%, 0.996% and 4.73%, significant increased and been activated. Mature DC (CD45+CD14-HLA-DR+CD80+) were 0.516%, 0.453% and 2.82%, significantly increased.

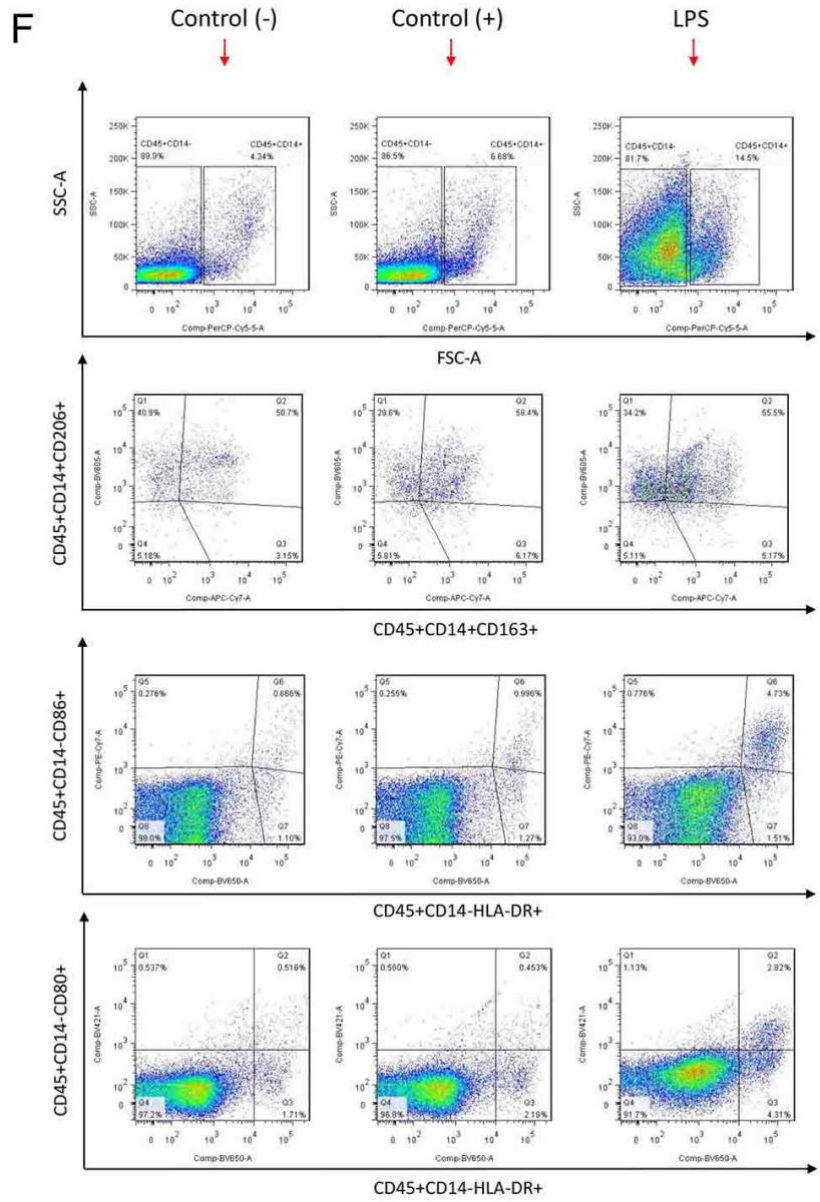

Figure 14: Analysis of the proportion of whole cell subtypes in different groups

Fig 14 | F: Analyzed cell subsets, including monocytes (CD45+CD14+), MΦ-2 cells (CD45+CD14+CD163+CD206+), DC (CD45+CD14-), immature DC (CD45+CD14-HLA-DR+CD86+) and mature DC (CD45+CD14-HLA-DR+CD80+).

4.6.2 Summary subset cell differences in VSV-Spike LPS-stimulated PBMCs

The main reason for the decrease in lymphocytes and T cells may be that the stimulated T cells undergo apoptosis and many cells die autonomously. Another possible mechanism is that the spike protein of SARS-CoV-2 can be embedded in the cytoskeletal protein of

lymphocytes, leading to cell death and inhibiting the normal function of immune cells [200], which is also a new target for the treatment of COVID-19.

Data from (Table 7) and (Figure 15) show that the LPS-activated PBMC group exhibit increased expression of GFP following VSV-Spike infection.The percentage of T cells decreased, and subsets of central memory T and killer T cell (CD8+ T cells) activation is limited, which may lead to the impairment of antiviral immune function. The inhibition of effector CD8+ PD-1+ T cells may also be one of the mechanisms of immune escape after the virus invades the body. The decrease in the number of CD4+ naïve T cell subsets also partially inhibits the function of helper T cells, a while more activation of MΦ cells and Monocytes cells, show that after VSV-Spike infection, the innate immune mechanism quickly responds to the antiviral mechanism. Both immature DC and mature DC cell subsets are significantly activated and expanded and have the potential to function in helping to activate T and B cell populations.

Our findings demonstrate that while innate immune cell subsets such as MΦ cells, monocytes, immature DC, and mature DC had significant increases in GFP expressing cells following LPS activation, adaptive immune cell subsets such as T cells, CD8+ memory T cells, CD4+ naive T cells, central memory T cells, and PD1+ T cells were significantly reduced in absolute numbers.

Table 7: Overall differences cell subtype ratios in Control(-), Control(+) and LPS groups

Group	Control(-)	Control(+)	LPS
PBMC(CD45+)	99.5%	94.5%	97.9%
T cell (CD45+CD3+)	59.5%	64.1%	**57.1%**
B cell (CD45+CD3-CD19+)	2.04%	4.23%	3.41%
NK-T cell (CD3+CD56+CD16+)	0.064%	0.112%	0.143%
NK cell (CD3-CD56+CD16+)	5.25%	3.06%	4.88%
CD8+ T cell (CD3+CD8+)	34.4%	34.2%	**31.9%**
CD4+ T cell (CD3+CD4+)	43.7%	42.7%	46.7%
CD8+ naïve T cell(CD8+CD45RA+)	31.0%	26.4%	35.5%

CD8+ memory T cell(CD8+CD45RO+)	53.5%	54.6%	**46.1%**
CD4+ naïve T cell(CD4+CD45RA+)	30.5%	29.2%	**25.9%**
CD4+ memory T cell(CD4+CD45RO+)	61.4%	61.7%	64.2%
Central memory T (CD27+CD45RO+)	38.9%	40.7%	**32.9%**
Naïve T (CD27+CD45RO-)	25.8%	22.9%	23.5%
Effector memory T (CD27-CD45RO+)	25.2%	26.6%	**32.4%**
Effector T (CD27-CD45RO-)	10.1%	9.74%	11.2%
PD1+ T cell (CD3+PD-1+)	5.43%	6.19%	3.98%
Effector CD8+ PD-1+ T cell(CD3+CD8+CD27+PD-1+)	13.0%	12.8%	**9.43%**
Effector CD8+ T cell(CD3+CD8+CD27+)	39.2%	37.2%	39.4%
Treg cell (CD3+CD4+CD25+)	6.63%	7.21%	6.7%
MΦ cell (CD14+CD11b+)	2.34%	1.54%	**3.57%**
MΦ-1 cell (CD14+HLA-DR+)	2.55%	2.12%	2.95%
Monocytes (CD45+CD14+)	4.34%	6.68%	**14.5%**
MΦ-2 cell (CD45+CD14+CD163+CD206+)	50.7%	58.4%	55.5%
DC (CD45+CD14-)	89.9%	86.5%	**81.7%**
Immature DC(CD45+CD14-HLA-DR+CD86+)	0.666%	0.996%	**4.73%**
Mature DC(CD45+CD14-HLA-DR+CD80+)	0.516%	0.453%	**2.82%**

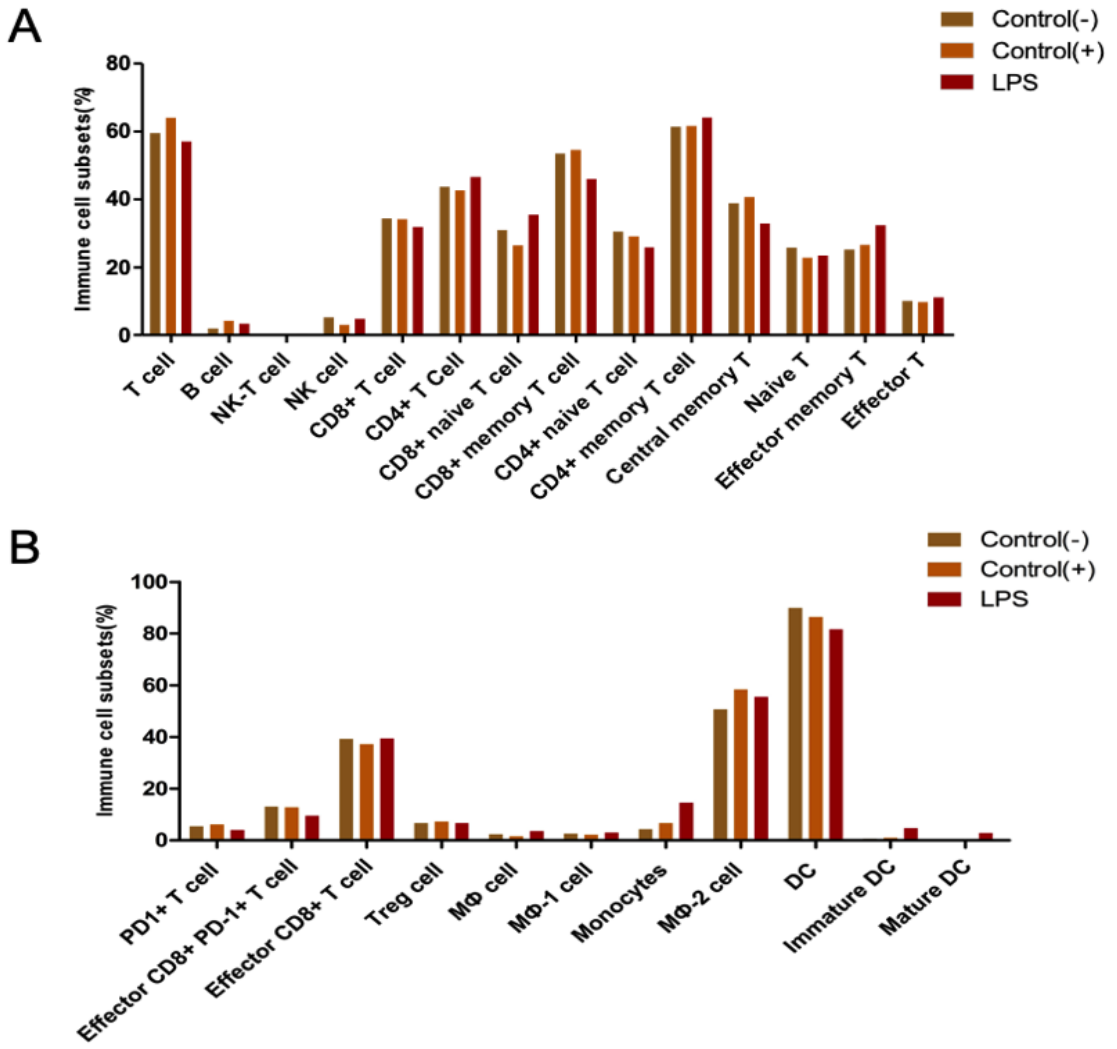

Figure 15 : The differences in cell subtype ratios in Control(-), Control(+) and LPS groups

Fig 15 | **A:** Comparison of the differences in the proportion of cell subtypes among different groups, including T cells, B cells and NK cells. **B:** Comparison of the differences in the proportion of cell subtypes among different groups include Partial T cell subsets, Marcrophage Momocytes and DC.

4.7 RNAseq analysis of VSV-Spike infected cells and SARS-CoV-2 infected people

4.7.1 RNA extraction of cell preparation samples from healthy controls

RNA samples were extracted from the same PBMC samples and healthy controls as used in the flow cytometric experiments reported earlier in the thesis. In 5 groups, P-1: Control (-), P-2: Control (+), P-3: Con A, P-4: LPS, P-5: PMA+ Ionomycin, from 3 independent experiments. RNA was extracted according to the RNA extraction protocol

(specify manufacturer), and the final sample volume was 20ul. Before RNA sequencing, various QC tests were required, including RNA Integrity Number (RIN), concentration and the purity, OD260/280 between 1.8-2.1 (Table 8). The RNA sequencing was completed by Novogene company, the Error Rate, Distribution of A/T/G/C Base and Raw data filtering were passed by protocol, to ensure the validity of the sequencing data.

Table 8: Sample quality inspection

No.	Sample No.	Concentration (ng/μl)	Volume(μl)	RIN	QC Results
P-1	Control(-)	68.31	20	9.8	Pass
P-2	Control(+)	70.52	20	9.2	Pass
P-3	LPS	467.8	20	9.8	Pass
P-4	Con A	359.63	20	9.9	Pass
P-5	PMA+Ionomycin	192.52	20	10	Pass

Before RNA sequencing, the RNA library li needs to go through a variety of QC tests. The key is to assess the integrity of the RNA. The RIN from 1 to 10 indicates the integrity of RNA. The higher the number, the better the integrity. Little RNA degradation is optimal, and the qualified standard is 7. The Integrity test results are pictured for 5 samples (Figure 16); the results of all samples are greater than 9.2.

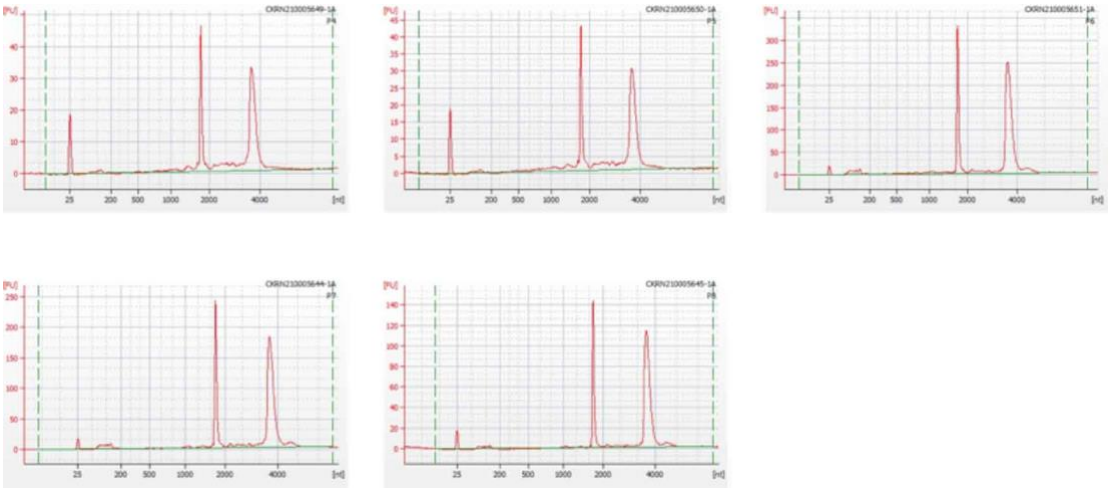

Figure 16: P1 to P5: RNA quality contol with RIN

Fig 16 | Graph of results using Agilent 2100, RIN score for P-1,P-2,P-3,P-4 and P-5 based on an instrument proprietary algorithm.

4.7.2 COVID-19 positive samples

Samples were taken from the 1st, 5th, 10th, and 15th day following admission to the hospital. Two individuals were with four time points were used for this analysis. The samples were from the elderly patients (>65 years old). RNA extraction was performed as mentioned above, and met the quality required by RNA sequencing (Table 9). Before RNA sequencing by the Novogene company, rRNA depletion and DNA library were performed according to the protocol (NEB).

Table 9：Sample quality inspection

No.	Sample No.	Concentration (ng/μl)	volume(μl)	RIN	QC Results
S-1	I4 D1	56.0	20	8.3	Pass
S-2	I4 D5	60.0	20	8.3	Pass
S-3	I4 D10	59.0	20	8.4	Pass
S-4	I4 D15	57.0	20	8.0	Pass
S-5	R4 D1	48.7	20	8.9	Pass
S-6	R4 D5	53.0	20	8.2	Pass
S-7	R4 D10	42.6	20	8.3	Pass
S-8	R4 D15	54.0	20	8.5	Pass

4.8 Analysis of RNA-sequencing data

The samples were sent for sequencing, and the P-1 to P-5 groups analyzed the immune responses induced by VSV-Spike under the function of different drugs; S-1 to S-8 were

samples from patients infected by SARS-CoV-2, which were divided into groups according to the number of days of infection, Two samples per group were analyzed as follows: Group A: Day1 (S-1 and S-5); Group B: Day5 (S-2 and S-6); Group C: Day10 (S-3 and S-7); Group D :Day15 (S-4 and S-8). The control group consisted of samples from healthy controls. The sequenced data of all samples are analyzed and processed by bioinformatics to compare and analyze the immune status of SARS-CoV-2 patients/VSV-Spike group and the main immune signaling pathways affected.

4.8.1 DEG analysis of RNA-sequencing data

After sequencing, the original data was obtained, the data was filtered and normalized, the sequencing reads were aligned to the transcripts, and the number of reads compared with the transcripts were quantified to analyze the differences between the gene/transcript statistics among the sample groups. For differential expression genes analysis, we screened out genes with significantly differential expression and the conditions were set as: p-value<0.05 and |log2| fold change ≥ 2.

4.8.1.1 Analysis of cell culture samples

We set up blank control group A: Control(-) and positive VSV-Spike control group B: Control(+), each two groups were compared, including group C: LPS, group D: Con A, and group E: PMA+Ionomycin, in order to understand the influence of VSV-Spike viral protein on immune-related genes (Figure 17A). Comparing groups A and B, 283 genes were up-regulated and 483 genes were down-regulated; from A to C, 1876 genes were up-regulated and 4746 genes were down-regulated; 3398 genes were down-regulated, whereas 1186 genes were up-regulated from A to D. A to E: 4279 down-regulated genes and 2621 up-regulated genes; B to C: 2127 up-regulated genes and 4200 down-regulated genes; B to D: 1469 down-regulated genes and 2923 up-regulated genes; B to E: 2962 up-regulated genes and 3657 down-regulated genes (Figure 17B). The biggest distinction was seen in A to C and B to C since both immune systems are triggered by LPS, which might increase VSV-ability Spike's to attach to it.

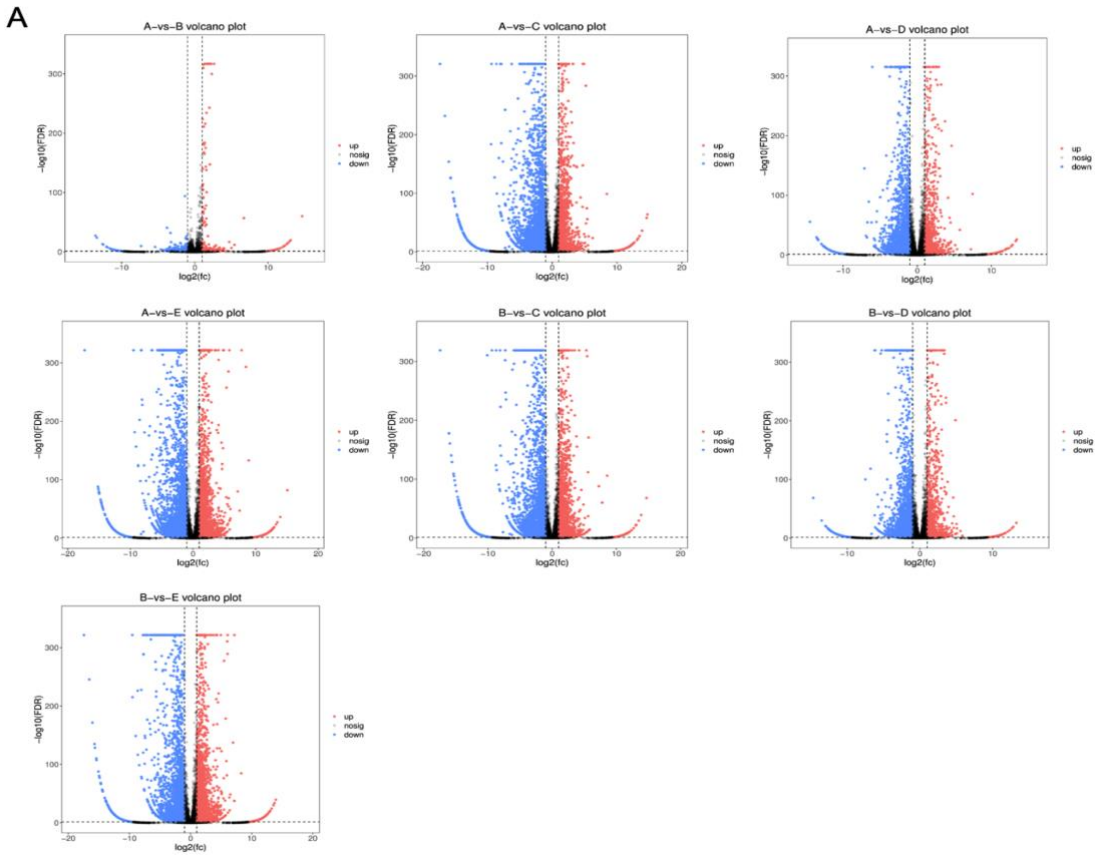

Figure 17: Volcanic map of differential genes

Fig 17 | **A:** Differential gene volcano plot analysis of cell experiments.

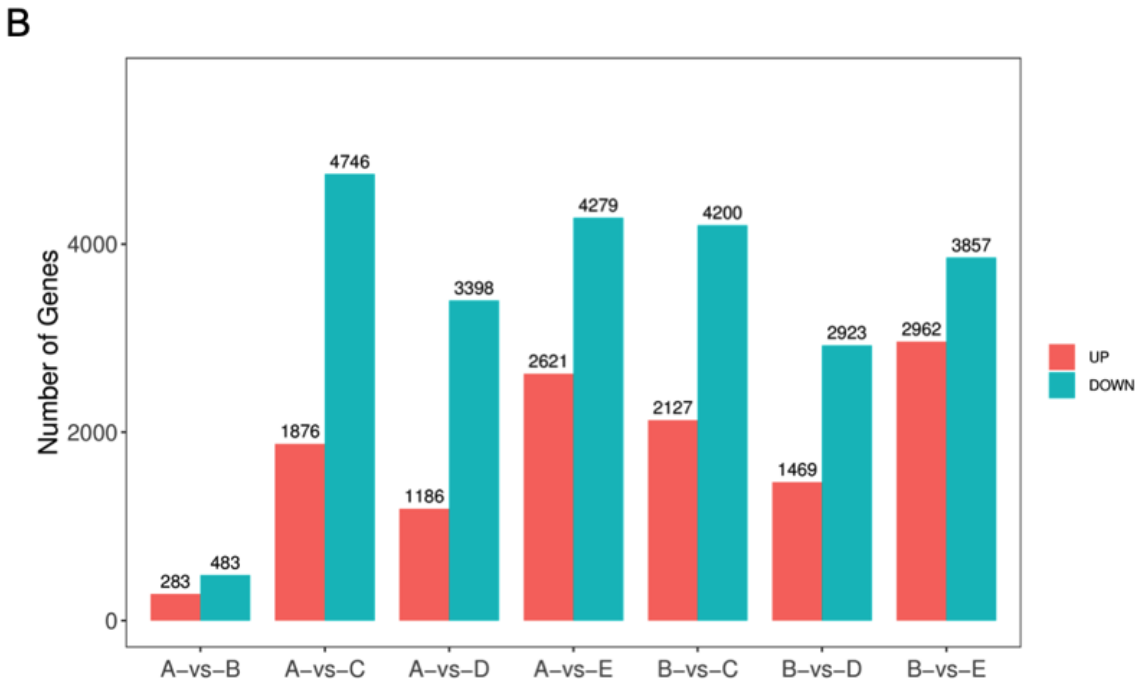

Figure 17: Differential gene expression statistics

Fig 17 | **B:** Histogram of differential genes in volcanic map.

4.8.1.2 Analysis of patient samples

To better understand the expression changes of immune system genes in the elderly after infection with SARS-CoV-2 relative to healthy controls, we compared the gene expression differences of Day1, Day5, Day10 and Day15 and health controls (Figure 18A). Comparing with Day1: 2095 genes were upregulated, 4803 genes were down regulated; To Day5: 1290 genes were up-regulated, 3323 genes were down-regulated; To Day10: 1001 genes up-regulated, 3062 genes were down-regulated; To Day15: 768 genes were up-regulated, 3216 down-regulated genes (Figure 18B). The number of differential genes that are upregulated from Day1 through Day15 becomes progressively smaller, suggesting that the gene changes caused by the virus slowly decrease over time.

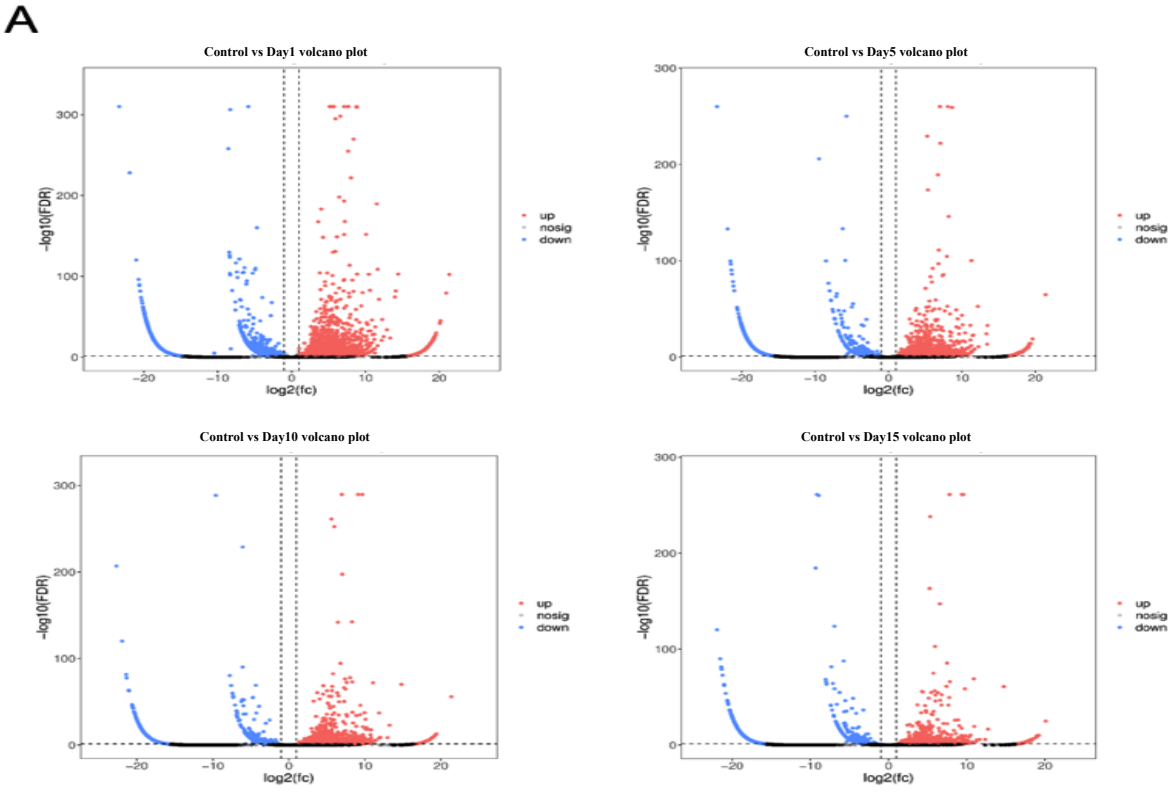

Figure 18: Volcanic map of differential genes

Fig 18 | **A:** Differential gene volcano plot analysis of COVID-19 compared to healthy groups after different days of infection. Days 1, 5, 10 and 15 following hospital admission.

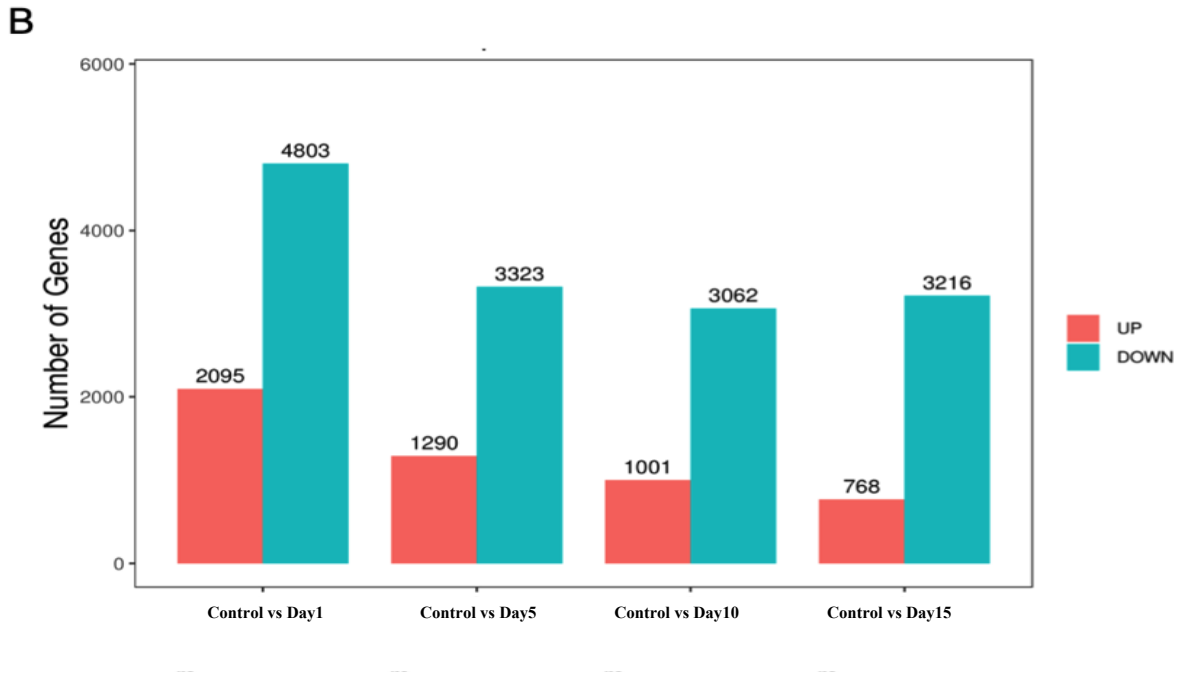

Figure 18: Differential gene expression statistics

Fig 18 | **B:** Histogram of differential genes in volcanic map

4.8.2 Venn analysis

Venn analysis is a cluster analysis of differential genes. Compared with A and B can intuitively see the whole impact of VSV-Spike on genes, but after the addition of LPS stimulation in group C, the gene changes after the combination of immune cells and spike can be seen. To determine the genes that changed significantly in the VSV-Spike group compared with the blank group after immune activation: A to C and B to C groups can exclude the effect of LPS alone on gene differences, so as to find out the genes that changed significantly in the VSV-Spike group compared with the blank group after immune activation. In this study, Venn analyses of the common differential genes among different groups of A and B, A and C, B and C found a total of 205 key common genes (Figure 19A), which were compared with the genetic changes of patients with COVID-19 on the Day 1, Day 5, Day 10, and Day 15 after hospital admission. A total of 3182 key common genes were found (Figure 19B). The key gene changes stimulated by SARS-CoV-2 spike protein in cell experiments or caused by COVID-19 patients with SARS-CoV-2 have importantly elucidate how SARS-

CoV-2 invades the human immune system and how the immune system fights the virus, especially with relation to determining how the key common genes plays a crucial role in the study of the pathogenic mechanism of the virus. Therefore, the intersection of 205 genes and the 3182 genes of patients were subjected to venn analysis, and the 38 genes with the most correlation were found (Fig C).

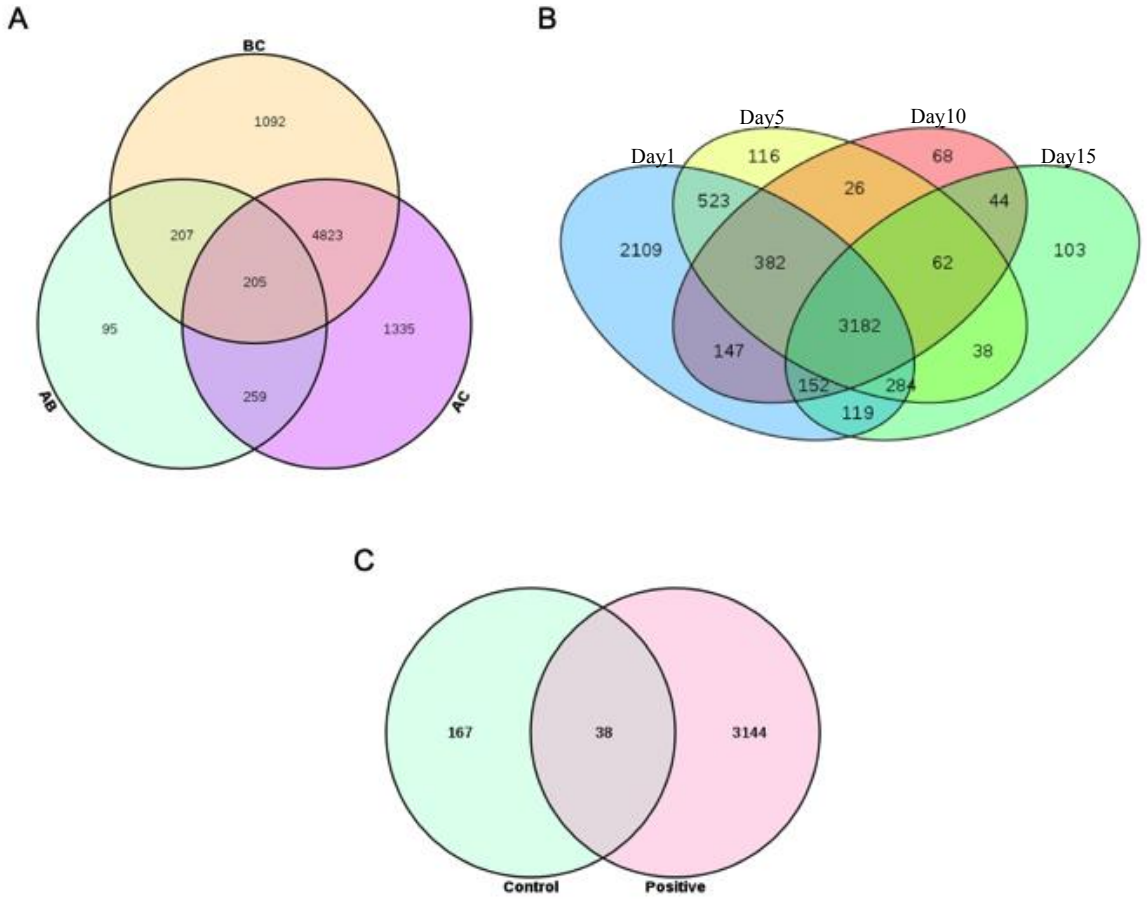

Figure 19: Venn difference analysis

Fig 19 | Venn difference analysis: **A:** Venn analysis of cell experiments **B:** Venn analysis of COVID-19 patients compared to healthy controls on different days after infection. **C:** Venn analysis of common key genes in cell experiments and COVID-19.

We performed gene function analysis on these 38 genes and found that all these genes are related to immune and antiviral functions, Among the 38 common genes, 29 genes were

less-regulated and 9 genes were high-regulated; the 29 less-regulated genes included CXCL10, HSH2D and CCL8. Genes related to adaptive immunity were mostly less-regulated. On the other hand, among the 9 high-regulated genes, two genes, IFI35 and SAMD9L which are related to macrophage and innate immunity, were activated.

The results suggest that innate immunity plays a very important antiviral role in the cellular experiments in which the spike protein activates the immune response or immune system in the COVID-19 patients, and that adaptive immunity may be inhibited in the initial phase of the antiviral response. In innate immunity, a variety of innate immune cells such as macrophages, dendritic cells, natural killer cells, etc. are activated, with macrophages, which promote the release of inflammation, being more activated due to their high expression of ACE2, and associated genes such as IFI35 and SAMD9L are all upregulated, which is particularly important for elderly COVID-19 patients, to resist the virus, but down-expression of inflammatory factors CXCL10, HSH2D, and CCL8, for the elderly, their innate immune system is vulnerable, and the inflammatory factors are down-regulated, which puts them at a disadvantage in resisting the COVID-19. From this point of view, the use of targeted drugs that boost the inflammatory factors of the innate immune system could reduce the severity and mortality of COVID-19 in the elderly.

Table 10：The 38 genes with the most correlation

Gene ID	Gene Name	Gene Function	log2(fc)	Regulation Type	p-Value
ENSG00000078081.8	**LAMP3**	Immature DCs efficiently and induce primary T-cell responses	-16.80233965	Down	2.76E-07
ENSG00000169245.6	**CXCL10**	Stimulation of monocytes, natural killer and T-cell migration	-17.3124753	Down	4.73E-10
ENSG00000196684.12	**HSH2D**	T-cell activation	-16.63040934	Down	1.17E-06
ENSG00000108691.9	**CCL2**	Activity for monocytes and basophils	-17.04633536	Down	8.05E-09
ENSG00000108700.5	**CCL8**	Chemotactic activity for monocytes, lymphocytes, basophils and eosinophils	-16.03036539	Down	8.99E-05
ENSG00000168961.17	**LGALS9**	Immunodeficiency	-17.14390133	Down	3.94E-09

ENSG00000134321.12	**RSAD2**	Cellular antiviral response and innate immune signaling	-17.72640445	Down	4.20E-13
ENSG00000089127.13	**OAS1**	Associated with susceptibility to viral infection	-16.90548103	Down	6.74E-08
ENSG00000111331.13	**OAS3**	Inhibition of cellular protein synthesis and viral infection resistance	-18.87369643	Down	7.87E-28
ENSG00000181381.13	**DDX60L**	Anti-viral immunity	-17.44540289	Down	5.71E-11
ENSG00000137965.11	**IFI44**	Immune response	-17.65592198	Down	1.71E-12
ENSG00000137959.16	**IFI44L**	Defense response to virus	-18.98740281	Down	6.50E-30
ENSG00000138646.9	**HERC5**	Antiviral immune response	-16.36033272	Down	1.02E-05
ENSG00000185885.16	**IFITM1**	Interferon induced antiviral proteins	-5.34357361	Down	2.20E-26
ENSG00000157601.14	**MX1**	Cellular antiviral response	-18.79245988	Down	2.43E-26
ENSG00000183486.13	**MX2**	Upregulated by interferon-alpha	-4.530033575	Down	8.79E-08
ENSG00000119917.14	IFIT3	Negative regulation of cell population proliferation	-5.788442371	Down	2.97E-16
ENSG00000130813.18	SHFL	Inhibits viral replication	-17.37839647	Down	2.31E-10
ENSG00000189060.5	H1F0	Responsible for the nucleosome structure	-4.978415863	Down	3.43E-09
ENSG00000205413.8	SAMD9	Regulating cell proliferation and apoptosis	-18.08565917	Down	1.95E-16
ENSG00000111275.13	ALDH2	Active form of the mitochondrial isozyme	-16.02756048	Down	8.99E-05
ENSG00000137628.17	DDX60	RNA binding	-17.67065625	Down	1.69E-12
ENSG00000126709.15	IFI6	Regulation of apoptosis	-17.7412958	Down	2.09E-13
ENSG00000172183.15	ISG20	Negative regulation of viral genome replication	-17.3940607	Down	1.15E-10
ENSG00000187608.9	ISG15	Chemotactic activity towards neutrophils	-17.06086478	Down	1.61E-08
ENSG00000130589.16	HELZ2	Nuclear transcriptional co-activator	-3.322440774	Down	3.22E-12
ENSG00000108771.13	DHX58	Negative regulation of type I interferon production	-16.36666372	Down	1.02E-05
ENSG00000133106.14	EPSTI1	Promote tumor invasion	-17.87147213	Down	2.57E-14
ENSG00000152778.9	IFIT5	Negative regulation of viral genome replication	-3.964586242	Down	0.000102817
ENSG00000068079.7	**IFI35**	Macrophage activation	2.021925990	Up	5.54E-58

ENSG00000177409.12	**SAMD9L**	Innate immune response to viral infection	2.188065910	Up	8.89E-34
ENSG00000130513.6	GDF15	Pleiotropic cytokine	5.000341248	Up	1.41E-19
ENSG00000145020.15	AMT	Glycine encephalopathy	6.283362522	Up	3.70E-28
ENSG00000279833.1	AL031846.2	LncRNA	5.353046431	Up	2.85E-61
ENSG00000176020.8	AMIGO3	Positive regulation of synapse assembly	3.844269865	Up	7.96E-05
ENSG00000121454.6	LHX4	Control of differentiation	6.807247737	Up	1.32E-30
ENSG00000042062.12	RIPOR3	Protein coding	5.173175591	Up	1.43E-09
ENSG00000228492.2	RAB11FIP1P1	Processed pseudogene	4.839097834	Up	1.26E-10

4.8.3 PPI network analysis of the 38 key genes

Thirty-eight key genes were analyzed using the PPI network method and divided into 3 clusters using the online STRING database program (https://string-db.org/). The 38 key genes involved in the biological process are mostly related to response to virus, defense response to virus, and response to type I interferon, according to the results of functional enrichment and signaling pathway analysis. RNA helicase activity, double-stranded RNA binding, and RNA binding were the key molecular functions. Influenza A, RIG-I-like receptor signaling pathway, and viral protein interaction with cytokines and cytokine receptors were the primary KEGG pathways. Interferon alpha/beta signaling, interferon signaling, and cytokine signaling in the immune system were the key Reactome Pathways. The primary annotated keywords were immunity, innate immunity, and antiviral defense (Table 11).

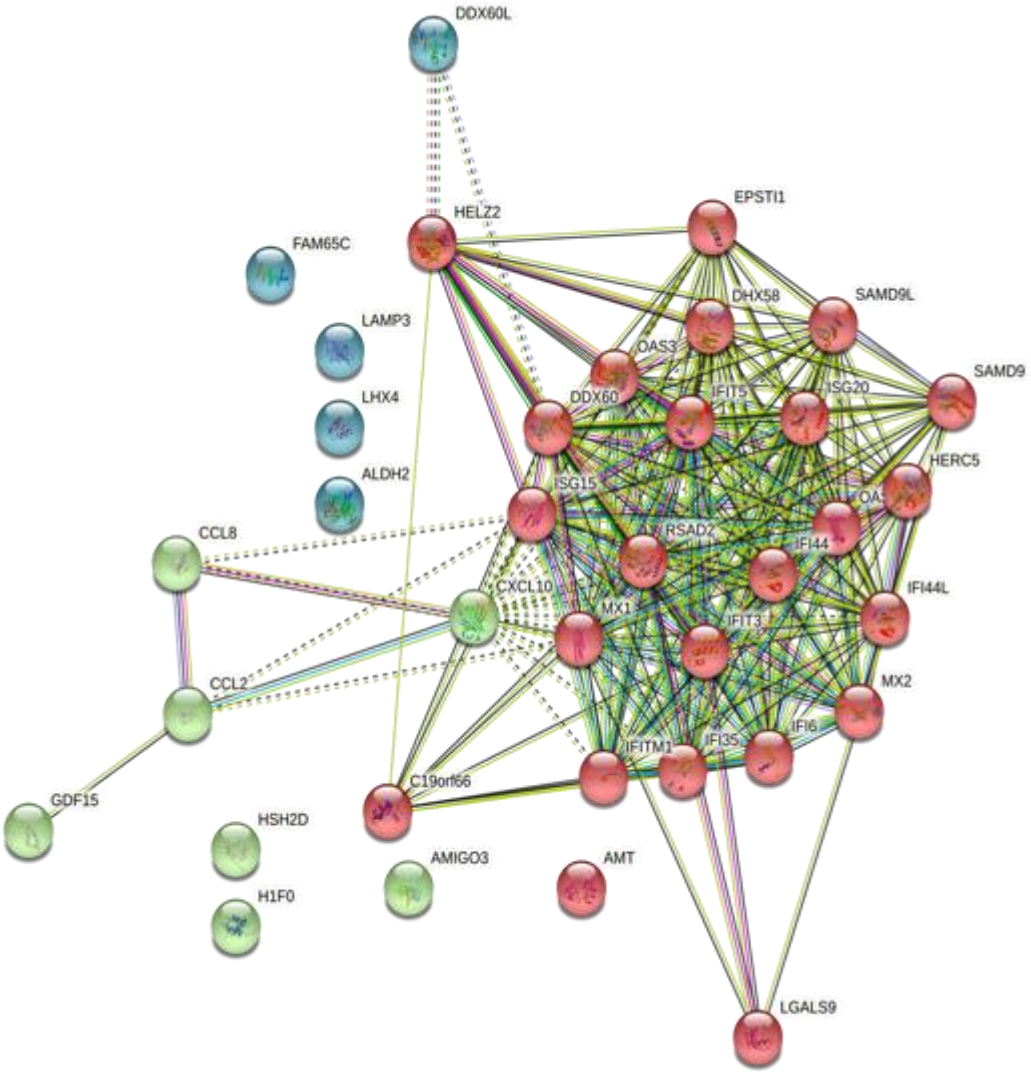

Figure 20: The PPI interaction network

Fig 20 | The nodes represent the different proteins; the lines between the nodes represent the interactions between the proteins.

Table 11. The 38 genes enrichment in network.

Term		Description	Strength	False Discovery Rate
Biological Process	**GO:0009615**	Response to virus	1.57	4.71e-23
	GO:0051607	Defense response to virus	1.64	3.00e-20
(Gene Ontology)	**GO:0034340**	Response to type I interferon	1.96	8.34e-17
Term		**Description**	**Strength**	**False Discovery Rate**
Molecular Function	**GO:0003724**	RNA helicase activity	1.46	0.0402
	GO:0003725	Double-stranded RNA binding	1.47	0.0402
(Gene Ontology)	**GO:0003723**	RNA binding	0.6	0.0402
Term		**Description**	**Strength**	**False Discovery Rate**

KEGG Pathways	**hsa05164**	Influenza A	1.36	8.02e-06
	hsa04622	RIG-I-like receptor signaling pathway	1.37	0.0272
	hsa04061	Viral protein interaction with cytokine and cytokine receptor	1.23	0.0443
Term		**Description**	**Strength**	**False Discovery Rate**
Reactome Pathways	**HSA-909733**	Interferon alpha/beta signaling	1.98	2.66e-17
	HSA-913531	Interferon Signaling	1.56	3.20e-14
	HSA-1280215	Cytokine Signaling in Immune system	1.11	1.50e-11
Term		**Description**	**Strength**	**False Discovery Rate**
Annotated Keywords (UniProt)	**KW-0051**	Antiviral defense	1.84	1.18e-22
	KW-0399	Innate immunity	1.37	1.24e-13
	KW-0391	Immunity	1.22	1.24e-13

4.8.4 Immune cell type enrichment analysis

Analysis of the changes in immune cell subsets of RNAseq data obtained from clinical COVID-19 patients and healthy controls, contributes to our understanding of immune system resistance to SARS-CoV-2.

4.8.4.1 Analysis of the enrichment of different subsets of immune cells

To compare the differences in immune cell types between the cell experiment group with COVID-19 sample group, it is important to choose an appropriate immune scoring tool. Common tools used to determine immune cell ratios have been studied and compared. including for example: Heatmap for immune responses based on TIMER, CIBERSORTx, QUANTISEQ, MCP-counter, xCell and other tools [201].

A cell population's immune cell density can be calculated using gene expression data via the analytic program CIBERSORTx. After CIBERSORTx analysis, it is possible to assess changes and proportions of cell type expression. From one to fifteen days following infection, eight COVID-19 samples were used for this investigation. Five samples were collected from the healthy control group, and their exon fragments per kilobase per million mapped fragments (FPKM) analysis was used.

The results showed that cells related to innate immunity accounted for a relatively large proportion in the COVID-19 group, while cells related to adaptive immunity accounted for a relatively large proportion in the healthy control group (Figure 21,22).

Input Sample	B cells naive	B cells memory	Plasma cells	T cells CD8	T cells CD4 naive	T cells CD4 memory resting	T cells CD4 memory activated	T cells follicular helper	T cells regulatory (Tregs)	T cells gamma delta	NK cells resting	NK cells activated	Monocytes	Macrophages M0	Macrophages M1	Macrophages M2	Dendritic cells resting	Dendritic cells activated	Mast cells resting	Mast cells activated	Eosinophils	Neutrophils	P-value	Correlation
Healthy-1	0.048	0	0	0.104	0	0	0.215	0.009	0.025	0	0	0.061	0.009	0.005	0.015	0	0	0	0	0.009	0	0.000	0.000	0.830
Healthy-2	0.027	0.001	0	0.247	0	0	0.228	0.059	0.179	0	0.075	0.008	0.017	0.022	0.023	0.003	0	0.006	0.001	0	0	0.003	0.000	0.754
Healthy-3	0.056	0	0	0.104	0	0	0.293	0.019	0.002	0	0.006	0	0.008	0	0.001	0	0	0.001	0	0.011	0	0.000	0.000	0.706
Healthy-4	0.07	0.039	0	0.21	0	0.096	0.097	0	0.13	0	0.03	0.136	0.012	0.092	0.023	0	0	0.042	0.012	0	0.011	0.000	0.000	0.747
Healthy-5	0.063	0.022	0	0.213	0.083	0	0.181	0	0.094	0	0.022	0.117	0.009	0.086	0.043	0	0	0.037	0.026	0	0.003	0.000	0.000	0.737
COVID.19.S1.D1	0	0.038	0.006	0.242	0	0	0	0.027	0.096	0	0	0.153	0.173	0.081	0	0	0.014	0.063	0.093	0	0	0.014	0.092	0.114
COVID.19.S1.D2	0.025	0.018	0	0.108	0	0.161	0	0.095	0	0	0	0.079	0.035	0	0.03	0	0.045	0.131	0	0.2	0.021	0.050	0.369	0.042
COVID.19.S1.D3	0	0.086	0.041	0	0	0.338	0	0	0	0.018	0	0.054	0.247	0.112	0.029	0	0	0.028	0	0.036	0.013	0.000	0.211	0.071
COVID.19.S1.D4	0.004	0.083	0.008	0	0.208	0	0	0	0.113	0	0.069	0.099	0	0.232	0	0.105	0.014	0	0	0	0	0.067	0.119	0.101
COVID.19.S2.D1	0	0.095	0	0.024	0.071	0	0	0.017	0.005	0.007	0	0.055	0	0	0	0.104	0.029	0.024	0.047	0.003	0	0.520	0.259	0.058
COVID.19.S2.D2	0	0.162	0.018	0	0	0.187	0	0	0.009	0	0.138	0	0.077	0	0	0.028	0.072	0.081	0	0.079	0.05	0.098	0.287	0.053
COVID.19.S2.D3	0.014	0.076	0.039	0.119	0	0.125	0	0.062	0.006	0	0	0.064	0.113	0.114	0.044	0.032	0.073	0	0.051	0	0	0.068	0.224	0.067
COVID.19.S2.D4	0	0.068	0.075	0.138	0.213	0	0	0.043	0	0	0.1	0.014	0.063	0.007	0.011	0	0.048	0.036	0.152	0	0	0.032	0.300	0.051

Figure 21: Comparing proportions of immune cell types in COVID-19 and healthy controls

Fig 21 | Relative proportions of 22 immune cells in COVID-19 and healthy controls.

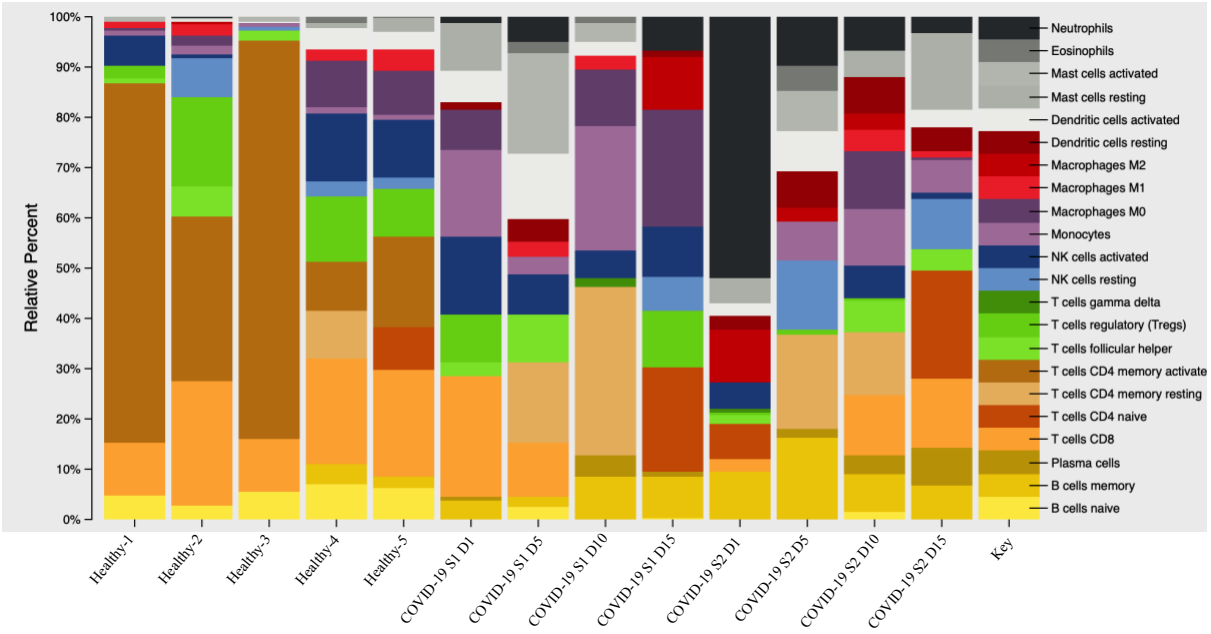

Figure 22: Comparing abundance of immune cell types in COVID-19 and healthy controls

Fig 22 | Bar charts of 22 immune cell proportions in COVID-19 and healthy controls.

4.8.4.2 Heatmap of immune cell type enrichment analysis

xCell is an optimized tool that can reliably describe the expression profile of immune cells based on gene signatures. In this study, the xCell webtool platform was used, and 64 Immune and stromal cell types were extracted from the gene expression data for enrichment analysis. After data processing, heat map analysis was performed and weak signatures were filtered. The findings indicated that the expression of DC, monocytes, epithelial, endothelial, and eosinophil cells, as well as other innate immune cells, was considerably elevated in the COVID-19 group, indicating that innate immunity may be involved in viral infection. B cells, CD4+ T cells, CD8+ T cells, and other adaptive immune cells were also downregulated (Figure 23), which suggests that SARS-CoV-2 may be inhibiting host adaptive immune function. The results were similar to those in the cell experimental group. The results of flow cytometric analysis of LPS-stimulated S protein in PBMC were similar, but no significant changes were found in macrophages in COVID-19; furthermore NK cells were significantly downregulated, indicating that innate immunity plays an important role in the antiviral process. The role is very complex and further research is needed.

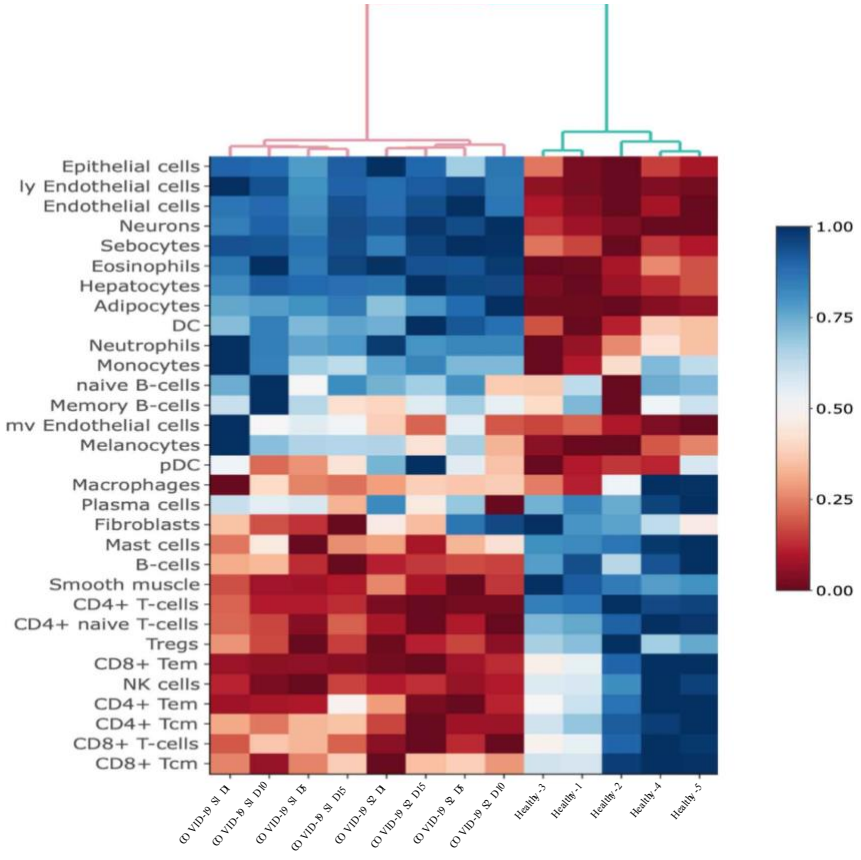

Figure 23: Heatmap of immune cell types in COVID-19 and healthy controls

Fig 23 | The bluer the color, the higher the frequency of expression, and the redder the color, the lower the frequency of expression.

4.8.4.3 Intergroup plot of immune cell type enrichment analysis

Differences exist in the expression of many immune cell markers between COVID-19 patients and healthy controls. The expressions of 21 distinct immune cell markers were noticeably different, as shown in (Figure 24). The expression of six different immune cell markers—basophils, DC, monocytes, NKT, neutrophils, and pro-B cells—is noticeably greater in the COVID-19 group. When compared to healthy controls, 13 different immune cell markers—B cells, CD4+ T cells, CD4+ Tcm, CD4+ Tem, CD4+ memory T cells, CD4+ nave T cells, CD8+ T cells, CD8+ Tcm, CD8+ Tem, Mast cells, NK cells, Th1 cells, Th2 cells, and Tregs—have a reduced expression. The findings demonstrate that innate immune cells, particularly DC, monocytes, NKT, neutrophils, etc., are crucial in preventing SARS-CoV-2 from replicating.

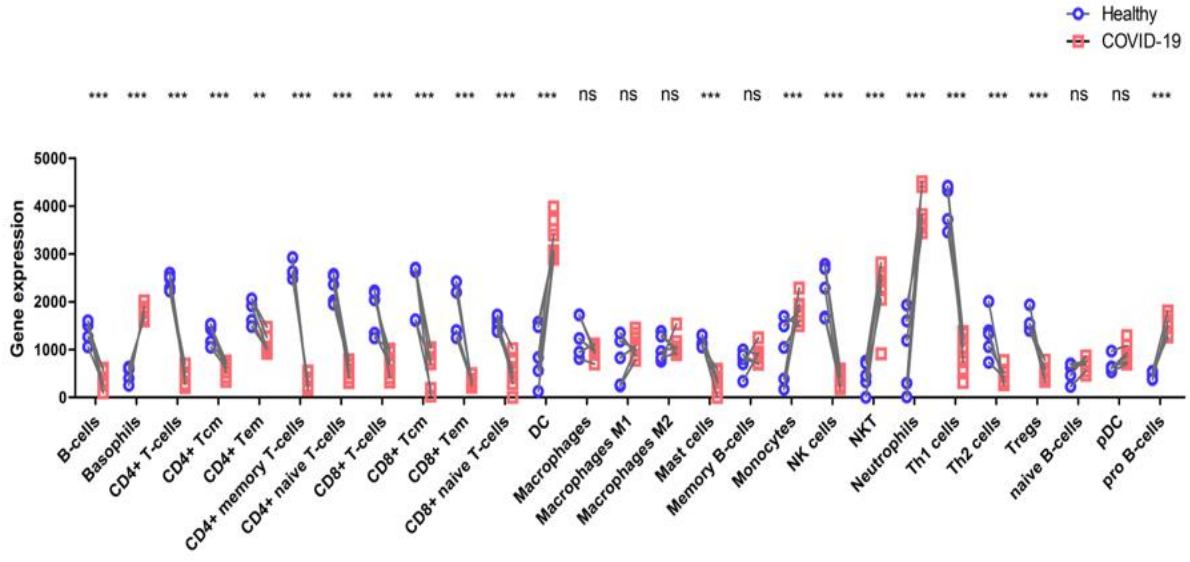

Figure 24: Intergroup plot of immune cell types in COVID-19 and healthy controls

Fig 24 | Blue circles represent data from healthy samples and red boxes represent data from COVID-19 samples, Differential expression of different immune cell types between COVID-19 and healthy controls. *means $P < 0.05$, **means $P < 0.01$, ***means $P < 0.001$, ns $P > 0.05$ no significant difference.

4.8.5 38 key genes Immunological clinical indication gene analysis

After obtaining 38 key genes, we analyzed the main characteristics of gene groups in COVID-19 and healthy controls, and used Spearman correlation to analyze the group relationship between key genes and subsets of immune cells while screening out immune-related hub genes. The *p*-value < 0.05 was considered statistically significant. ROC (Receiver Operating Characteristic) analysis was used to reveal the clinical relationship between hub genes and SARS-CoV-2.

4.8.5.1 PCA analysis of 38 key genes

PCA (Principal Components Analysis) can extract the two eigenvectors that best reflect the data characteristics from the data to show the difference between the data. Comparing the 38 key genes of the COVID-19 patients and healthy control groups shows can be found that principal component 1 (PC1) can reflect 80.4% of the feature differences, and principal component 2 (PC2) can reflect 10.5% of the feature differences of the data.

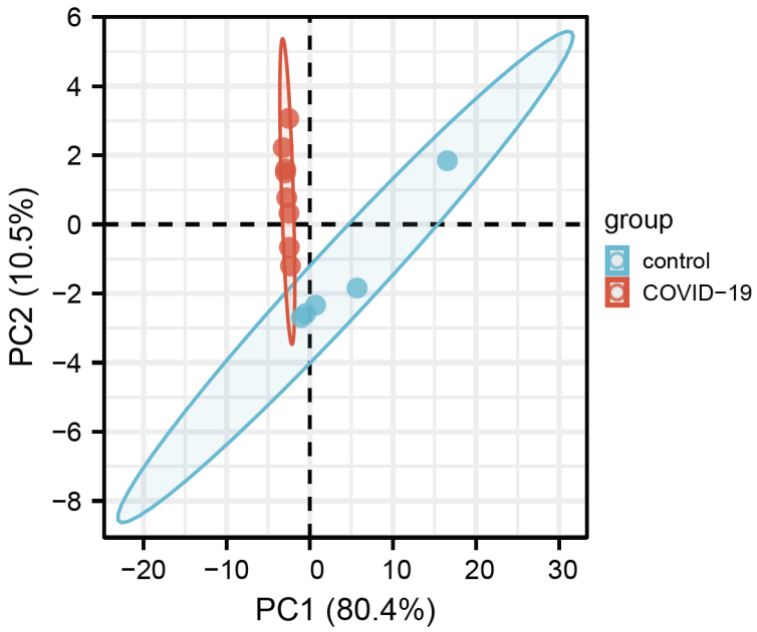

Figure 25: PCA analysis of 38 key genes in COVID-19 patients and healthy controls

Fig 25 | PCA diagram. Blue represents the healthy control group and red represents the COVID-19 group.

4.8.5.2 Correlation between 38 key genes and innate immune cell subsets

Through the correlation analysis among innate immune cell subsets (dendritic cells, monocytes, macrophages, mast cells, and neutrophils) and 38 key genes, the results showed that a large number of genes in dendritic cells resting and neutrophils were significantly correlated, and other innate immune cell subsets were not closely correlated. SPSS 26.0 was performed for data analysis. Using Spearman correlation analysis, 38 key and innate immune cell subsets correlation. Value of $p < 0.05$ was considered statistically significant.

Table 12. Correlation analysis between the 38 key genes and immune cell subtypes (Significant differences marked in red).

Immune Cell Type	Dendritic cells resting		Dendritic cells activated		Monocytes		Macrophages M0		Macrophages M1		Macrophages M2		Mast cells resting		Neutrophils	
Gene ID	SC	*P*-Value	SC	*P*-Value	SC	*P*-Value	SC	*P*-Value	SC	*P*-Value	SC	*P*-Value	SC	*P*-Value	SC	*P*-Value
RIPOR3	0.317	0.292	0.216	0.479	0.163	0.596	0.269	0.374	-0.001	0.996	0.121	0.694	0.252	0.407	0.359	0.228
IFI35	-0.75	0.003	-0.091	0.767	-0.37	0.213	0.052	0.865	0.349	0.242	-0.371	0.211	-0.069	0.822	-0.712	0.006
LAMP3	-0.75	0.003	-0.091	0.767	-0.37	0.213	0.052	0.865	0.349	0.242	-0.371	0.211	-0.069	0.822	-0.712	0.006
OAS1	-0.75	0.003	-0.091	0.767	-0.37	0.213	0.052	0.865	0.349	0.242	-0.371	0.211	-0.069	0.822	-0.712	0.006
CCL2	-0.75	0.003	-0.091	0.767	-0.37	0.213	0.052	0.865	0.349	0.242	-0.371	0.211	-0.069	0.822	-0.712	0.006
CCL8	-0.75	0.003	-0.123	0.689	-0.364	0.222	0.033	0.914	0.343	0.251	-0.339	0.257	-0.076	0.806	-0.693	0.009
DHX58	-0.75	0.003	-0.091	0.767	-0.37	0.213	0.052	0.865	0.349	0.242	-0.371	0.211	-0.069	0.822	-0.712	0.006
ALDH2	-0.75	0.003	-0.072	0.814	-0.37	0.213	0.043	0.889	0.318	0.29	-0.371	0.211	-0.076	0.806	-0.712	0.006
OAS3	-0.531	0.062	0.228	0.453	-0.287	0.342	-0.151	0.621	0.539	0.057	-0.48	0.097	-0.217	0.477	-0.553	0.05
IFIT3	-0.688	0.009	0.09	0.77	-0.161	0.598	0.121	0.693	0.2	0.513	-0.449	0.123	0.154	0.616	-0.682	0.01
LHX4	0.824	0.001	0.221	0.468	0.336	0.262	0.025	0.935	-0.181	0.554	0.435	0.137	0.563	0.045	0.808	0.001
IFI6	-0.613	0.026	0.162	0.597	-0.305	0.311	-0.079	0.798	0.509	0.076	-0.449	0.123	-0.166	0.587	-0.608	0.027
GDF15	0.483	0.095	0.26	0.392	0.165	0.59	0.098	0.751	-0.396	0.181	0.36	0.227	0.147	0.631	0.599	0.03
HELZ2	-0.437	0.136	-0.076	0.806	0.172	0.575	0.503	0.08	0.573	0.04	-0.178	0.561	0.341	0.254	-0.456	0.118
C19orf66	-0.512	0.074	-0.134	0.663	-0.229	0.453	0.135	0.661	0.645	0.017	-0.292	0.334	-0.008	0.98	-0.562	0.046
EPSTI1	-0.75	0.003	-0.091	0.767	-0.37	0.213	0.052	0.865	0.349	0.242	-0.371	0.211	-0.069	0.822	-0.712	0.006
RSAD2	-0.572	0.041	0.222	0.466	-0.305	0.311	-0.121	0.693	0.515	0.072	-0.48	0.097	-0.188	0.537	-0.59	0.034
DDX60	-0.75	0.003	-0.091	0.767	-0.37	0.213	0.052	0.865	0.349	0.242	-0.371	0.211	-0.069	0.822	-0.712	0.006
IFI44L	-0.572	0.041	0.21	0.491	-0.299	0.321	-0.106	0.73	0.527	0.064	-0.48	0.097	-0.188	0.537	-0.59	0.034
IFI44	-0.75	0.003	-0.091	0.767	-0.37	0.213	0.052	0.865	0.349	0.242	-0.371	0.211	-0.069	0.822	-0.712	0.006
HERC5	-0.75	0.003	-0.091	0.767	-0.37	0.213	0.052	0.865	0.349	0.242	-0.371	0.211	-0.069	0.822	-0.712	0.006
AMT	0.471	0.104	0.133	0.666	0.303	0.315	0.139	0.65	-0.326	0.277	0.282	0.351	0.338	0.259	0.52	0.069
IFIT5	-0.716	0.006	0.036	0.907	-0.209	0.492	0.103	0.738	0.227	0.456	-0.449	0.123	0.101	0.744	-0.707	0.007
MX1	-0.653	0.015	0.096	0.755	-0.329	0.272	-0.064	0.836	0.485	0.093	-0.449	0.123	-0.166	0.587	-0.645	0.017
LGALS9	-0.75	0.003	-0.091	0.767	-0.37	0.213	0.052	0.865	0.349	0.242	-0.371	0.211	-0.069	0.822	-0.712	0.006
CXCL10	-0.75	0.003	-0.11	0.72	-0.389	0.189	0.04	0.898	0.343	0.251	-0.404	0.171	-0.092	0.764	-0.731	0.004
ISG20	-0.75	0.003	-0.091	0.767	-0.37	0.213	0.052	0.865	0.349	0.242	-0.371	0.211	-0.069	0.822	-0.712	0.006
AMIGO3	0.497	0.084	0.333	0.266	0.42	0.153	0.137	0.655	-0.126	0.682	0.183	0.55	-0.177	0.562	0.466	0.108
SAMD9L	-0.75	0.003	-0.091	0.767	-0.37	0.213	0.052	0.865	0.349	0.242	-0.371	0.211	-0.069	0.822	-0.712	0.006
DDX60L	-0.559	0.047	-0.234	0.441	-0.239	0.431	0.224	0.462	0.545	0.054	-0.228	0.453	0.069	0.822	-0.584	0.036
MX2	-0.555	0.049	0.198	0.518	-0.433	0.14	-0.227	0.456	0.435	0.137	-0.384	0.195	-0.141	0.645	-0.49	0.089
IFITM1	-0.696	0.008	-0.051	0.868	-0.614	0.026	-0.109	0.723	0.289	0.337	-0.248	0.414	-0.193	0.527	-0.541	0.056
ISG15	-0.694	0.008	0.042	0.892	-0.359	0.229	-0.064	0.836	0.448	0.125	-0.449	0.123	-0.166	0.587	-0.682	0.01
H1F0	-0.745	0.004	-0.012	0.969	-0.305	0.311	0.021	0.945	0.188	0.539	-0.511	0.074	-0.003	0.992	-0.768	0.002
HSH2D	-0.75	0.003	-0.091	0.767	-0.37	0.213	0.052	0.865	0.349	0.242	-0.371	0.211	-0.069	0.822	-0.712	0.006
SAMD9	-0.75	0.003	-0.091	0.767	-0.37	0.213	0.052	0.865	0.349	0.242	-0.371	0.211	-0.069	0.822	-0.712	0.006
RAB11FIP1P1	0.509	0.076	0.022	0.943	0.388	0.19	0.407	0.168	0.022	0.942	0.473	0.103	0.084	0.785	0.565	0.044
AL031846.2	0.523	0.067	0.403	0.172	0.38	0.201	0.114	0.71	-0.162	0.598	0.222	0.465	0.205	0.501	0.56	0.047

4.8.5.3 Venn difference analysis of correlation genes

Venn analysis of common key genes in dendritic cells resting and neutrophils. A total of 38 key genes and 29 significantly related genes were found in dendritic cells resting, while 31 significantly related genes were found in neutrophils and 27 common hub genes were found.

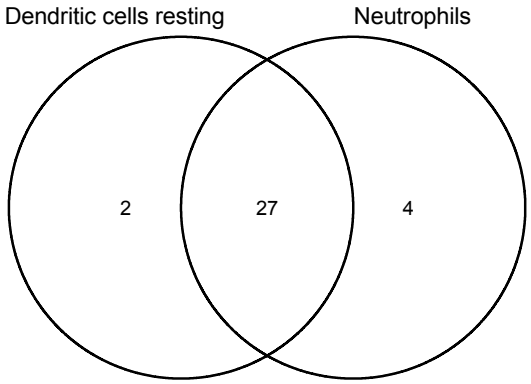

Figure 26: Venn difference analysis

Fig 26 | Venn analysis of common hub genes in Dendritic cells resting and Neutrophils.

4.8.5.4 ROC analysis of hub gene

ROC analysis was performed on the hub genes, and the area under the ROC curve was between 0.5 and 1. The closer the AUC is to 1, the higher the close correlation between the gene and the disease. Results showed some correlation among LAMP3 (AUC=0.775, CI=0.431-1.000), MX1 (AUC=0.725, CI=0.378-1.000), SAMD9L (AUC=0.850, CI=0.593-1.000) and CXCL10 (AUC=0.825, CI=0.479 -1.000), while SAMD9 (AUC = 0.925, CI = 0.783-1.000) has a higher correlation. Joint ROC analysis showed that AUC=1, suggesting that innate immunity-related hub genes are highly correlated with clinical diagnostic indicators of SARS-CoV-2.

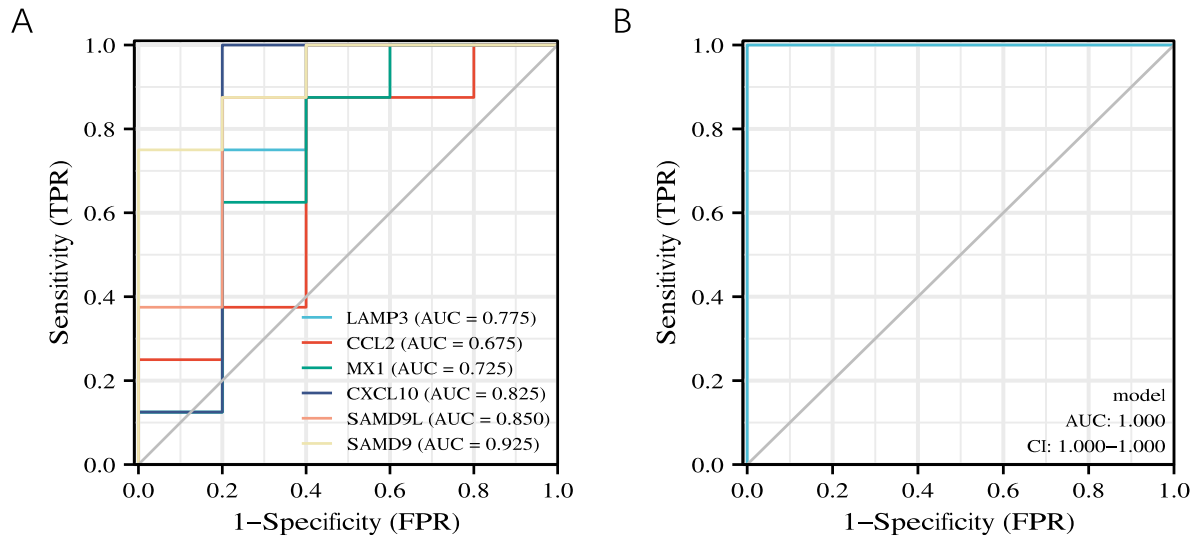

Figure 27: ROC analysis of hub gene

Fig 27 | **A:** ROC curves of the hub genes in COVID-19 patients compared to healty control. **B:** The joint ROC curves of the hub genes relate to innate immunity.

4.8.6 Toll-like receptor signal pathway analysis

The TLR signaling pathway is essential for the elimination of SARS-CoV-2 and other pathogenic bacteria. TLRs can bind to viral ssRNA/dsRNA and S, E, and N proteins to form complexes via MyD88 or TRIF, to activate NF-κB and other signaling pathways, and then activate type I and III interferon or downstream proinflammatory cytokines.

An impaired type I interferon response was seen in individuals with severe and serious COVID-19, although the production of the inflammatory molecules TNF-α and IL-6 was elevated [202]. The specific mechanism is uncertain; however, it may be caused by the suppression SARS-CoV-2 of TLR signaling. Patients who are obese or elderly experience the same [203]. Additionally, a delayed type I interferon response can cause tissue damage and inflammation while failing to suppress the infection [204].

In this study, samples from senior COVID-19 patients and healthy controls were chosen as the experimental group on the first, fifth, and tenth and fifteenth days following SARS-CoV-2 infection. After RNA sequencing, TLR pathway analysis was performed. TLRs become active on day 1 following SARS-CoV-2 infection, activating the NF-κB pathway through the downstream MyD88 complex and releasing inflammatory factors including TNF-

α and IL-8. However, because TLRs are unable to activate IRF3/7, type I interferon activation is unsuccessful (IFN-α and IFN-β) (Figure 28).

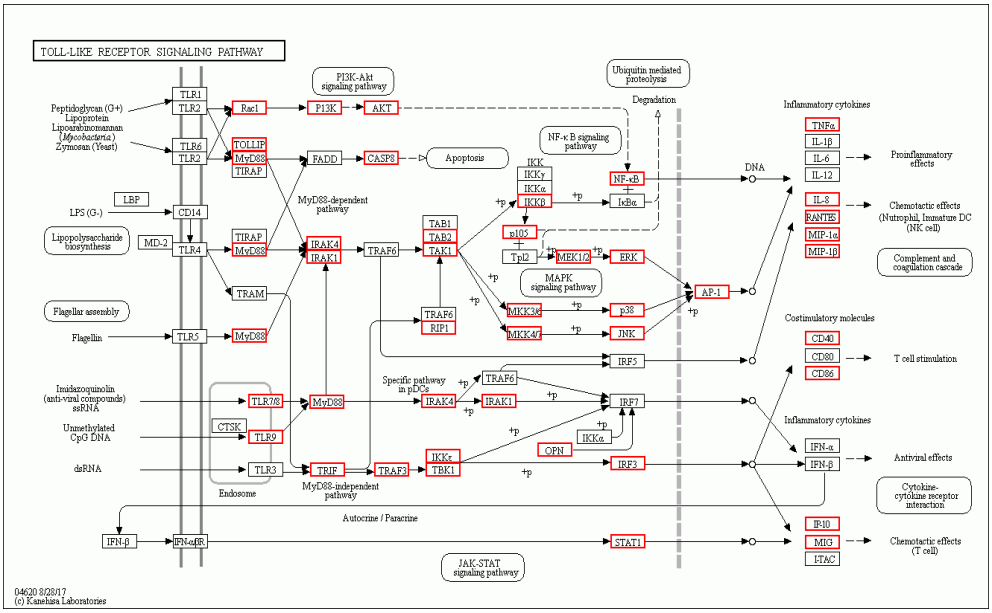

Figure 28: TLR signaling pathway analysis(Day1)

Fig 28 | The red border means activated, the black border means inactive.

On day 5 shows the same result (Figure 29).

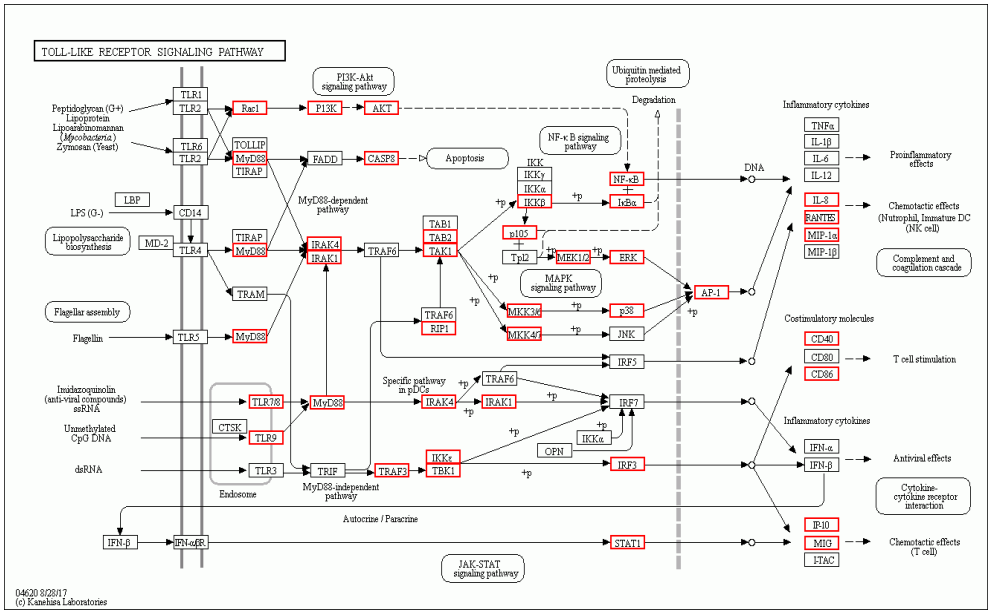

Figure 29: TLR signaling pathway analysis(Day5)

Fig 29 | The red border means activated, the black border means inactive.

On day 10, TLRs are activated, which then triggers the NF-κB pathway via the downstream MyD88 complex, releasing inflammatory factors including IL-8. However, because TLRs are unable to activate IRF3/7, type I interferon (IFN-α and IFN-β) activation is ineffective (Figure 30).

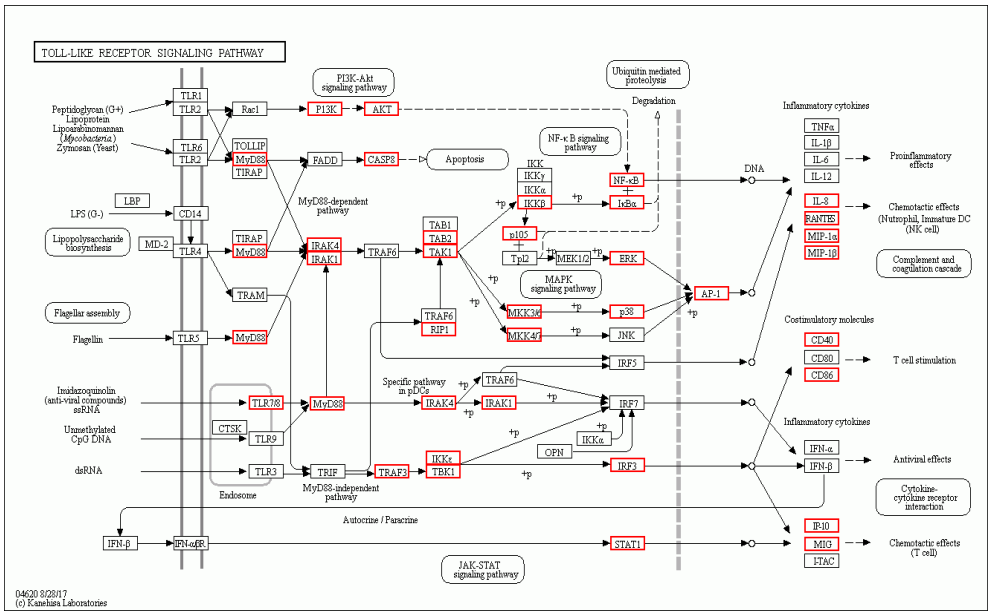

Figure 30: TLR signaling pathway analysis(Day10)

Fig 30 | The red border means activated, the black border means inactive.

Results from day 15 are similar to those of the previous days (Figure 31).

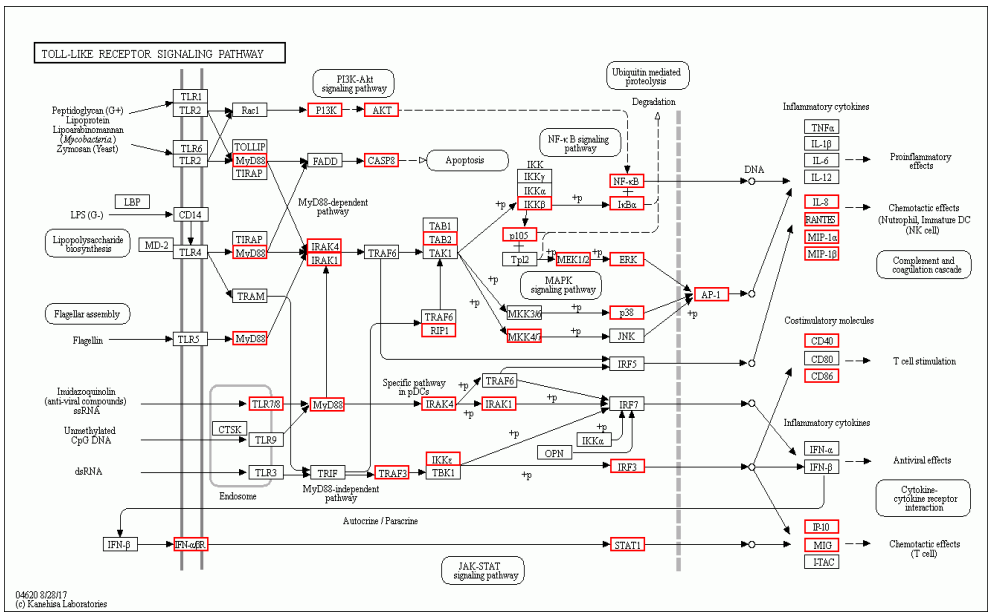

Figure 31: TLR signaling pathway analysis(Day15)

Fig 31 | The red border means activated, the black border means inactive.

4.8.7 Heatmap analysis of Toll-like receptor and NF-κB pathway

To evaluate the primary impacts on clinical illness symptoms, it is crucial to identify relevant regulatory genes in the TLR and NF-κB signaling pathways, and to analyze the variations in regulatory genes between healthy control and COVID-19 patient groups. The DEGs of the two main signaling pathways, TLR and NF-κB signaling pathways, were thoroughly studied.

The results demonstrates that the COVID-19 patient groups highly expressed the majority of relevant genes in these signaling pathways when compared to the healthy controls (HC) (Figure 32A). We selected the most altered genes in these pathways and discovered that in the TLR signaling pathway, TLR2,TLR5, TLR7 and TLR8 were highly expressed, IRAK3 was downstream and is also activated and expressed by the cascade, leading to the expression of inflammatory factors(IL-6,IL-8,IL10 and CXCL3) were highly, but both TLR3/6 and its downstream IRF3/7 are downregulated, leading to downregulation of NF-κB signaling gene (CCL4,CD40,CARD11,TRIM25) and blockage of type I interferon(IFNA1,IFNB1) expression. These data suggest that the TLR signaling pathway is deeply involved in the progression of COVID-19 disease and plays an important bidirectional regulatory role. Inhibition of type I interferon expression may lead to activation of compensatory immune system mechanisms and activation of more inflammatory factor signaling pathways, triggering a cytokine storm and worsening the patient's condition (Figure 32B).

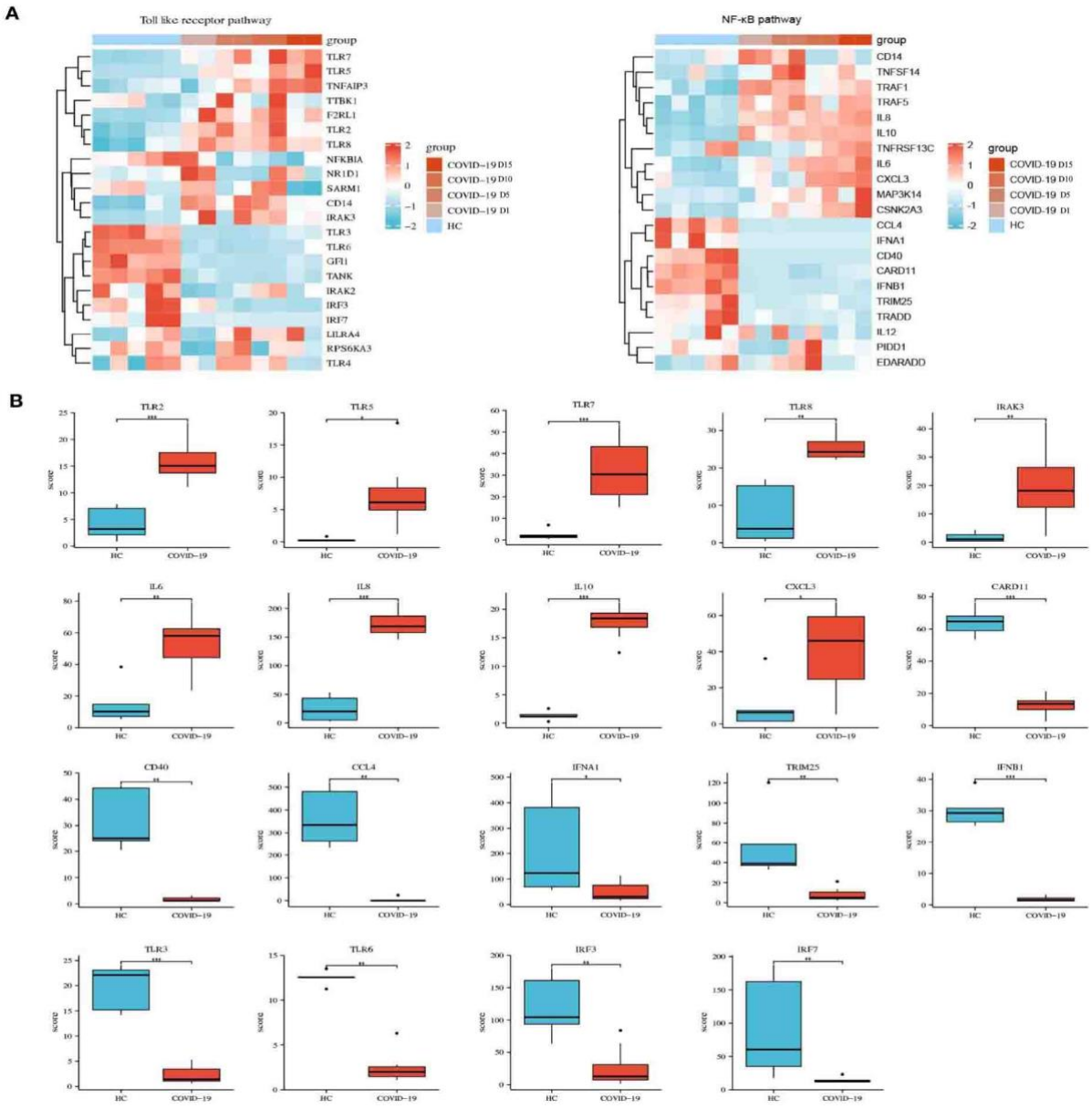

Figure 32: TLR and NF-κB signaling pathway analysis

Fig 32 | Identification of hub immune genes in the diagnosis of severe COVID-19. **(A)** The heat map of major associated immune response processes comparing HC and COVID-19 group. **(B)** Group boxplot diagrams of the key immunity genes. Statistically significant differences are calculated using Welch's t-test. Data are shown as means ± SD, *p < 0.05; **p < 0.01; ***p < 0.001; ns which stands for not significant.

In summary, our study found that viral proteins are involved in the inhibition or delay of the type I IFN response. The block of type I IFN response may also be a unique phenomenon in elderly COVID-19 patients, and that the result may lead to innate immune escape of SARS-CoV-2, exacerbating COVID-19 disease conditions.

4.8.8 Gene Ontology (GO) Enrichment Analysis

The GO annotation outputs can be ascribed to the secondary classification. The secondary GO histogram map can be created, and the secondary classification map of the GO analysis can also be created using the GO analysis technique (OmicShare tools) to comprehend the functions of DEGs. To further understand how various genes work, they are mapped to three ontology sub-categories, including BP: Biological Process, CC: Cellular Component, and MF: Molecular Function.

GO was used to annotate the functions of DEGs in cell experiments: Control (-) versus Control (+), Control (-) versus the LPS group, and Control (+) versus the LPS group; SARS-CoV-2 samples were compared with samples from healthy controls (HC) (3 samples mixed) and patients from day1to day15. The figure's various color depths correspond to various gene counts. The number of genes rapidly reduces as the color transitions from dark to bright.

4.8.8.1 GO Enrichment analysis: Control(-) versus Control(+)

The three biological processes where DEGs were most enriched in BP compared to the Control(-) and Control(+) groups were the immunological effector process, the cell surface receptor signaling pathway, and the viral defense response. Membrane, protein-containing complex, and extracellular area DEGs were most enriched in CC. Binding, cytokine activity, and molecular function regulator were the DEGs with the greatest enrichment in MF (Figure 33).

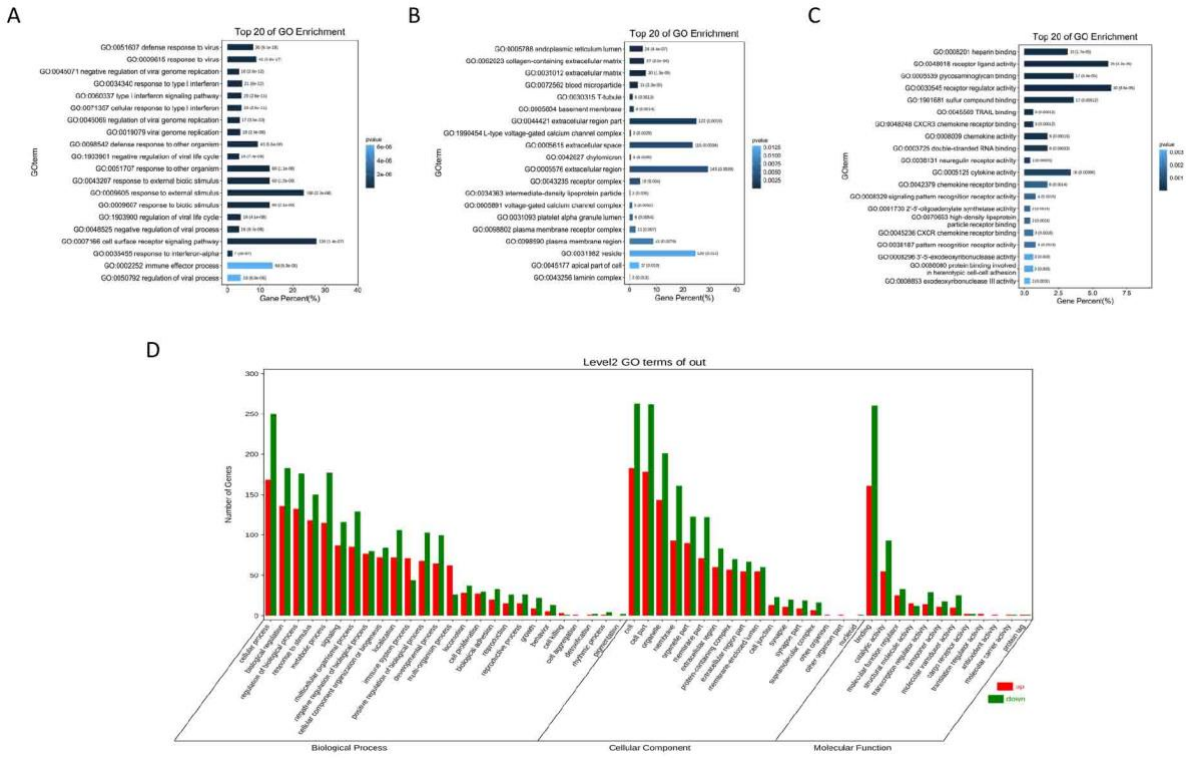

Figure 33: GO Enrichment analysis

Fig 33 | Top 20 GO annotation enrichment analysis of DEGs (Compared with Control(-) and Control(+)) . The vertical axis is the GO Term and the specific information of each GO number, while the horizontal axis is the percentage of the number of genes. **A:** BP; **B:** CC; **C:** MF. **D:** Red and green in the secondary classification histogram of the GO annotation analysis of DEGs stand for up- and down-regulation of gene expression, respectively.

4.8.8.2 GO Enrichment analysis: Control(-) versus the LPS group

Cellular process, metabolic process, and stimulus response exhibited the greatest enrichment of DEGs in BP as compared to the Control(-) and LPS groups. DEGs were mostly enriched in the membrane, intracellular, and cytoplasmic parts of cells in CC. DEGs in MF were mostly enriched for binding and catalytic activity (Figure 34).

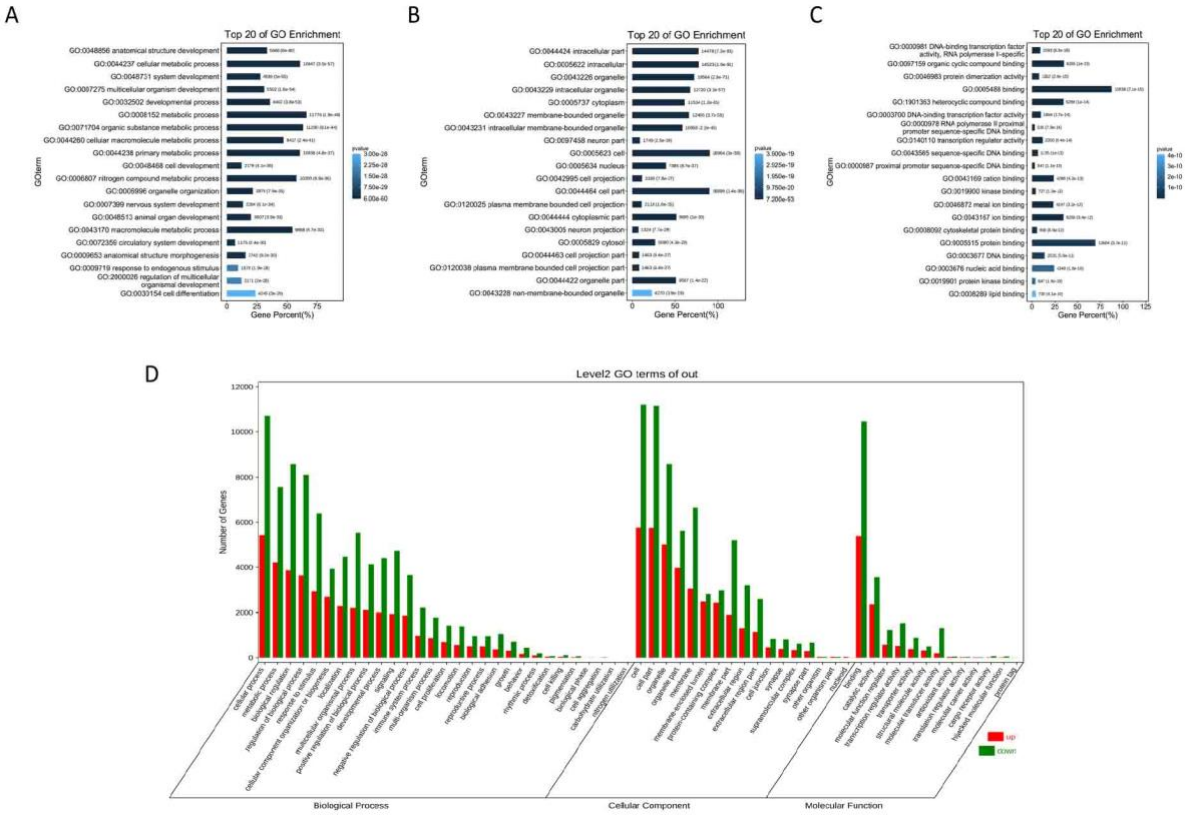

Figure 34: GO Enrichment analysis

Fig 34 | Top 20 GO annotation enrichment analysis of DEGs (Compared with Control(-) and LPS group) , The vertical axis is the GO Term and the specific information of each GO number, while the horizontal axis is the percentage of the number of genes. **A:** BP; **B:** CC; **C:** MF. **D:** Red and green in the secondary classification histogram of the GO annotation analysis of DEGs stand for up- and down-regulation of gene expression, respectively.

4.8.8.3 GO Enrichment analysis: Control(+) versus the LPS group

Cellular process, biological regulation, and stimulus response exhibited the greatest enrichment of DEGs in BP as compared to the Control(+) and LPS groups. Intracellular, membrane-bounded organelle and organelle were the primary sources of DEG enrichment in CC. Binding, catalytic activity, and molecular function regulator were the DEGs with the greatest enrichment in MF (Figure 35).

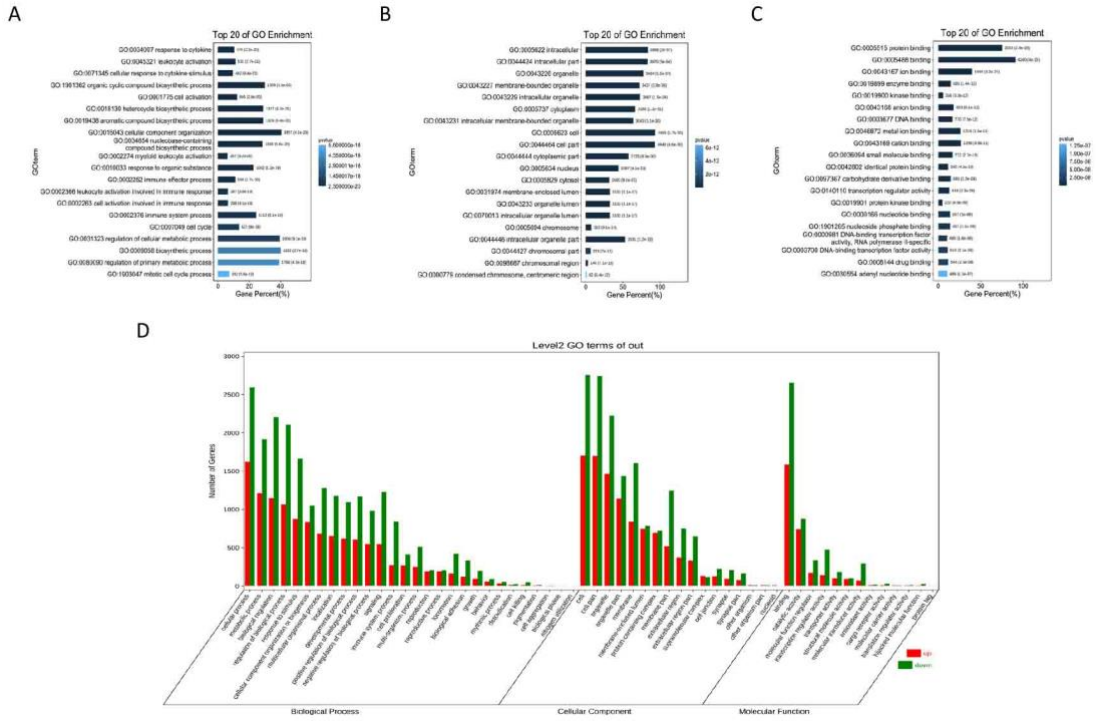

Figure 35: GO Enrichment analysis

Fig 35 | Top 20 GO annotation enrichment analysis of DEGs (Compared with Control(+) group and LPS group) , The vertical axis is the GO Term and the specific information of each GO number, while the horizontal axis is the percentage of the number of genes. **A:** BP; **B:** CC; **C:** MF. **D:** Red and green in the secondary classification histogram of the GO annotation analysis of DEGs stand for up- and down-regulation of gene expression, respectively.

All groups in the vitro cell studies were analyzed, and the findings revealed that cellular processes, biological control, and stimulus response accounted for the majority of DEG enrichment in BP. The top three were the immunological effector process, the cell surface receptor signaling pathway, and the viral defense response. Cells, cell parts, and organelles were the key DEGs that were enriched in CC. Organelles that were membrane-bound and intracellular were at the top. Binding, catalytic activity, and molecular function regulator were the DEGs with the highest enrichment in MF. Protein binding, enzyme binding, and DNA binding were at the top. An illustration of the key genes that the spike protein regulates in order to control certain physiological processes.

4.8.8.4 GO Enrichment analysis: HC (3 samples mixed) versus A:S-1 and S-5 (Day1)

Cellular process, biological regulation, and protein localisation were the key areas of enrichment of DEGs in BP when compared to the groups of HC samples and COVID-19 patient samples(Day1). Organelle and intracellular, membrane-bounded organelle were the primary DEGs that were enriched in CC. Binding, catalytic activity, and transcription regulator activity accounted for the majority of DEG enrichment in MF (Figure 36).

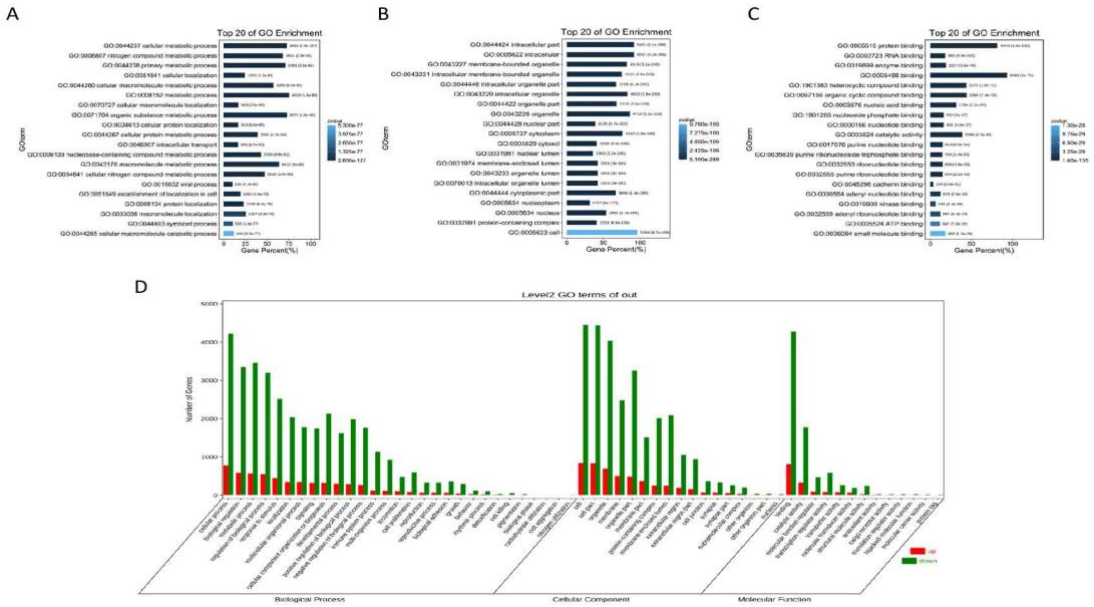

Figure 36: GO Enrichment analysis

Fig 36 | Top 20 GO annotation enrichment analysis of DEGs (Day1). The vertical axis is the GO Term and the specific information of each GO number, while the horizontal axis is the percentage of the number of genes. **A:** BP; **B:** CC; **C:** MF. **D:** Red and green in the secondary classification histogram of the GO annotation analysis of DEGs stand for up- and down-regulation of gene expression, respectively.

4.8.8.5 GO Enrichment analysis: HC (3 samples mixed) versus B:S-2 and S-6 (Day5)

Cellular process, biological regulation, and metabolic process were the key areas of enrichment of DEGs in BP when compared to the groups of HC samples and COVID-19 patient samples(Day5). The cytoplasm and intracellular, membrane-bounded organelle showed the greatest concentration of DEGs in CC. Binding, catalytic activity, and transcription regulator activity were the DEGs with the highest enrichment in MF (Figure 37).

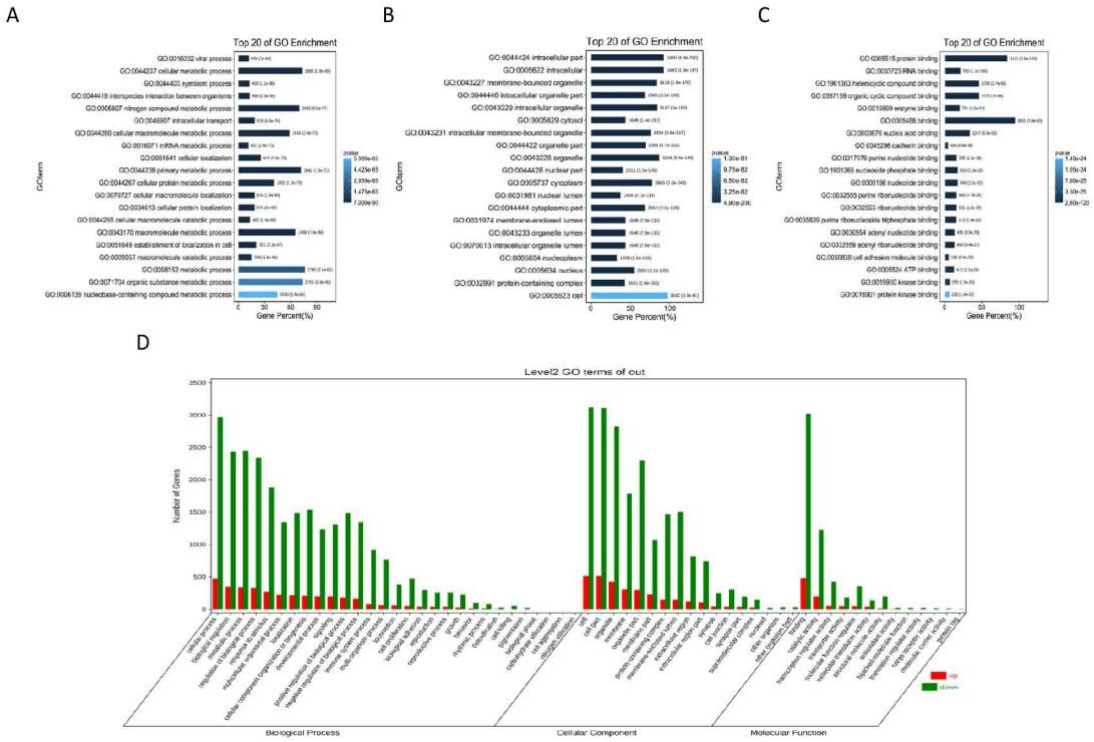

Figure 37: GO Enrichment analysis

Fig 37 | Top 20 GO annotation enrichment analysis of DEGs (Day5) , The vertical axis is the GO Term and the specific information of each GO number, while the horizontal axis is the percentage of the number of genes. **A:** BP; **B:** CC; **C:** MF. **D:** Red and green in the secondary classification histogram of the GO annotation analysis of DEGs stand for up- and down-regulation of gene expression, respectively.

4.8.8.6 GO Enrichment analysis: HC (3 samples mixed) versus C:S-3 and S-7 (Day10)

Cellular process, biological regulation, and metabolic process were the key areas of enrichment of DEGs in BP when compared to the groups of HC samples and COVID-19 patient samples(Day10). Intracellular, organelle, and cytoplasm DEG enrichments were primarily seen in CC. Binding, catalytic activity, and molecular function regulator were the DEGs with the greatest enrichment in MF (Figure 38).

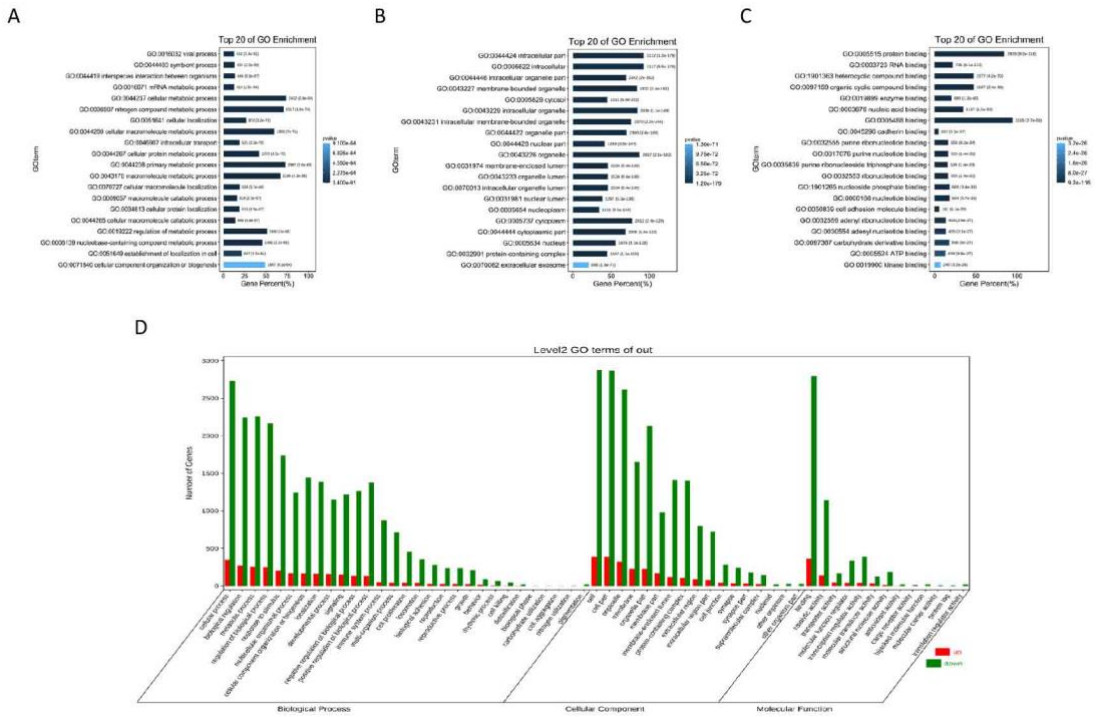

Figure 38: GO Enrichment analysis

Fig 38 | Top 20 GO annotation enrichment analysis of DEGs (Day10). The vertical axis is the GO Term and the specific information of each GO number, while the horizontal axis is the percentage of the number of genes. **A:** BP; **B:** CC; **C:** MF. **D:** Red and green in the secondary classification histogram of the GO annotation analysis of DEGs stand for up- and down-regulation of gene expression, respectively.

4.8.8.7 GO Enrichment analysis: HC (3 samples mixed) versus D: S-4 and S-8 (Day15)

Cellular process, biological regulation, and metabolic process were the key areas of enrichment of DEGs in BP when compared to the groups of HC samples and COVID-19 patient samples(Day15). The intracellular, organelle, and cytoplasm were the primary areas of DEG enrichment in CC. DEGs with the highest levels of binding, catalytic, and transporter activity were found in MF (Figure 39).

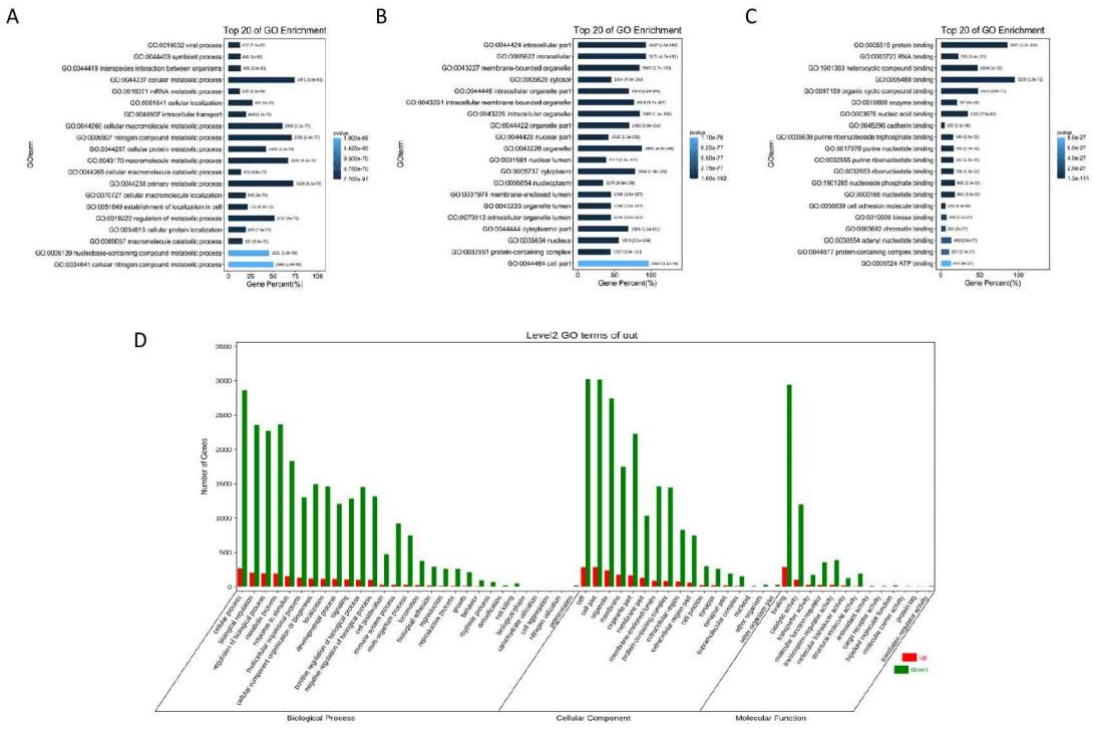

Figure 39: GO Enrichment analysis

Fig 39 | Top 20 GO annotation enrichment analysis of DEGs (Day15) , The vertical axis is the GO Term and the specific information of each GO number, while the horizontal axis is the percentage of the number of genes. **A:** BP; **B:** CC; **C:** MF. **D:** Red and green in the secondary classification histogram of the GO annotation analysis of DEGs stand for up- and down-regulation of gene expression, respectively.

After comparing sample data from HC and COVID-19 patients on various days, the findings revealed that cellular process, biological regulation, and metabolic process had the greatest enrichment of DEGs in BP. The top three metabolic processes were those of cells, nitrogen compounds, and macromolecules. Cells, cell parts, and organelles were the key DEGs that were enriched in CC. Organelles that were membrane-bound and intracellular were at the top. Binding, catalytic activity, and molecular function regulator were the DEGs with the greatest enrichment in MF. Protein binding, enzyme binding, and RNA binding were at the top.

The result is that the biological functions of the different GOs affected by DEGs are similar both in in vitro cell experiments and in COVID-19 patients.

4.8.9 KEGG Pathway Enrichment analysis

Using the tools provided by OmicShare to analyze KEGG pathways in order to comprehend how DEGs are classified. Not only can the KEGG enrichment analysis be used to identify gene pathways engaged in diverse activities, but it can also be used to evaluate the relevance of any important signaling pathways that are discovered. In cell studies and SARS-CoV-2 samples, the signal route of DEGs was annotated using KEGG. The biological pathway's relevance under the identical circumstances is shown by the *p* value. The significance of the biological signaling route is more important, as shown by the lower the *p* value, the higher the significant difference.

4.8.9.1 KEGG Pathway Enrichment analysis: Control(-) versus Control(+)

The KEGG pathway annotation for infectious illnesses, signal transduction, immune system, global and overview maps, and translation was different from the groups of Control(-) and Control(+) (Figure 40A). Influenza A, Cytosolic DNA-sensing pathway, and Cytokine-cytokine receptor interaction were the top KEGG pathways that were enriched (Figure 40B).

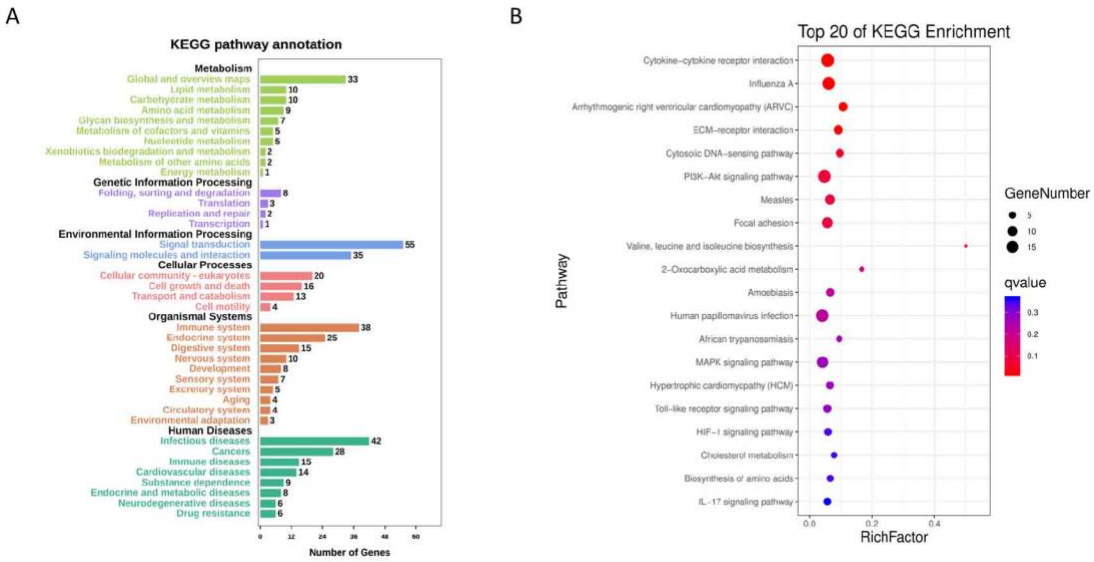

Figure 40: KEGG pathway Enrichment analysis

Fig 40 | KEGG annotation enrichment analysis of DEGs (Compared with Control(-) and Control(+)). **A:** DEG annotation for KEGG pathways. **B:** Analysis of the top 20 enriched KEGG pathways for DEGs.

4.8.9.2 KEGG Pathway Enrichment analysis: Control(-) versus LPS group

In comparison to the Control(-) and LPS groups, the KEGG pathway annotation were global and overview maps, immune system, signal transduction, and infectious illnesses (Figure 41A). Metabolic processes, actin cytoskeleton regulation, Ras signaling route, Jak-STAT signaling system, and Apelin signaling pathway were the top KEGG pathways that were enriched (Figure 41B).

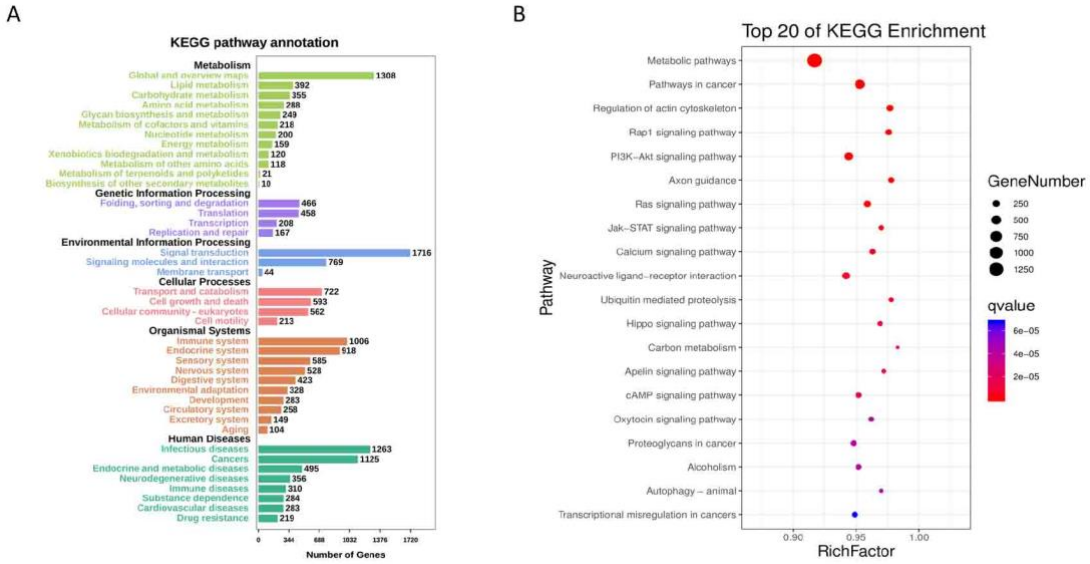

Figure 41: KEGG pathway Enrichment analysis

Fig 41 | KEGG annotation enrichment analysis (Compared with Control(-) and LPS group). **A:** DEG annotation for KEGG pathways. **B:** Analysis of the top 20 enriched KEGG pathways for DEGs.

4.8.9.3 KEGG Pathway Enrichment analysis: Control(+) versus LPS group

In contrast to the Control(+) and LPS groups, the KEGG pathway annotation was characterized by illnesses of the immune system; signal transduction; cell development and death; transport and catabolism; and global and overview maps (Figure 42A). Cell cycle, DNA replication, cytokine-cytokine receptor interaction, apoptosis, and the p53 signaling pathway were the top KEGG pathways that were enriched (Figure 42B).

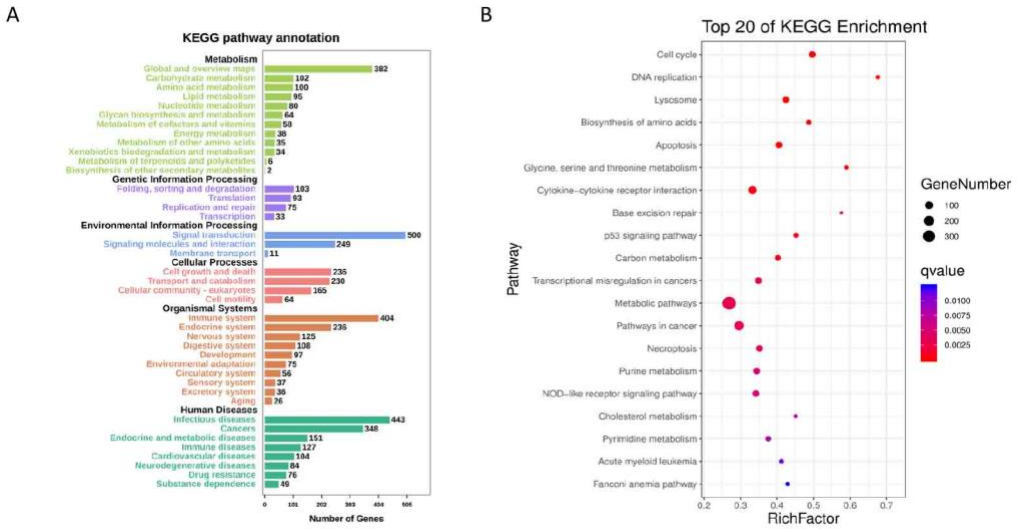

Figure 42: KEGG pathway Enrichment analysis

Fig 42 | KEGG annotation enrichment analysis of (Compared with Control(+) group and LPS group), **A:** DEG annotation for KEGG pathways. **B:** Analysis of the top 20 enriched KEGG pathways for DEGs.

All of the groups in the in vitro cell studies were examined, and the findings revealed that the KEGG pathway annotations for infectious disorders, signal transduction, cell growth and death, transport and catabolism, immune system, and global and overview maps, were the most prevalent. Cell cycle, DNA replication, cytokine-cytokine receptor interaction, apoptosis, and the p53 signaling pathway were the top KEGG pathways that were enriched. These data suggest that these are the primary biological processes controlled by various Spike protein-influenced gene expression signaling pathways.

4.8.9.4 KEGG Pathway Enrichment analysis: HC (3 samples mixed) versus A:S-1 and S-5 (Day1)

The KEGG pathway annotation included infectious disorders, signal transduction, transport and catabolism, immune system, and global and overview maps, as compared to the groupings of HC samples and COVID-19 patient samples (Day1) (Figure 43A). Ribosome, RNA transport, Neurotrophin signaling pathway, T cell receptor signaling pathway, Parkinson disease, and protein processing in the endoplasmic reticulum were the top KEGG pathways that were enriched (Figure 43B).

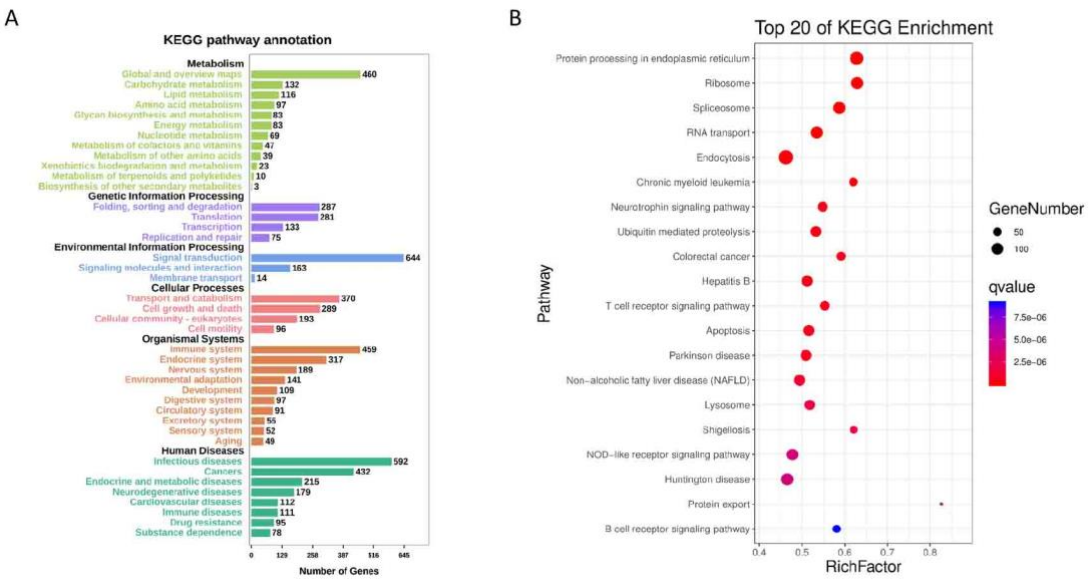

Figure 43: KEGG pathway Enrichment analysis

Fig 43 | KEGG annotation enrichment analysis of (Day1), **A:** DEG annotation for KEGG pathways. **B:** Analysis of the top 20 enriched KEGG pathways for DEGs.

4.8.9.5 KEGG Pathway Enrichment analysis: HC (3 samples mixed) versus B:S-2 and S-6 (Day5)

In comparison to the groups of HC samples and COVID-19 patient samples (Day 5), the KEGG pathway annotation was the immune system, global and overview maps, signal transduction illnesses, transport and catabolism, and infectious disorders (Figure 44A). Ribosome, Protein processing in the endoplasmic reticulum, T cell receptor signaling pathway, Parkinson's disease, Neurotrophin signaling pathway, RNA transport, and B cell receptor signaling pathway were the top KEGG pathways that were enriched (Figure 44B).

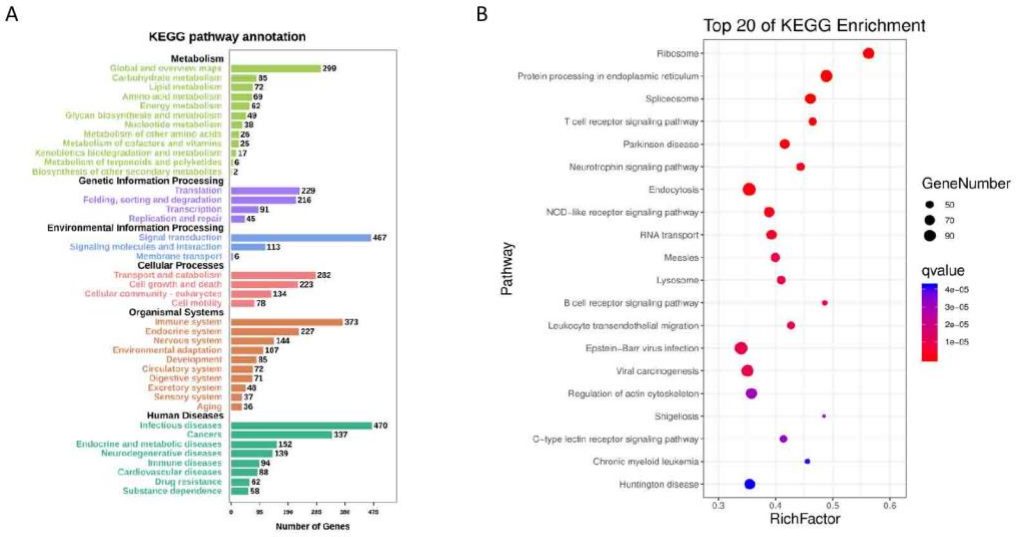

Figure 44: KEGG pathway Enrichment analysis

Fig 44 | KEGG annotation enrichment analysis of (Day5), **A:** DEG annotation for KEGG pathways. **B:** Analysis of the top 20 enriched KEGG pathways for DEGs.

4.8.9.6 KEGG Pathway Enrichment analysis: HC (3 samples mixed) versus C:S-3 and S-7 (Day10)

Comparatively to the COVID-19 patient samples and the groups of HC samples, the KEGG pathway annotation for Day 10 was immune system, global and overview maps, signal transduction illnesses, transport and catabolism, and infectious disorders (Figure 45A). Proteasome, NOD-like receptor signaling route, Neurotrophin signaling pathway, T cell receptor signaling pathway, Parkinson's disease, and protein processing in the endoplasmic reticulum were the top KEGG pathways that were enriched (Figure 45B).

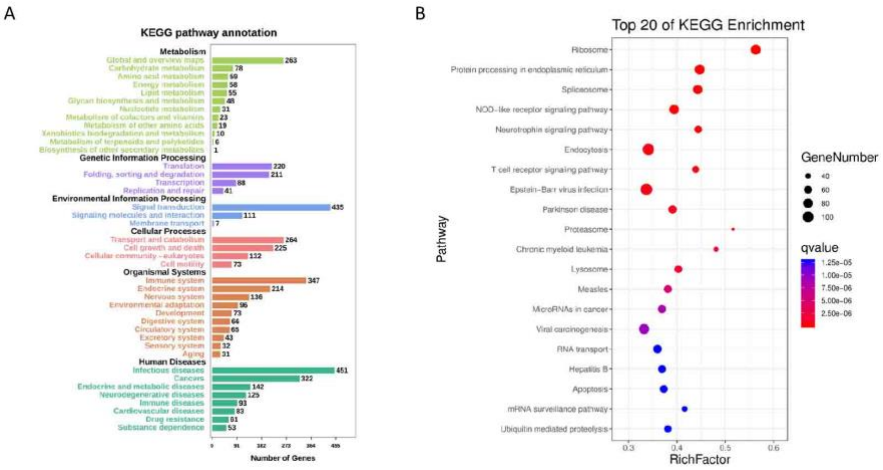

Figure 45: KEGG pathway Enrichment analysis

Fig 45 | KEGG annotation enrichment analysis of (Day10), **A:** DEG annotation for KEGG pathways. **B:** Analysis of the top 20 enriched KEGG pathways for DEGs.

4.8.9.7 KEGG Pathway Enrichment analysis: HC (3 samples mixed) versus D: S-4 and S-8 (Day15)

In comparison to the groups of HC samples and COVID-19 patient samples (Day 15), the KEGG pathway annotation was immune system, global and overview maps, signal transduction illnesses, transport and catabolism, and infectious disorders (Figure 46A). Ribosome, Protein processing in the endoplasmic reticulum, Neurotrophin signaling pathway, T cell receptor signaling pathway, RNA transport, Proteasome, and B cell receptor signaling pathway were the top KEGG pathways that were enriched (Figure 46B).

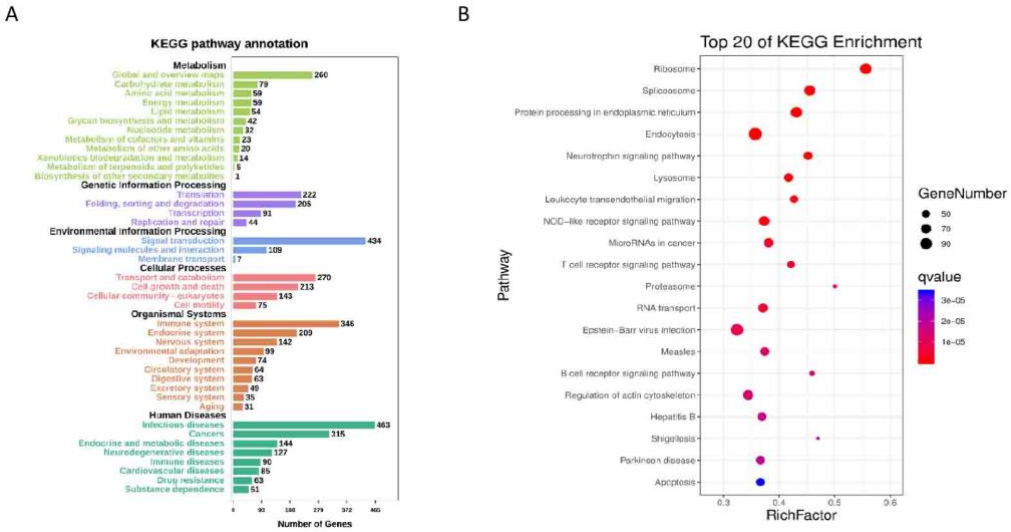

Figure 46: KEGG pathway Enrichment analysis

Fig 46 | KEGG annotation enrichment analysis of (Day15), **A:** DEG annotation for KEGG pathways. **B:** Analysis of the top 20 enriched KEGG pathways for DEGs.

After comparing sample data from HC and COVID-19 patients on various days, the findings revealed that the KEGG pathway annotation was comprised of the immune system, signal transduction, cell development and death, transport, and catabolism. Ribosome, protein processing in the endoplasmic reticulum, Neurotrophin signaling pathway, T cell receptor signaling pathway, RNA transport, Proteasome, and B cell receptor signaling pathway were the top KEGG pathways that were enriched.

The result is that the biological annotations of the different KEGG pathways affected by DEGs were similar in both in vitro cell experiments and in COVID-19 patients, but the Top KEGG pathways were significantly different.

4.9 Multi-cytokine detection and analysis in cell experiments

To study the expression of the key cytokines compared with the groups of Control (+) and Control (-), and the groups of Control (+) plus LPS, after collected the cell culture supernatant from the cell experiment and carried out multi-cell experiments. The cytokines, including IL-2, IL-4, IL-6, IL-10, TNF-α, IFN-γ were determined using the BD Cytometric Bead Array (CBA) Human Th1/Th2 Cytokine Kit II.

4.9.1 Obtain standard curve

Open a new vial of recombinant standards, reconstitute the standards with assay diluent and dilute them in the following order: 1:2,1:4,1:8;1:16,1:32,1:64,1:128 and 1:256. Mix the cytokine beads with the recombinant standards, and use the PE-conjugated detection antibodies to mark them. The intensity of PE fluorescence provides information about the concentration of the respective cytokine. After the samples were collected on a flow cytometer, software was used to generate results in graphical and tabular form. The results of the analysis showed that in the standard of IL-2, $R^2 = 0.9948$, IL-4, $R^2 = 0.9987$. IL-6, $R^2 = 0.9955$, IL-10, $R^2 = 0.9947$, TNF-α, $R^2 = 0.9955$, IFN-γ, $R^2 = 0.9996$ (Figure 47). Standard curves for each cytokine cover concentrations from 20 to 5000 pg/mL. R^2 were obtained by squaring this R(coefficient of correlation), In general, the closer R^2 is to 1, the better the correlation between the independent variable and the dependent variable in regression analysis In this standard curve, a significant linear correlation is defined as $R^2 > 0.99$.

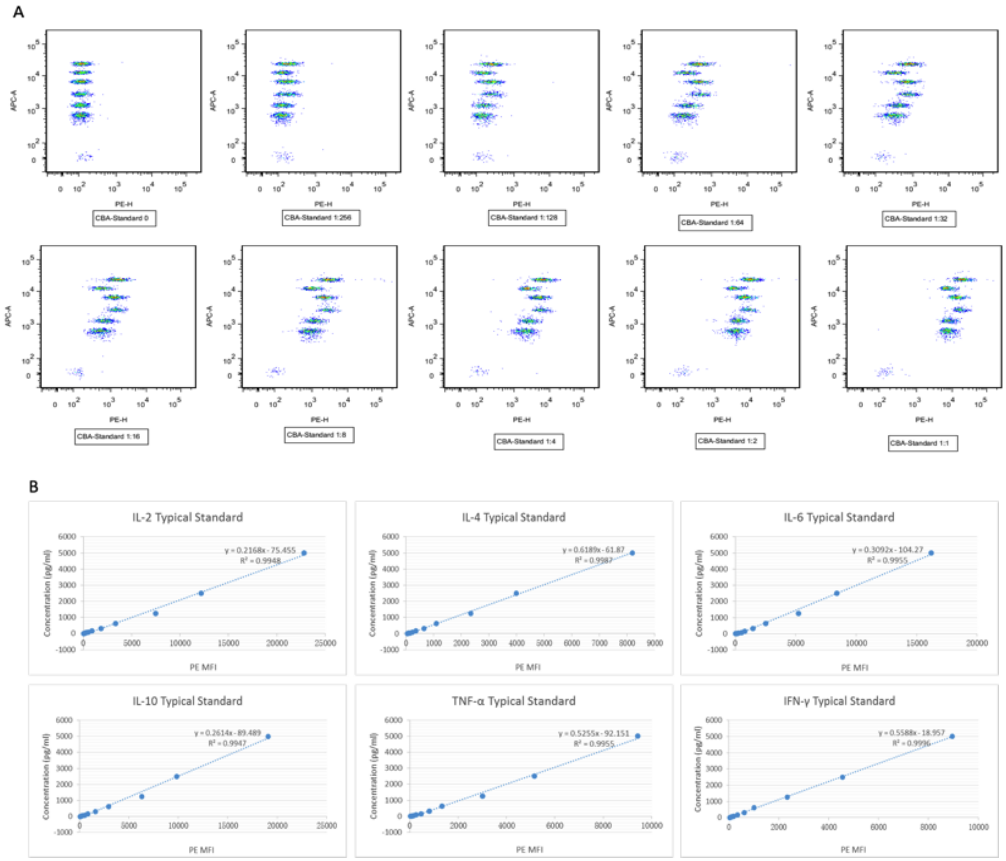

Figure 47: Multi-cytokine detection standard curve

Fig 47 | **A:** Standards detection of different dilution concentrations, the dilution ratio includes 1:1,1:2,1:4,1:8;1:16,1:32,1:64,1:128 and 1:256. **B:** Standard curve of cytokines, R^2>0.99.

4.9.2 Detection of cytokines expression

The pathogenesis of the human coronavirus involves the release of a cytokine storm, which is caused by a large number of proinflammatory cytokines and chemokines [205].

A number of cytokines, including IL-2, IL-6, IL-8, IL-17, GCSF, IL-10, TNF-α and IFN-γ, are released as a result of SARS-CoV-2 activating the innate and adaptive immune systems after invading host cells. Abnormally high expression of these cytokines can cause tissue damage that results in respiratory failure or multi-organ failure [206-208]. Notably, when comparing survivors with non-survivors, it is discovered that the level of IL-6 is higher in non-survivors, indicating infection with SARS-CoV-2, which is associated with a fatal outcome and persistently high expression of IL-6. Among them, IL-6 is a key cytokine that is highly expressed in the serum of COVID-19 patients. In individuals with severe illnesses,

tocilizumab clinical usage to suppress IL-6 has demonstrated considerable effectiveness [209].

Our findings further demonstrate that, in contrast to the control(+) and control(-) groups, the expression of IL-6 is higher in cell experiments. Comparing the control(+) plus LPS groups reveals that following LPS stimulation, the group that expresses the spike protein can drive PBMC to express IL-6 at a high level, demonstrating that the SARS-CoV-2 spike protein can cause high production of IL-6 at the cellular level in vitro (Figure 48). Similarly, severe COVID-19 patients have high levels of TNF-α and IFN-γ, which combined cause a cytokine storm [210]. The results of our in vitro cell experiments also show that compared with control(+) and control(-) groups,IL-6, TNF-α and IFN-γ expression is higher in control(+) plus LPS groups (Table 13).

Table 13: Cytokine expression in three groups, concentration（pg/mL）

Samples	IL-2	IL-4	IL-6	IL-10	TNF-α	IFN-γ
Control(-)	1549	487	5066	1036	605	2178
Control(+)	1352	470	7650	1353	669	4131
LPS	4599	494	166000	2439	34100	164000

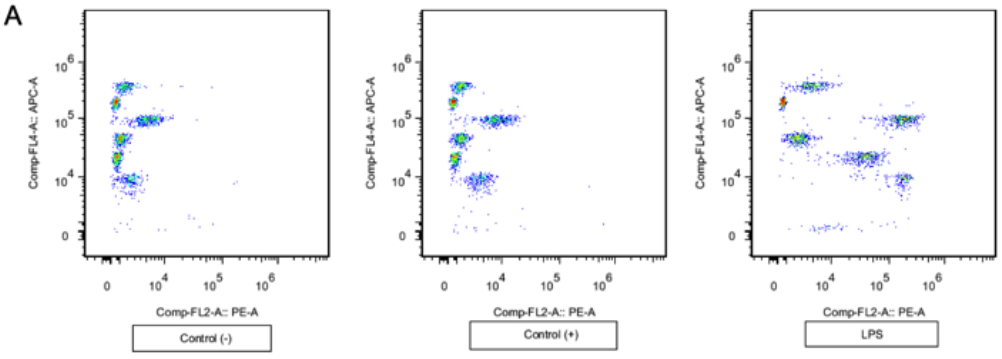

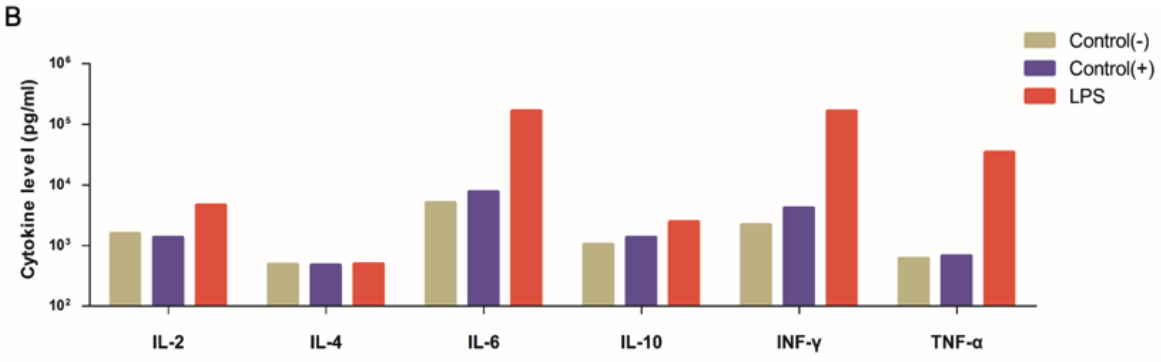

Figure 48: Detection of cytokine expression levels in different groups

Fig 48 | **A:** Flow chart of cytokine expression. **B:** Histogram of cytokine expression level

5. Discussion

SARS-CoV-2 has been raging worldwide since its emergence in December 2019 all over the world. And it is now gaining from the rising popularity of vaccinations globally and the decrease in toxicity of the virus itself, different mutant strains are causing it to spread more quickly. Although the fatality rate has decreased dramatically since the outbreak's commencement, SARS-CoV-2 continues to pose a major threat to people's health all over the world due to its quick and unpredictable mutation rate. There is no denying that the immune system is essential for preventing viral replication and getting rid of the virus. Immune escape and cytokine storm, particularly in older individuals with COVID-19, are the major factors that cause severe illness and mortality in patients with SARS-CoV-2. Gaining a thorough grasp of the signaling regulatory mechanisms involved in the function of immune cells and innate immunity to viruses is not impossible.

When creating brand-new therapies or novel vaccinations for COVID-19 patients, a thorough understanding of the innate immune system's mode of action in resistance to SARS-CoV-2 is crucial. Particularly in senior COVID-19 patients, innate immunity is essential for resistance to SARS-CoV-2 infection because as people age, their ability to generate inflammatory macrophages increases, rendering them more vulnerable to the symptoms of a cytokine storm. The loss of function of activation of the TLR pathway, which results in delayed or low production of type I interferon, is another indication of the innate immune system's lack of antiviral activity.

SARS-CoV-2 primarily recognizes the host ACE2 through the S protein, fuses with the surface of the cell membrane, injects viral RNA into the host cell, performs transcription and translation, and then combines the newly produced protein and RNA to form new virus particles that are then released from the cell through the exocytosis pathway. The type I interferons and pro-inflammatory cytokines that are created as a result of this process include

ssRNA, dsRNA, viral protein fragments S, E, and N. These molecules may be identified by TLRs and activate downstream signaling pathways including NF-κB. Our study provides proof that certain TLRs, including TLR2, TLR5, TLR7, and TLR8, are activated in the elderly COVID-19 patient group and then activate the NF-κB pathway by forming the MyD88 complex to promote the production of inflammatory factors, but these were unable to activate IRF3/7, which prevented the activation of type I interferons. Further study is necessary to determine why other TLRs are not activated, whether viral nonstructural proteins suppress them, and how this phenomena influences the activation of innate immunity. The block of TLRs may potentially be a sign of immunodeficiency in the older population.

Our findings from in vitro cell tests indicate that LPS-stimulated PBMCs may fuse the S protein-expressing vector into subsets of macrophages and DCs, which raises the possibility that these innate immune cells are highly expressed ACE2 in our bodies. At the same time, it is demonstrated in the flow cytometric that only a small percentage of the central memory T and killer T cell (CD8+ T cell) subtypes of the T cell subset of the LPS group were activated. However, there is an increase in the number of macrophages, which may be the result of LPS alone. Another possibility is that LPS makes it easier for the S protein to attach to macrophages, enhancing innate immunity while suppressing adaptive immunity. Additional investigation is required to determine the precise circumstance. One of our hypotheses is that the S protein enhanced by LPS activates the intracellular TLR signaling pathway, leading to high expression of cytokines. However, which TLRs are activated and whether this occurs through the NF-κB pathway remain unknown. The results of multi-cytokine detection experiments also revealed that IL-6, TNF-α and IFN-γ were strongly expressed in the LPS group, causing a cytokine storm phenomenon similar to that in clinically critical patients.

RNA-seq analysis was performed in the cell experimental group and the group compared with healthy and postinfected elderly, and it was discovered that in the COVID-19 group, as days passed after infection, the activated genes in the differential genes continued to decrease while the suppressed genes continued to increase, and these changes in the expression of

these genes may have had a significant impact in regulating the in vivo antiviral after infection with the virus.

We identified 38 significant core genes that were shared by all groups by integrating RNA-seq analysis of cell experiments with HC vs COVID-19 data. All of the innate immunity-related genes have up-regulated expression, and the majority of these genes are engaged in immunity. This demonstrating that innate immunity, which is impaired in the elderly, may have a major impact on viral infection in its early stages and may be a contributing factor to the high severity rate and high fatality rate. Additionally, PPI analysis was conducted on these 38 important genes. The findings demonstrated a high correlation between the proteins they transcribed, particularly when it came to cytokine signaling in the immune system, innate immunity, reaction to viruses, protection against viruses, response to type I interferon, and other activities.

Innate immune-related cell subsets like DC, monocytes, etc. were considerably elevated when comparing COVID-19 patients with HC, but adaptive immune-related cell subsets like B cells, T cells, etc. were downregulated, which was demonstrated by immune cell enrichment analysis. These findings match those of cell experimentation using flow cytometry. The LPS-stimulated S protein in PBMC indicates that SARS-CoV-2 activates innate immunity while suppressing adaptive immunity, which may affect the clinical outcome in older patients. A greater death rate and more severe illness are more likely in older people with impaired innate immunity. Additionally, our hub gene analysis revealed that innate immunity-related hub genes are highly linked to SARS-CoV-2 in clinical settings.

We performed GO and KEGG enrichment analyses to better comprehend the roles of differentially expressed genes in cellular studies and in COVID-19 patients. We discovered that their biological roles were similar using GO and KEGG analyses. Protein binding and RNA binding are analogous to the activities associated with viral invasion, reproduction, and packaging in GO analysis, where DEGs mostly influence cellular processes. Signal transduction, cell growth and death, immune, and other signaling pathways related to anti-viral immune system defense are the main signaling pathways affected. according to KEGG

analysis, highlighting the significance of the endogenous immune system and anti-viral defense following SARS-CoV-2 infection.

In conclusion, cell studies were used to examine the impact of S protein on immune cells. It can attach to macrophages and DC cells, indicating that they express ACE2 at high levels, and it may be that the activation of S protein is what causes the proliferation of macrophages and DCs. Regarding innate immunity, it was shown that B cells and T cells were dramatically downregulated in the COVID-19 group whereas immune cells such as DC were significantly increased when compared to HC. Older patients are more susceptible to innate immunity, possibly as a result of inadequate macrophage activation; furthermore innate immune cells such macrophages and DCs, which play a major role in early resistance to SARS-CoV-2, are lacking. Because RI3/RIF7 activation is compromised in the TLR pathway, downstream genes cannot be expressed. Our study also found evidence that this may be because TLR3/6 and its downstream gene, IRF3/7, are both downregulated. This lead to the downregulation of NF-κB signaling genes and blocks the expression of type I interferon, which may worsen the elderly's decreased resistance to SARS-CoV-2, increase the storm of inflammatory factors, and increase clinical mortality and severity.

Our research on the relationship between SARS-CoV-2 and host innate immunity will help shed light on SARS-CoV-2 immunological escape and pathogenesis in further investigations. Further study is required to understand the pathophysiology of the TLR signaling route in older COVID-19 patients, and antagonists of the TLR signaling pathway may represent a key target for the creation of novel drugs.

References

1. Guo YR, Cao QD, Hong ZS, et al. **The origin, transmission and clinical therapies on coronavirus disease 2019 (COVID-19) outbreak - an update on the status.** *Mil Med Res*. 2020;**7**(1):11.
2. Yang X, Yu Y, Xu J, et al. **Clinical course and outcomes of critically ill patients with SARS-CoV-2 pneumonia in Wuhan, China: a single-centered, retrospective, observational study**. *Lancet Respir Med*. 2020;**8**(5):475-481.
3. McKimm-Breschkin JL, Jiang S, Hui DS, Beigel JH, Govorkova EA, Lee N. **Prevention and treatment of respiratory viral infections: Presentations on antivirals, traditional therapies and host-directed interventions at the 5th ISIRV Antiviral Group conference.** *Antiviral Res*. 2018;**149**:118-142.
4. Chen Y, Liu Q, Guo D. **Emerging coronaviruses: Genome structure, replication, and pathogenesis.** *J Med Virol*. 2020;**92**(4):418-423.
5. Corman VM, Muth D, Niemeyer D, Drosten C. **Hosts and Sources of Endemic Human Coronaviruses.** *Adv Virus Res*. 2018;**100**:163-188.
6. Cui J, Li F, Shi ZL. **Origin and evolution of pathogenic coronaviruses.** *Nat Rev Microbiol*. 2019;**17**(3):181-192.
7. Rossi GA, Sacco O, Mancino E, Cristiani L, Midulla F. **Differences and similarities between SARS-CoV and SARS-CoV-2: spike receptor-binding domain recognition and host cell infection with support of cellular serine proteases.** *Infection*. 2020;**48**(5):665-669.
8. Chafekar A, Fielding BC. **MERS-CoV: Understanding the Latest Human Coronavirus Threat.** *Viruses*. 2018;**10**(2):93.
9. **World Health Organization. Coronavirus Disease (COVID-19) Pandemic**. Available online at: https://www.who.int/emergencies/diseases/novel-coronavirus-2019.
10. World Health Organization. **Summary of Probable SARS Cases With Onset of Illness From 1 November 2002 to 31 July 2003.** Available online at:https://www.who.int/publications/m/item/summary-of-probable-sars-cases-with-onset-of-illness-from-1-november-2002-to-31-july-2003.
11. World Health Organization. **Middle East Respiratory Syndrome Coronavirus (MERS-CoV).** Available online at:https://www.who.int/emergencies/mers-cov/en/.
12. Zhu N, Zhang D, Wang W, et al. **A Novel Coronavirus from Patients with Pneumonia in China, 2019.** *N Engl J Med*. 2020;**382**(8):727-733.
13. Velavan TP, Meyer CG. **The COVID-19 epidemic.** *Trop Med Int Health*. 2020;**25**(3):278-280.
14. Hasöksüz M, Kiliç S, Saraç F. **Coronaviruses and SARS-COV-2.** *Turk J Med Sci*. 2020;**50**(SI-1):549-556.
15. Weiss SR, Leibowitz JL. **Coronavirus pathogenesis.** *Adv Virus Res*. 2011;**81**:85-164.
16. Su S, Wong G, Shi W, et al. **Epidemiology, Genetic Recombination, and Pathogenesis of Coronaviruses.** *Trends Microbiol*. 2016;**24**(6):490-502.
17. Perlman S. **Another Decade, Another Coronavirus.** *N Engl J Med*. 2020;**382**(8):760-762.
18. Masters PS. **The molecular biology of coronaviruses.** *Adv Virus Res*. 2006;**66**:193-292.
19. Hartenian E, Nandakumar D, Lari A, Ly M, Tucker JM, Glaunsinger BA**. The molecular virology of coronaviruses.** *J Biol Chem*. 2020;**295**(37):12910-12934.
20. Hui DSC, Zumla A. **Severe Acute Respiratory Syndrome: Historical, Epidemiologic, and Clinical Features.** *Infect Dis Clin North Am*. 2019;**33**(4):869-889.

21. Singh SP, Pritam M, Pandey B, Yadav TP. **Microstructure, pathophysiology, and potential therapeutics of COVID-19: A comprehensive review.** *J Med Virol*. 2021;**93**(1):275-299.
22. Kadam SB, Sukhramani GS, Bishnoi P, Pable AA, Barvkar VT. **SARS-CoV-2, the pandemic coronavirus: Molecular and structural insights.** *J Basic Microbiol*. 2021;**61**(3):180-202.
23. Ke Z, Oton J, Qu K, et al. **Structures and distributions of SARS-CoV-2 spike proteins on intact virions**. *Nature*. 2020;**588**(7838):498-502.
24. Lu R, Zhao X, Li J, et al. **Genomic characterisation and epidemiology of 2019 novel coronavirus: implications for virus origins and receptor binding.** *Lancet*. 2020;**395**(10224):565-574.
25. Malik YA. **Properties of Coronavirus and SARS-CoV-2.** *Malays J Pathol*. 2020;**42**(1):3-11.
26. Forni D, Cagliani R, Clerici M, Sironi M. **Molecular Evolution of Human Coronavirus Genomes.** *Trends Microbiol*. 2017;**25**(1):35-48.
27. de Wit E, van Doremalen N, Falzarano D, Munster VJ. **SARS and MERS: recent insights into emerging coronaviruses.** *Nat Rev Microbiol*. 2016;**14**(8):523-534.
28. Masson P, Hulo C, De Castro E, et al. **ViralZone: recent updates to the virus knowledge resource. *Nucleic Acids Res*.** 2013;**41**:D579-D583.
29. Chan JF, Kok KH, Zhu Z, et al. **Genomic characterization of the 2019 novel human-pathogenic coronavirus isolated from a patient with atypical pneumonia after visiting Wuhan.** *Emerg Microbes Infect*. 2020;**9**(1):221-236.
30. Kim D, Lee JY, Yang JS, Kim JW, Kim VN, Chang H**. The Architecture of SARS-CoV-2 Transcriptome.** *Cell*. 2020;**181**(4):914-921.e10.
31. Angeletti S, Benvenuto D, Bianchi M, Giovanetti M, Pascarella S, Ciccozzi M. **COVID-2019: The role of the nsp2 and nsp3 in its pathogenesis.** *J Med Virol*. 2020;**92**(6):584-588.
32. Zhang L, Shen FM, Chen F, Lin Z. **Origin and Evolution of the 2019 Novel Coronavirus.** *Clin Infect Dis*. 2020;**71**(15):882-883.
33. van Dorp L, Acman M, Richard D, et al. **Emergence of genomic diversity and recurrent mutations in SARS-CoV-2.** *Infect Genet Evol*. 2020;**83**:104351.
34. Zhou, Y., Hou, Y., Shen, J. *et al.* **Network-based drug repurposing for novel coronavirus 2019-nCoV/SARS-CoV-2.** *Cell Discov*. 2020; **6,** 14.
35. Bar-On YM, Flamholz A, Phillips R, Milo R. **SARS-CoV-2 (COVID-19) by the numbers.** *Elife*. 2020;**9**:e57309.
36. Chen Y, Qiu F. **Spike protein in the detection and treatment of novel coronavirus.** *Sheng Wu Yi Xue Gong Cheng Xue Za Zhi*. 2020;**37**(2):246-250.
37. Xia X. **Domains and Functions of Spike Protein in Sars-Cov-2 in the Context of Vaccine Design.** *Viruses*. 2021;**13**(1):109.
38. Arya R, Kumari S, Pandey B, et al. **Structural insights into SARS-CoV-2 proteins.** *J Mol Biol*. 2021;**433**(2):166725.
39. Salleh MZ, Derrick JP, Deris ZZ. **Structural Evaluation of the Spike Glycoprotein Variants on SARS-CoV-2 Transmission and Immune Evasion.** *Int J Mol Sci*. 2021;**22**(14):7425.
40. Papa G, Mallery DL, Albecka A, et al. **Furin cleavage of SARS-CoV-2 Spike promotes but is not essential for infection and cell-cell fusion.** *PLoS Pathog*. 2021;**17**(1):e1009246.
41. Walls AC, Park YJ, Tortorici MA, Wall A, McGuire AT, Veesler D. **Structure, Function, and Antigenicity of the SARS-CoV-2 Spike Glycoprotein**. *Cell*. 2020;**181**(2):281-292.e6.

42. Mannar D, Saville JW, Zhu X, et al. **SARS-CoV-2 Omicron variant: Antibody evasion and cryo-EM structure of spike protein-ACE2 complex.** *Science*. 2022;**375**(6582):760-764.
43. Hoffmann M, Kleine-Weber H, Schroeder S, et al**. SARS-CoV-2 Cell Entry Depends on ACE2 and TMPRSS2 and Is Blocked by a Clinically Proven Protease Inhibitor.** *Cell*. 2020;**181**(2):271-280.e8.
44. Kuba K, Imai Y, Ohto-Nakanishi T, Penninger JM. **Trilogy of ACE2: a peptidase in the renin-angiotensin system, a SARS receptor, and a partner for amino acid transporters.** *Pharmacol Ther*. 2010;**128**(1):119-128.
45. Li F, Li W, Farzan M, Harrison SC**. Structure of SARS coronavirus spike receptor-binding domain complexed with receptor.** *Science*. 2005;**309**(5742):1864-1868.
46. Zhang L, Ghosh SK, Basavarajappa SC, et al. **Molecular dynamics simulations and functional studies reveal that hBD-2 binds SARS-CoV-2 spike RBD and blocks viral entry into ACE2 expressing cells.** Preprint. *bioRxiv*. 2021;**2021**.01.07.425621.
47. Tian X, Li C, Huang A, et al. **Potent binding of 2019 novel coronavirus spike protein by a SARS coronavirus-specific human monoclonal antibody.** *Emerg Microbes Infect*. 2020;**9**(1):382-385.
48. Song W, Gui M, Wang X, Xiang Y. **Cryo-EM structure of the SARS coronavirus spike glycoprotein in complex with its host cell receptor ACE2.** *PLoS Pathog*. 2018;**14**(8):e1007236.
49. Wrapp D, Wang N, Corbett KS, et al**. Cryo-EM structure of the 2019-nCoV spike in the prefusion conformation.** *Science*. 2020;**367**(6483):1260-1263.
50. Lan J, Ge J, Yu J, et al. **Structure of the SARS-CoV-2 spike receptor-binding domain bound to the ACE2 receptor.** *Nature*. 2020;**581**(7807):215-220.
51. Garmaroudi FS, Marchant D, Hendry R, et al. **Coxsackievirus B3 replication and pathogenesis.** *Future Microbiol*. 2015;**10**(4):629-653.
52. Mulay A, Konda B, Garcia G Jr, et al. **SARS-CoV-2 infection of primary human lung epithelium for COVID-19 modeling and drug discovery.** *Cell Rep*. 2021;**35**(5):109055.
53. Zumla A, Chan JF, Azhar EI, Hui DS, Yuen KY. **Coronaviruses - drug discovery and therapeutic options.** *Nat Rev Drug Discov*. 2016;**15**(5):327-347.
54. Maginnis MS. **Virus-Receptor Interactions: The Key to Cellular Invasion.** *J Mol Biol*. 2018;**430**(17):2590-2611.
55. Zhou P, Yang XL, Wang XG, et al. **A pneumonia outbreak associated with a new coronavirus of probable bat origin.** *Nature*. 2020;**579**(7798):270-273.
56. Hoffmann M, Kleine-Weber H, Pöhlmann S. **A Multibasic Cleavage Site in the Spike Protein of SARS-CoV-2 Is Essential for Infection of Human Lung Cells.** *Mol Cell*. 2020;**78**(4):779-784.e5.
57. Rabaan AA, Al-Ahmed SH, Haque S, et al. **SARS-CoV-2, SARS-CoV, and MERS-COV: A comparative overview.** *Infez Med*. 2020;**28**(2):174-184.
58. Wan Y, Shang J, Graham R, Baric RS, Li F. **Receptor Recognition by the Novel Coronavirus from Wuhan: an Analysis Based on Decade-Long Structural Studies of SARS Coronavirus.** *J Virol*. 2020;**94**(7):e00127-20.
59. Morgello S. **Coronaviruses and the central nervous system**. *J Neurovirol*. 2020;**26**(4):459-473.
60. Xu X, Chen P, Wang J, et al. **Evolution of the novel coronavirus from the ongoing Wuhan outbreak and modeling of its spike protein for risk of human transmission.** *Sci China Life Sci*. 2020;**63**(3):457-460.

61. Hu B, Guo H, Zhou P, Shi ZL. **Characteristics of SARS-CoV-2 and COVID-19.** *Nat Rev Microbiol*. 2021;**19**(3):141-154.
62. Du L, He Y, Zhou Y, Liu S, Zheng BJ, Jiang S**. The spike protein of SARS-CoV--a target for vaccine and therapeutic development.** *Nat Rev Microbiol*. 2009;**7**(3):226-236.
63. Diamond MS, Kanneganti TD**. Innate immunity: the first line of defense against SARS-CoV-2.** *Nat Immunol*. 2022;**23**(2):165-176.
64. **Clade and lineage nomenclature aids in genomic epidemiology studies of active hCoV-19 viruses.** GISAID https://go.nature. com/3pgSIt6, 2021.
65. Bedford, T., Hodcroft, E. B. & Neher, R. A. **Updated Nextstrain SARS-CoV-2 clade naming strategy.** Nextstrain https://go.nature.com/3c9Riep, 2021.
66. https://www.who.int/en/activities/tracking-SARS-CoV-2-variants/
67. Groves DC, Rowland-Jones SL, Angyal A. **The D614G mutations in the SARS-CoV-2 spike protein: Implications for viral infectivity, disease severity and vaccine design.** *Biochem Biophys Res Commun*. 2021;**538**:104-107.
68. Korber B, Fischer WM, Gnanakaran S, et al. **Tracking Changes in SARS-CoV-2 Spike: Evidence that D614G Increases Infectivity of the COVID-19 Virus.** *Cell*. 2020;**182**(4):812-827.e19.
69. Public Health England. **Investigation of novel SARS-CoV-2 variant: variant of concern 202012/01: techinical briefing,** Available at: https://assets.publishing.service.gov.uk/government/uploads/system/uploads/attachment_data/file/959360/Variant_of_Concern_VOC_202012_01_Technical_Briefing_3.pdf.
70. Tegally H, Wilkinson E, Giovanetti M, et al. **Detection of a SARS-CoV-2 variant of concern in South Africa.** *Nature*. 2021;**592**(7854):438-443.
71. Fujino T, Nomoto H, Kutsuna S, et al. **Novel SARS-CoV-2 Variant in Travelers from Brazil to Japan.** *Emerg Infect Dis*. 2021;**27**(4):1243-1245.
72. **MInistry of Health and Family Welfare. Genome sequencing by INSACOG shows variants of concern and a novel variant in India.** Available at: https://pib.gov.in/PressReleaseIframePage.aspx?PRID=1707177.
73. Davies NG, Abbott S, Barnard RC, et al. **Estimated transmissibility and impact of SARS-CoV-2 lineage B.1.1.7 in England.** *Science*. 2021;**372**(6538):eabg3055.
74. Starr TN, Greaney AJ, Hilton SK, et al. **Deep Mutational Scanning of SARS-CoV-2 Receptor Binding Domain Reveals Constraints on Folding and ACE2 Binding.** *Cell*. 2020;**182**(5):1295-1310.e20.
75. Chen J, Wang R, Wang M, Wei GW. **Mutations Strengthened SARS-CoV-2 Infectivity.** *J Mol Biol*. 2020;**432**(19):5212-5226.
76. Avanzato VA, Matson MJ, Seifert SN, et al. **Case Study: Prolonged Infectious SARS-CoV-2 Shedding from an Asymptomatic Immunocompromised Individual with Cancer**. *Cell*. 2020;**183**(7):1901-1912.e9.
77. Ong SWX, Chiew CJ, Ang LW, et al. **Clinical and virological features of SARS-CoV-2 variants of concern: a retrospective cohort study comparing B.1.1.7 (Alpha), B.1.315 (Beta), and B.1.617.2 (Delta).** *Clin Infect Dis*. 2021;**ciab721**.
78. Halfmann PJ, Iida S, Iwatsuki-Horimoto K, et al. **SARS-CoV-2 Omicron virus causes attenuated disease in mice and hamsters.** *Nature*. 2022;**603**(7902):687-692.
79. Data Source, https://www.istat.it/en/archivio/253831.

80. Bikdeli B, Madhavan MV, Jimenez D, et al. **COVID-19 and Thrombotic or Thromboembolic Disease: Implications for Prevention, Antithrombotic Therapy, and Follow-Up: JACC State-of-the-Art Review.** *J Am Coll Cardiol*. 2020;**75**(23):2950-2973.
81. Connors JM, Levy JH. **Thromboinflammation and the hypercoagulability of COVID-19.** *J Thromb Haemost*. 2020;**18**(7):1559-1561.
82. Flaherty GT, Hession P, Liew CH, et al. **COVID-19 in adult patients with pre-existing chronic cardiac, respiratory and metabolic disease: a critical literature review with clinical recommendations.** *Trop Dis Travel Med Vaccines*. 2020;6:16.
83. Tay MZ, Poh CM, Rénia L, MacAry PA, Ng LFP. **The trinity of COVID-19: immunity, inflammation and intervention.** *Nat Rev Immunol*. 2020;**20**(6):363-374.
84. van Beek AA, Van den Bossche J, Mastroberardino PG, de Winther MPJ, Leenen PJM. **Metabolic Alterations in Aging Macrophages: Ingredients for Inflammaging?.** *Trends Immunol*. 2019;**40**(2):113-127.
85. Qin Z, Fang X, Sun W, et al. **Deactylation by SIRT1 enables liquid-liquid phase separation of IRF3/IRF7 in innate antiviral immunity.** *Nat Immunol*. 2022;**23**(8):1193-1207.
86. Booth A, Reed AB, Ponzo S, et al. **Population risk factors for severe disease and mortality in COVID-19: A global systematic review and meta-analysis.** *PLoS One*. 2021;**16**(3):e0247461.
87. Guan WJ, Ni ZY, Hu Y, et al. **Clinical Characteristics of Coronavirus Disease 2019 in China.** *N Engl J Med*. 2020;**382**(18):1708-1720.
88. Wu C, Chen X, Cai Y, et al. **Risk Factors Associated With Acute Respiratory Distress Syndrome and Death in Patients With Coronavirus Disease 2019 Pneumonia in Wuhan, China.** *JAMA Intern Med*. 2020;**180**(7):934-943.
89. Li R, Pei S, Chen B, et al**. Substantial undocumented infection facilitates the rapid dissemination of novel coronavirus (SARS-CoV-2)**. *Science*. 2020;**368**(6490):489-493.
90. Chen Y, Klein SL, Garibaldi BT, et al. **Aging in COVID-19: Vulnerability, immunity and intervention.** *Ageing Res Rev*. 2021;**65**:101205.
91. Livingston E, Bucher K. **Coronavirus Disease 2019 (COVID-19) in Italy.** *JAMA*. 2020;**323**(14):1335.
92. Jackson BR, Gold JAW, Natarajan P, et al. **Predictors at Admission of Mechanical Ventilation and Death in an Observational Cohort of Adults Hospitalized With Coronavirus Disease 2019.** *Clin Infect Dis*. 2021;**73**(11):e4141-e4151.
93. Wu Z, McGoogan JM. **Characteristics of and Important Lessons From the Coronavirus Disease 2019 (COVID-19) Outbreak in China: Summary of a Report of 72 314 Cases From the Chinese Center for Disease Control and Prevention.** *JAMA*. 2020;**323**(13):1239-1242.
94. CDC COVID-19 Response Team. **Severe Outcomes Among Patients with Coronavirus Disease 2019 (COVID-19) - United States, February 12-March 16, 2020.** *MMWR Morb Mortal Wkly Rep*. 2020;**69**(12):343-346.
95. Onder G, Rezza G, Brusaferro S. **Case-Fatality Rate and Characteristics of Patients Dying in Relation to COVID-19 in Italy.** *JAMA*. 2020;**323**(18):1775-1776.
96. Salje H, Tran Kiem C, Lefrancq N, et al. **Estimating the burden of SARS-CoV-2 in France.** *Science*. 2020;**369**(6500):208-211.
97. Konno Y, Kimura I, Uriu K, et al. **SARS-CoV-2 ORF3b Is a Potent Interferon Antagonist Whose Activity Is Increased by a Naturally Occurring Elongation Variant.** *Cell Rep*. 2020;**32**(12):108185.

98. Anka AU, Tahir MI, Abubakar SD, et al. **Coronavirus disease 2019 (COVID-19): An overview of the immunopathology, serological diagnosis and management.** *Scand J Immunol*. 2021;**93**(4):e12998.
99. Tan W, Lu Y, Zhang J, Wang J, Dan Y, Tan Z, et al. **Viral kinetics and antibody responses in patients with COVID-19.** *medRxiv*. 2020; **2020**.03.24.20042382.
100. Toor SM, Saleh R, Sasidharan Nair V, Taha RZ, Elkord E. **T-cell responses and therapies against SARS-CoV-2 infection.** *Immunology*. 2021;**162**(1):30-43.
101. Iwasaki A, Yang Y. **The potential danger of suboptimal antibody responses in COVID-19.** *Nat Rev Immunol*. 2020;**20**(6):339-341.
102. To KK, Tsang OT, Leung WS, et al. **Temporal profiles of viral load in posterior oropharyngeal saliva samples and serum antibody responses during infection by SARS-CoV-2: an observational cohort study.** *Lancet Infect Dis*. 2020;**20**(5):565-574.
103. Guo L, Ren L, Yang S, et al. **Profiling Early Humoral Response to Diagnose Novel Coronavirus Disease (COVID-19).** *Clin Infect Dis*. 2020;**71**(15):778-785.
104. BAO L L, DENG W, GAO H, et al. **Reinfection could not occur in SARS-CoV-2 infected rhesus macaques.** *bioRxiv*,2020; **99**0226.
105. Islam MN, Hossain KS, Sarker PP, et al. **Revisiting pharmacological potentials of Nigella sativa seed: A promising option for COVID-19 prevention and cure.** *Phytother Res*. 2021;**35**(3):1329-1344.
106. Zheng J, Wang Y, Li K, Meyerholz DK, Allamargot C, Perlman S. **Severe Acute Respiratory Syndrome Coronavirus 2-Induced Immune Activation and Death of Monocyte-Derived Human Macrophages and Dendritic Cells.** *J Infect Dis*. 2021;**223**(5):785-795.
107. Vabret N, Britton GJ, Gruber C, et al. **Immunology of COVID-19: Current State of the Science.** *Immunity*. 2020;**52**(6):910-941.
108. Zhang S, Wang L, Cheng G. **The battle between host and SARS-CoV-2: Innate immunity and viral evasion strategies.** *Mol Ther*. 2022;**30**(5):1869-1884.
109. Campana P, Parisi V, Leosco D, Bencivenga D, Della Ragione F, Borriello A. **Dendritic Cells and SARS-CoV-2 Infection: Still an Unclarified Connection.** *Cells*. 2020;**9**(9):2046.
110. Thevarajan I, Nguyen THO, Koutsakos M, et al. **Breadth of concomitant immune responses prior to patient recovery: a case report of non-severe COVID-19.** *Nat Med*. 2020;**26**(4):453-455.
111. Taefehshokr N, Taefehshokr S, Hemmat N, Heit B**. Covid-19: Perspectives on Innate Immune Evasion.** *Front Immunol*. 2020;**11**:580641.
112. Li G, Fan Y, Lai Y, et al. **Coronavirus infections and immune responses.** *J Med Virol*. 2020;**92**(4):424-432.
113. Stockinger B, Bourgeois C, Kassiotis G. **CD4+ memory T cells: functional differentiation and homeostasis.** *Immunol Rev*. 2006;**211**:39-48.
114. Lees JR, Farber DL. **Generation, persistence and plasticity of CD4 T-cell memories.** *Immunology*. 2010;**130**(4):463-470.
115. Sette A, Crotty S. **Adaptive immunity to SARS-CoV-2 and COVID-19.** *Cell*. 2021;**184**(4):861-880.
116. Fan YY, Huang ZT, Li L, et al. **Characterization of SARS-CoV-specific memory T cells from recovered individuals 4 years after infection.** *Arch Virol*. 2009;**154**(7):1093-1099.
117. Tan AT, Linster M, Tan CW, et al. **Early induction of functional SARS-CoV-2-specific T cells associates with rapid viral clearance and mild disease in COVID-19 patients.** *Cell Rep*. 2021;**34**(6):108728.

118. Amanat F, Stadlbauer D, Strohmeier S, et al. **A serological assay to detect SARS-CoV-2 seroconversion in humans.** *Nat Med*. 2020;**26**(7):1033-1036.
119. Deng W, Bao L, Liu J, et al. **Primary exposure to SARS-CoV-2 protects against reinfection in rhesus macaques.** *Science*. 2020;**369**(6505):818-823.
120. Li XY, Du B, Wang YS, et al. **The keypoints in treatment of the critical coronavirus disease 2019 patient**. *Zhonghua Jie He He Hu Xi Za Zhi*. 2020;**43**(4):277-281.
121. Chu CM, Poon LL, Cheng VC, et al. **Initial viral load and the outcomes of SARS.** *CMAJ*. 2004;171(11):1349-1352.
122. Oh MD, Park WB, Choe PG, et al. **Viral Load Kinetics of MERS Coronavirus Infection.** *N Engl J Med*. 2016;**375**(13):1303-1305.
123. Totura AL, Whitmore A, Agnihothram S, et al. **Toll-Like Receptor 3 Signaling via TRIF Contributes to a Protective Innate Immune Response to Severe Acute Respiratory Syndrome Coronavirus Infection.** *mBio*. 2015;**6**(3):e00638-15.
124. Zaki AM, van Boheemen S, Bestebroer TM, Osterhaus AD, Fouchier RA. **Isolation of a novel coronavirus from a man with pneumonia in Saudi Arabia**. *N Engl J Med*. 2012;**367**(19):1814-1820.
125. Ng ML, Tan SH, See EE, Ooi EE, Ling AE. **Proliferative growth of SARS coronavirus in Vero E6 cells.** *J Gen Virol*. 2003;**84**(Pt 12):3291-3303.
126. Kaur S, Bansal R, Kollimuttathuillam S, et al. **The looming storm: Blood and cytokines in COVID-19.** *Blood Rev*. 2021;**46**:100743.
127. Bastard P, Michailidis E, Hoffmann HH, et al. **Auto-antibodies to type I IFNs can underlie adverse reactions to yellow fever live attenuated vaccine.** *J Exp Med*. 2021;**218**(4):e20202486.
128. Huang C, Wang Y, Li X, et al. **Clinical features of patients infected with 2019 novel coronavirus in Wuhan**, China. *Lancet*. 2020. **395**(10223):497-506.
129. Diao B, Wang C, Tan Y, et al. **Reduction and Functional Exhaustion of T Cells in Patients With Coronavirus Disease 2019 (COVID-19).** *Front Immunol*. 2020;**11**:827.
130. Wu F, Zhao S, Yu B, et al. A new coronavirus associated with human respiratory disease in China. *Nature*. 2020;579(7798):265-269.
131. MEREDITH W, JENNIFER C-F, JOCELYN K AND CATHERINE M. **A rampage through the body**. *Science*, 2020, **368** (6489):356-360.
132. Shemesh M, Aktepe TE, Deerain JM, et al. **SARS-CoV-2 suppresses IFNβ production mediated by NSP1, 5, 6, 15, ORF6 and ORF7b but does not suppress the effects of added interferon**. *PLoS Pathog*. 2021;**17**(8):e1009800.
133. Blanco-Melo D, Nilsson-Payant BE, Liu WC, et al**. Imbalanced Host Response to SARS-CoV-2 Drives Development of COVID-19.** *Cell*. 2020;**181**(5):1036-1045.e9.
134. Fajgenbaum DC, June CH**. Cytokine Storm.** *N Engl J Med*. 2020;**383**(23):2255-2273.
135. Pontarotti P, Paganini J. **COVID-19 Pandemic: Escape of Pathogenic Variants and MHC Evolution.** *Int J Mol Sci*. 2022;**23**(5):2665.
136. Manik M, Singh RK. **Role of toll-like receptors in modulation of cytokine storm signaling in SARS-CoV-2-induced COVID-19.** *J Med Virol*. 2022;**94**(3):869-877.
137. Amor S, Fernández Blanco L, Baker D. **Innate immunity during SARS-CoV-2: evasion strategies and activation trigger hypoxia and vascular damage.** *Clin Exp Immunol*. 2020;**202**(2):193-209.

138. Xiong Y, Liu Y, Cao L, et al. **Transcriptomic characteristics of bronchoalveolar lavage fluid and peripheral blood mononuclear cells in COVID-19 patients.** *Emerg Microbes Infect*. 2020;**9**(1):761-770.
139. Masselli E, Vaccarezza M, Carubbi C, et al**. NK cells: A double edge sword against SARS-CoV-2.** *Adv Biol Regul*. 2020;**77**:100737.
140. Kanneganti TD. **Intracellular innate immune receptors: Life inside the cell.** *Immunol Rev*. 2020;**297**(1):5-12.
141. Thiel V, Weber F. **Interferon and cytokine responses to SARS-coronavirus infection.** *Cytokine Growth Factor Rev*. 2008;**19**(2):121-132.
142. Hu W, Yen YT, Singh S, Kao CL, Wu-Hsieh BA**. SARS-CoV regulates immune function-related gene expression in human monocytic cells.** *Viral Immunol*. 2012;**25**(4):277-288.
143. Kawai T, Akira S. **Toll-like receptors and their crosstalk with other innate receptors in infection and immunity.** *Immunity*. 2011;**34**(5):637-650.
144. Kim AY, Shim HJ, Kim SY, Heo S, Youn HS. **Differential regulation of MyD88- and TRIF-dependent signaling pathways of Toll-like receptors by cardamonin.** *Int Immunopharmacol*. 2018;**64**:1-9.
145. Akira S, Takeda K. **Toll-like receptor signalling.** *Nat Rev Immunol*. 2004;**4**(7):499-511.
146. Yang L, Seki E. **Toll-like receptors in liver fibrosis: cellular crosstalk and mechanisms.** *Front Physiol*. 2012;**3**:138.
147. Kawasaki T, Kawai T. **Toll-like receptor signaling pathways.** *Front Immunol*. 2014;**5**:461.
148. Yu L, Feng Z**. The Role of Toll-Like Receptor Signaling in the Progression of Heart Failure.** *Mediators Inflamm*. 2018;**2018**:9874109.
149. Vaure C, Liu Y. **A comparative review of toll-like receptor 4 expression and functionality in different animal species.** *Front Immunol*. 2014;**5**:316.
150. Dela Cruz EJ, Fiedler TL, Liu C, et al. **Genetic Variation in Toll-Like Receptor 5 and Colonization with Flagellated Bacterial Vaginosis-Associated Bacteria.** *Infect Immun*. 2021;**89**(3):e00060-20.
151. Fore F, Budipranama M, Destiawan RA. **TLR10 and Its Role in Immunity.** *Handb Exp Pharmacol*. 2022;**276**:161-174.
152. Schlee M, Hartmann G. **Discriminating self from non-self in nucleic acid sensing.** *Nat Rev Immunol*. 2016;**16**(9):566-580.
153. Abdelwahab SF, Hamdy S, Osman AM, et al. **Association of the polymorphism of the Toll-like receptor (TLR)-3 and TLR-9 genes with hepatitis C virus-specific cell-mediated immunity outcomes among Egyptian health-care workers.** *Clin Exp Immunol*. 2021;**203**(1):3-12.
154. Jung HE, Lee HK. **Current Understanding of the Innate Control of Toll-like Receptors in Response to SARS-CoV-2 Infection.** *Viruses*. 2021;**13**(11):2132.
155. Lynn GM, Chytil P, Francica JR, et al. **Impact of Polymer-TLR-7/8 Agonist (Adjuvant) Morphology on the Potency and Mechanism of CD8 T Cell Induction.** *Biomacromolecules*. 2019;**20**(2):854-870.
156. Dominguez-Molina B, Machmach K, Perales C, et al. **Toll-Like Receptor 7 (TLR-7) and TLR-9 Agonists Improve Hepatitis C Virus Replication and Infectivity Inhibition by Plasmacytoid Dendritic Cells.** *J Virol*. 2018;**92**(23):e01219-18.
157. Khan S, Shafiei MS, Longoria C, Schoggins JW, Savani RC, Zaki H. **SARS-CoV-2 spike protein induces inflammation via TLR2-dependent activation of the NF-κB pathway.** *Elife*. 2021;**10**:e68563.

158. Zheng M, Karki R, Williams EP, et al. **TLR2 senses the SARS-CoV-2 envelope protein to produce inflammatory cytokines.** *Nat Immunol*. 2021;**22**(7):829-838.
159. Choudhury A, Mukherjee S. **In silico studies on the comparative characterization of the interactions of SARS-CoV-2 spike glycoprotein with ACE-2 receptor homologs and human TLRs.** *J Med Virol*. 2020;**92**(10):2105-2113.
160. Frank MG, Nguyen KH, Ball JB, et al. **SARS-CoV-2 spike S1 subunit induces neuroinflammatory, microglial and behavioral sickness responses: Evidence of PAMP-like properties.** *Brain Behav Immun*. 2022;**100**:267-277.
161. Zhao Y, Kuang M, Li J, et al. **SARS-CoV-2 spike protein interacts with and activates TLR4**. *Cell Res*. 2021;**31**(7):818-820.
162. Bortolotti D, Gentili V, Rizzo S, et al. **TLR3 and TLR7 RNA Sensor Activation during SARS-CoV-2 Infection.** *Microorganisms*. 2021;**9**(9):1820.
163. Solanich X, Vargas-Parra G, van der Made CI, et al. **Genetic Screening for *TLR7* Variants in Young and Previously Healthy Men With Severe COVID-19.** *Front Immunol*. 2021;**12**:719115.
164. (https://www.fda.gov/consumers/consumer-updates/know-your-treatment-options-covid-19)
165. Qureshi QH, Ashraf T, Rehman K, Khosa MK, Akash MSH. **Therapeutic interventions of remdesivir in diabetic and nondiabetic COVID-19 patients: A prospective observational study conducted on Pakistani population.** *J Med Virol*. 2021;**93**(12):6732-6736.
166. de Wit E, Feldmann F, Cronin J, et al. **Prophylactic and therapeutic remdesivir (GS-5734) treatment in the rhesus macaque model of MERS-CoV infection.** *Proc Natl Acad Sci U S A*. 2020;**117**(12):6771-6776.
167. Lo MK, Feldmann F, Gary JM, et al. **Remdesivir (GS-5734) protects African green monkeys from Nipah virus challenge.** *Sci Transl Med*. 2019;**11**(494):eaau9242.
168. Tchesnokov EP, Feng JY, Porter DP, Götte M. **Mechanism of Inhibition of Ebola Virus RNA-Dependent RNA Polymerase by Remdesivir.** *Viruses*. 2019;**11**(4):326.
169. Beigel JH, Tomashek KM, Dodd LE, et al. **Remdesivir for the Treatment of Covid-19 - Final Report.** *N Engl J Med*. 2020;**383**(19):1813-1826.
170. Johnson MG, Puenpatom A, Moncada PA, et al. **Effect of Molnupiravir on Biomarkers, Respiratory Interventions, and Medical Services in COVID-19 : A Randomized, Placebo-Controlled Trial.** *Ann Intern Med*. 2022;**M22**-0729.
171. Qingxian Cai, Minghui Yang, Dongjing Liu, et al. **Experimental Treatment with Favipiravir for COVID-19: An Open-Label Control Study.***Engineering*,2020,**6**(10):1192-1198.
172. O'Shea JJ, Kontzias A, Yamaoka K, Tanaka Y, Laurence A. **Janus kinase inhibitors in autoimmune diseases.** *Ann Rheum Dis*. 2013;**72** Suppl 2(0 2):ii111-ii115.
173. Das D, Mukhopadhyay P, Banerjee D. **Mortality comparision in patients receiving either Remdesivir or Remdesivir plus Baricitinib combination in case of moderate to severe COVID-19 Pneumonia: A retrospective study.** *J Assoc Physicians India*. 2022;**70**(4):11-12.
174. Mahase E. **Covid-19: Pfizer's paxlovid is 89% effective in patients at risk of serious illness, company reports.** *BMJ*. 2021;**375**:n2713.
175. Gupta A, Gonzalez-Rojas Y, Juarez E, et al. **Early Treatment for Covid-19 with SARS-CoV-2 Neutralizing Antibody Sotrovimab.** *N Engl J Med*. 2021;**385**(21):1941-1950.

176. Lee JY, Ko JH, et al. **Effectiveness of Regdanvimab Treatment in High-Risk COVID-19 Patients to Prevent Progression to Severe Disease.** *Front Immunol*. 2021;**12**:772320.
177. Dougan M, Nirula A, Azizad M, et al. **Bamlanivimab plus Etesevimab in Mild or Moderate Covid-19.** *N Engl J Med*. 2021;**385**(15):1382-1392.
178. Nguyen Y, Flahault A, Chavarot N, et al. **Pre-exposure prophylaxis with tixagevimab and cilgavimab (Evusheld©) for COVID-19 among 1112 severely immunocompromised patients.** *Clin Microbiol Infect*. 2022;**S1198**-743X(22)00383-4.
179. Ganesh R, Philpot LM, Bierle DM, et al. **Real-World Clinical Outcomes of Bamlanivimab and Casirivimab-Imdevimab Among High-Risk Patients With Mild to Moderate Coronavirus Disease 2019.** *J Infect Dis*. 2021;**224**(8):1278-1286.
180. Kritas SK, Ronconi G, Caraffa A, Gallenga CE, Ross R, Conti P. **Mast cells contribute to coronavirus-induced inflammation: new anti-inflammatory strategy.** *J Biol Regul Homeost Agents*. 2020;**34**(1):9-14.
181. Bonaventura A, Vecchié A, Wang TS, et al. **Targeting GM-CSF in COVID-19 Pneumonia: Rationale and Strategies.** *Front Immunol*. 2020;**11**:1625.
182. Whittaker Brown SA, Iancu-Rubin C, Aboelela A, et al. **Mesenchymal stromal cell therapy for acute respiratory distress syndrome due to coronavirus disease 2019.** *Cytotherapy*. 2022;**24**(8):835-840.
183. Li X, Geng M, Peng Y, Meng L, Lu S. **Molecular immune pathogenesis and diagnosis of COVID-19.** *J Pharm Anal*. 2020;**10**(2):102-108.
184. Gusev E, Sarapultsev A, Solomatina L, Chereshnev V. **SARS-CoV-2-Specific Immune Response and the Pathogenesis of COVID-19.** *Int J Mol Sci*. 2022;**23**(3):1716.
185. Saif LJ. **Vaccines for COVID-19: perspectives, prospects, and challenges based on candidate SARS, MERS, and animal coronavirus vaccines.** *Euro Med J.* 2020; DOI/10.33590/ emj/200324.
186. Rittig MG, Kaufmann A, Robins A, et al**. Smooth and rough lipopolysaccharide phenotypes of Brucella induce different intracellular trafficking and cytokine/chemokine release in human monocytes.** *J Leukoc Biol*. 2003;**74**(6):1045-1055.
187. Li Y, Deng SL, Lian ZX, Yu K. **Roles of Toll-Like Receptors in Nitroxidative Stress in Mammals.** *Cells*. 2019;8(6):576.
188. Sumner JB, Gralën N, Eriksson-Quensel IB. **THE MOLECULAR WEIGHTS OF UREASE, CANAVALIN, CONCANAVALIN A AND CONCANAVALIN B.** *Science*. 1938;**87**(2261):395-396.
189. Lei HY, Chang CP. **Lectin of Concanavalin A as an anti-hepatoma therapeutic agent.** *J Biomed Sci*. 2009;**16**(1):10.
190. Dwyer JM, Johnson C. **The use of concanavalin A to study the immunoregulation of human T cells.** *Clin Exp Immunol*. 1981;**46**(2):237-249.
191. Blumberg PM. **Protein kinase C as the receptor for the phorbol ester tumor promoters: sixth Rhoads memorial award lecture.** *Cancer Res*. 1988;**48**(1):1-8.
192. "**Flow Cytometry Intracellular Staining Guide**". *eBioscience*, Inc. Retrieved 2011-09-25.
193. Hikmet F, Méar L, Edvinsson Å, Micke P, Uhlén M, Lindskog C. **The protein expression profile of ACE2 in human tissues.** *Mol Syst Biol*. 2020;16(7):e9610.
194. https://www.proteinatlas.org/ENSG00000130234-ACE2/immune+cell
195. Junqueira C, Crespo Â, Ranjbar S, et al. **FcγR-mediated SARS-CoV-2 infection of monocytes activates inflammation.** *Nature*. 2022;**606**(7914):576-584.

196. Muus C, Luecken MD, Eraslan G, et al. **Single-cell meta-analysis of SARS-CoV-2 entry genes across tissues and demographics.** *Nat Med*. 2021;**27**(3):546-559.
197. Wan S., Yi Q., Fan S., Lv J., Zhang X., Guo L. et al. **Characteristics of lymphocyte subsets and cytokines in peripheral blood of 123 hospitalized patients with 2019 novel coronavirus pneumonia (NCP)**. *medRxiv.* 2020; **10**.1101/2020.02.10.20021832
198. Sodeifian F, Nikfarjam M, Kian N, Mohamed K, Rezaei N. **The role of type I interferon in the treatment of COVID-19.** *J Med Virol*. 2022;**94**(1):63-81.
199. Hasanvand A. **COVID-19 and the role of cytokines in this disease.** *Inflammopharmacology*. 2022;**30**(3):789-798.
200. Zhang Z, Zheng Y, Niu Z, et al. **SARS-CoV-2 spike protein dictates syncytium-mediated lymphocyte elimination.** *Cell Death Differ*. 2021;**28**(9):2765-2777.
201. Yao J, Chen X, Liu X, Li R, Zhou X, Qu Y. **Characterization of a ferroptosis and iron-metabolism related lncRNA signature in lung adenocarcinoma.** *Cancer Cell Int*. 2021;**21**(1):340.
202. Hadjadj J, Yatim N, Barnabei L, et al. **Impaired type I interferon activity and inflammatory responses in severe COVID-19 patients.** *Science*. 2020;**369**(6504):718-724.
203. Cuevas AM, Clark JM, Potter JJ. **Increased TLR/MyD88 signaling in patients with obesity: is there a link to COVID-19 disease severity?.** *Int J Obes (Lond)*. 2021;**45**(5):1152-1154.
204. Mellett L, Khader SA. S100A8/A9 in COVID-19 pathogenesis: Impact on clinical outcomes. *Cytokine Growth Factor Rev*. 2022;63:90-97.
205. Channappanavar R, Perlman S. **Pathogenic human coronavirus infections: causes and consequences of cytokine storm and immunopathology.** *Semin Immunopathol*. 2017;39(5):529-539.
206. Channappanavar R, Fehr AR, Vijay R, et al. **Dysregulated Type I Interferon and Inflammatory Monocyte-Macrophage Responses Cause Lethal Pneumonia in SARS-CoV-Infected Mice.** *Cell Host Microbe*. 2016;**19**(2):181-193.
207. Zazzara MB, Bellieni A, Calvani R, Coelho-Junior HJ, Picca A, Marzetti E. **Inflammaging at the Time of COVID-19.** *Clin Geriatr Med*. 2022;**38**(3):473-481.
208. Azaiz MB, Jemaa AB, Sellami W, et al. **Deciphering the balance of IL-6/IL-10 cytokines in severe to critical COVID-19 patients.** *Immunobiology*. 2022;**227**(4):152236.
209. Rodríguez-Hernández MÁ, Carneros D, Núñez-Núñez M, et al. **Identification of IL-6 Signalling Components as Predictors of Severity and Outcome in COVID-19.** *Front Immunol*. 2022;**13**:891456.
210. Schultze JL, Aschenbrenner AC. **COVID-19 and the human innate immune system.** *Cell*. 2021;**184**(7):1671-1692.

ACKNOWLEDGMENTS

Recalling the passing years, I feel that the years are like songs. I spent the most precious years of my life in Sassari, Shantou and Halifax. I hesitated and retreated. Fortunately, I was accompanied by good teachers and friends from beginning to end to accompany me through those rough days.

First of all, I would like to thank my supervisor Professor Salvatore Rubino, who has been giving me guidance in life and study during my Ph.D, I deeply benefited from Professor Rubino's careful instruction.

Secondly, I would like to thank my supervisor Professor David J. Kelvin, Medical College in Shantou University and The Department of Microbiology and Immunology in Dalhousie University. He had providing me with experimental conditions, financial support and careful guidance for my research subject. As a teacher, he stirs up the maze and makes people feel like a spring breeze. Here I would like to express my most sincere respect and thanks. Also I am very grateful to my Dalhousie University colleagues Ali Toloue Ostadgavahi and Christopher Richardson for their help with cell experiments.

I would also like to thank Professor Leonardo A Sechi and Professor Giustina Casu Finlayson for their support in my life and study. Thank my classmates and friends who have always cared about and supported me, I will never forget the friendship with my classmates.

Last but not least, I want to thank my parents and family. Whenever I face difficulties and setbacks, they are always beside me to cheer me up; Whenever I face major choices, they give me advice and help from my point of view. No matter what my choice is, they fully believe in me and support me unconditionally. Their selfless love and care for me is the driving force for me to move forward and will always be the harbor I can rely on.

Once again, thank everyone who accompanied me on the journey!